Summer 8-15-2017

Type 1 and F17-like Pili Promote the Establishment of the Uropathogenic E. coli Intestinal Reservoir

Caitlin Nicole Spaulding
Washington University in St. Louis

WASHINGTON UNIVERSITY IN ST. LOUIS

Division of Biology and Biomedical Sciences
Molecular Microbiology and Microbial Pathogenesis

Dissertation Examination Committee:
Scott Hultgren, Chair
John Atkinson
Brian Edelson
Jeffrey Gordon
David Hunstad
Andrew Kau
Phillip Tarr

Type 1 and F17-like Pili Promote the Establishment of the Uropathogenic *E. coli* Intestinal Reservoir.

by

Caitlin N. Spaulding

A dissertation presented to
The Graduate School
of Washington University in
partial fulfillment of the
requirements for the degree
of Doctor of Philosophy

August 2017
St. Louis, Missouri

Table of Contents

List of Figures and Tables

Figures:

Supplementary Tables:

Acknowledgments

First and foremost I would like to thank Scott Hultgren for his support, guidance, and unwavering enthusiasm for scientific discovery and for training scientists. I am eternally grateful for his essential role throughout my graduate education and beyond. I am also tremendously grateful to Jeffrey Gordon for his roles in my thesis work as a collaborator, committee chair, and mentor and for his support of my thesis research and my scientific training.

Thank you to my thesis committee - Dr. Jeffrey Gordon, Dr. John Atkinson, Dr. Brian Edelson, Dr. David Hunstad, Dr. Andrew Kau, and Dr. Phil Tarr - for the constructive feedback that helped to shape my thesis work. I would especially like to thank my committee member and collaborator Dr. Andy Kau for his hard work on behalf of this project and for always having an open door to discuss experiments, science, and the next-steps in my scientific career.

I am grateful to collaborators that contributed directly to my thesis work, including: Dr. James Janetka, Dr. Han Remaut, Dr. Daved Fremont, and Dr. Segolene Ruer.

Thank you to the Department of Molecular Microbiology for fostering an excellent training environment for Ph.D. students.

The entire Hultgren lab, past and present, has contributed to this work through their input and feedback. I am grateful to be surrounded by intelligent, hard working individuals who create such a fun and enriching lab environment. Thank you especially to Roger Klein, Dr. Zac Cusumano, Dr. Karen Dodson, Jerry Pinkner, and Henry Schieber for their scientific contributions to this project. A special thank you to Karen Dodson for teaching me how to communicate science through writing, for patiently reading and editing an endless number of documents, and for being a wonderful scientist and mentor.

I am very thankful for funding that made this work possible. This work was supported by grants from the NIH (K08AI113184, R01AI048689, P50DK064540, RC1DK086378, DK30292, and 1F31DK107057), FWO-Flanders (G030411N), Hercules Foundation (UABR/09/005) and VIB PRJ9.

Thank you to my amazing friends and family, especially Zeina, Liam, Tracy, Sandy, Amanda, Katherine, Shannon, Natalie, Ana, and Greg, for making time outside of lab fun and relaxing.

To my brother, Aaron, thank you for you love and encouragement and for always being my biggest fan and my role model.

To my parents, Larry and Angela, thank you for all the sacrifices you have made to help me achieve my goals, for fostering my love for discovery, for your enthusiasm during times of success, and for your fortitude and compassion during times of failure. Without your unconditional love and unwavering support this work would not have been possible.

Finally, to my husband, Danny, thank you for being my steadfast source of empathy, tranquility, support, love, and laughter. Thank you for providing sanity in the midst of chaos, understanding and strength in the face of frustration, and for making each day better than the last.

Caitlin N. Spaulding

Washington University in St. Louis

August 2017

ABSTRACT OF THE DISSERTATION

Type 1 and F17-like Pili Promote the Establishment of the Uropathogenic *E. coli* Intestinal Reservoir.

By

Caitlin N. Spaulding

Doctor of Philosophy in Biology and Biomedical Sciences

Molecular Microbiology and Microbial Pathogenesis

Washington University in St. Louis, 2017

Dr. Scott J. Hultgren, Chair

Urinary tract infections (UTI) affect over 150 million individuals worldwide every year. These infections are associated with significant morbidity and have a sizeable economic impact, with $5 billion being spent on UTI treatment in the USA annually. Uropathogenic *E. coli* (UPEC) are responsible for 80% of community acquired UTIs and 65% of nosocomial UTI. The current standard of care for UTI is antibiotic therapy. However, 30-50% of women experience recurrent UTI (rUTI) despite receiving antibiotic therapy. The prevalence of single and multi-drug resistant UPEC strains has led to increased reliance on carbepenems, which are primarily reserved for multi-drug resistant infections, to treat an increasing number of patients. Consequently *E. coli* strains resistant to colistin, a drug of last resort for treating carbapenem-

resistant Enterobacteriaceae, have now been isolated in over 30 counties. The rate at which drug-resistant *E. coli* are spreading across the globe emphasizes the urgent nature of the antibiotic-resistance crisis we currently face and the dire need for new, antibiotic-sparing therapies that target UPEC virulence factors. To colonize host tissue, *E. coli* encode chaperone usher pathway (CUP) pili and single UPEC strains can encode up to 16 distinct CUP pilus operons. Although CUP pilus types that promote UPEC colonization of the urinary tract have been identified, no studies investigating a role for CUP pilus types in UPEC intestinal colonization have been published. Still, leading models of infection posit that UPEC in the gut seed UTI by being shed in the feces, and then colonizing the peri-urethral or vaginal tissue and subsequently ascending through the urethra to access the bladder. Using a mouse model of UPEC intestinal colonization I found that two (CUP) pili, F17-like pili and type 1 pili, provide a fitness advantages for UPEC in the gut. The X-ray crystal structure of the F17-like pilus adhesin lectin domain, coupled with molecular studies of glycan binding, disclosed a ligand specificity distinct from other pilus types known to facilitate gastrointestinal colonization. While phylogenomic studies revealed that F17-like pili are closely related to pilus types carried by intestinal pathogens, but are restricted to extra-intestinal pathogenic *E. coli*. Moreover, I found that high-affinity mannose analogues (mannosides) that target the function of type 1 pili and effectively treat UTI reduce intestinal colonization by clinical UPEC isolates, including a multi-drug resistant strain, without disrupting gut microbiota structure. By decreasing the intestinal UPEC reservoir that seeds bladder infection, mannosides could significantly reduce the rate of UTI and rUTI. Further, mannosides act like a molecular scalpel, specifically targeting intestinal UPEC with minimal effects on the overall gut microbiota. Ultimately, therapies like mannosides, which selectively target colonization by a specific pathogen, have potential to revolutionize treatment and prevention of

rUTI. Take together, this dissertation provides invaluable tools and insights into the understudied UPEC intestinal reservoir

Chapter 1: Adhesive Pili in UTI Pathogenesis and Drug Development

From:

Adhesive Pili in UTI Pathogenesis and Drug Development

Caitlin N. Spaulding and Scott J. Hultgren

Pathogens 2016, 5(1), 30. doi: 10.3390/pathogens5010030. PMID: 26999218

Abstract

Urinary tract infections (UTIs) are one of the most common bacterial infections, affecting 150 million people each year worldwide. High recurrence rates and increasing antimicrobial resistance among uropathogens are making it imperative to develop alternative strategies for the treatment and prevention of this common infection. In this Review, we discuss how understanding the: (i) molecular and biophysical basis of host-pathogen interactions; (ii) consequences of the molecular cross-talk at the host pathogen interface in terms of disease progression; and (iii) pathophysiology of UTIs is leading to efforts to translate this knowledge into novel therapeutics to treat and prevent these infections.

Keywords: UTI; rUTI; CAUTI; pili; UPEC; chaperone-usher pathway (CUP) pili; *Enterococcus*; vaccine; antibiotic-resistance

Introduction

Urinary tract infections (UTIs) can be acquired in the community or hospital setting and are one of the most common bacterial infections that occur, affecting more than 150 million people worldwide each year [1–3]. UTI is clinically divided into two major infections, characterized by the localization of the bacteria in the urinary tract, cystitis and pyelonephritis. Cystitis, or lower UTI, is infection of the bladder. Once in the bladder, bacteria can ascend the ureters and colonize the kidneys, causing pyelonephritis or upper UTI. While the incidence of pyelonephritis is fairly low (~0.3%–0.6%) it is particularly dangerous as uncontrolled bacterial infection can spread to the bloodstream, causing sepsis (which occurs in ~2% of pyelonephritis cases) [4,5]. UTIs are also categorized as uncomplicated or complicated infections. Complicated UTI occurs in patients with: (i) functional or structural urinary tract abnormalities; (ii) renal failure; (iii) immunosuppression; (iv) pregnancy; and/or (v) foreign bodies, such as indwelling catheters, placed within their urinary tract [6–8]. Catheter-associated UTIs (CAUTI), make up 70%–80% of all complicated UTI and are the most common type of nosocomial infection [4,9]. CAUTI are of particular concern as they result in high morbidity, increased mortality and are the most common cause of secondary sepsis in hospital patients. While complicated UTI affects individuals of both genders, uncomplicated UTI primarily affects otherwise healthy women [10]. Pyelonephritis often occurs in healthy, non-pregnant women but can be categorized as a complicated UTI because of the potential of developing a blood stream infection. For women, the lifetime risk of developing an uncomplicated UTI approaches 60% [5]. Of these women who

experience an initial UTI, 20%–30% will go on to experience a recurrent infection (rUTI) within 4–6 months, despite receiving appropriate antibiotic therapy [5,11]. To combat rUTI, these women are treated with frequent antibiotic therapy often to be taken at the time that symptoms arise or immediately following sexual intercourse [6]. However, a subset of these women will continue to experience rUTI as frequently as six or more times a year [12]. Due to its prevalence and high rates of recurrence, UTI is associated with significant economic costs. The financial burden of UTI in the United States, which reflects both direct medical costs and indirect costs such as lost work output and wages, is an estimated $5 billion annually [5]. These infections also result in significant patient morbidity resulting in serious deterioration in quality of life including: pain, discomfort, disruption of daily activities, and few treatment options other than long-term antibiotic prophylaxis [5,11,13].

While many bacterial organisms cause UTI, the most common causative agent of both uncomplicated and complicated UTI is the gram-negative pathogen uropathogenic *Escherichia coli* (*E. coli*) (UPEC). UPEC are responsible for 80%–90% of all uncomplicated UTI and approximately 65% of complicated UTIs [5,14,15]. Gram-positive *Enterococcus* species are the second leading cause of complicated UTI (11%) and the third leading cause of uncomplicated UTI (5%) [15]. The source population of UPEC and *Enterococcus* that lead to UTI is thought to be the gastrointestinal tract, where they can reside as either commensal or transient members of the gut microbiota [11,16,17]. When present in the gut, UPEC or *Enterococcus* spp. can be shed in the feces, inoculating peri-urethral or vaginal areas, and are subsequently introduced into the urinary tract during periods of physical manipulation such as during sexual activity or catheterization (Figure 1A) [18]. Upon entering the bladder, uropathogens must bind to an available epithelial receptor and/or, if present, abiotic-surface to establish and maintain

colonization. UPEC and enterococcal species both accomplish this through the expression of distinctive adhesive pili on their surface. After creating a foothold in the bladder, uropathogens employ a myriad of additional virulence factors to establish bladder colonization in the face of an active immune response, micturition, and rapid epithelial cell exfoliation. Historically, antibiotics have been used, very successfully, to treat patients with UTI. However, the rise of single and multi-drug resistant uropathogens as well as high rates of recurrence in women infected with both antibiotic sensitive and drug-resistant uropathogens has become a major concern, highlighting the need to develop alternative strategies to treat patients with UTI and CAUTI. In this review, we will discuss the role of adhesive pili during UTI or CAUTI. Here we will focus mainly on UTI and CAUTI caused by UPEC and *Enterococcus spp*. due to the high prevalence of these pathogens in community-acquired and nosocomial infections. We will also explore the development of alternative, non-antibiotic treatment strategies that target adhesive pili in order to prevent UPEC and *Enterococcus* spp. from initiating infection and thus causing disease.

The Role of Chaperone-Usher Pathway (CUP) Pili in UPEC Mediated UTI

CUP Pilus Assembly Mechanisms

Upon entering the bladder, UPEC must first adhere to the bladder epithelium, also referred to as the urothelium, or risk clearance during urine voiding. Recognition and attachment to host and environmental surfaces is mediated through the expression of non-flagellar, adhesive, extracellular fibers, called pili that bind to receptors present on the host cell surface. In UPEC, many of these adhesive pili belong to a large, conserved family of pili called the chaperone-usher pathway (CUP) pili [20]. CUP pili are assembled by the corresponding chaperone-usher machinery, which are encoded by operons that contain all the dedicated genetic information

necessary to assemble a mature pilus: an outer-membrane pore-forming usher protein, a periplasmic chaperone protein, pilus subunits, and in most cases, a tip adhesin protein. The first crystal structure of a CUP chaperone, PapD, which is involved in the assembly of P pili, revealed that it consists of two-immunoglobulin (Ig) domains [21]. Two key amino acid residues, R8 and K112, present in the cleft of the chaperone were subsequently identified as the active site of the protein [22]. Unlike the chaperone, pilus subunits are composed of an incomplete Ig fold, which lacks the C-terminal beta strand and requires the assistance of the dedicated chaperone for folding and stability (Figure 2B,D). Chaperone-assisted folding occurs by a reaction termed donor strand complementation (DSC) in which conserved alternating exposed hydrophobic residues on the chaperone's G1 strand are buried in complementary pockets in the pilus subunit, allowing for the completion of the subunits Ig fold (Figure 2C) [23,24]. This interaction allows pilus subunits to fold into a primed, high-energy state in complex with the chaperone, ultimately allowing the subunits to be targeted to the outer membrane usher (Figure 2E). The usher, a gated channel, is made up of five functional domains: a 24 stranded transmembrane β-barrel translocation domain (TD), a β-sandwich plug (PLUG) that resides in the pore of the TD in the apo-usher, an N-terminal periplasmic domain (NTD) and two C-terminal periplasmic domains (CTD1 and 2) [25–29]. The usher catalyzes pilus assembly by driving subunit polymerization in a concerted reaction termed donor strand exchange (DSE) (Figure 2E,F) [30–33]. Pilus subunits, excluding the adhesin, encode an N-terminal extension (Nte) comprised of conserved alternating hydrophobic residues. DSE occurs when the chaperone is displaced and an incoming subunit's Nte zips into the previously chaperone-bound groove of a nascently incorporated subunit at the growing terminus of the pilus. This "zip-in-zip-out mechanism" allows for the final folding of

the pilus subunit, such that every subunit in the pilus completes the Ig fold of its neighbor (Figure 2F).

The Role of Type 1 Pili during Uncomplicated UTI

A hallmark of the luminal surface of urothelial cells, also called superficial facet cells, are the presence of uroplakin plaques, which consist of 4 uroplakin integral membrane proteins, that function as a barrier between the toxic contents of the bladder and the underlying urothelium [34,35]. The surface of the uroplakin is studded with mannose [36,37]. The tip adhesin for type 1 pili, FimH, binds mannose with stereochemical specificity. Therefore, upon entering the bladder, FimH is able to bind mannosylated residues on the bladder surface, such as those found on uroplakin as well as β1-α3 integrin receptors (Figure 1B) [36,38–40]. FimH mediated interaction with the urothelium induces a signaling cascade that activates Rho family GTPases and results in actin rearrangement within urothelial cells, promoting UPEC invasion (Figure 1C,D) [38,41,42]. Studies in mice have revealed that once inside superficial facet cells, UPEC are able to escape the endocytic vesicle, via unknown mechanisms, into the cytoplasm where they replicate rapidly forming biofilm-like communities called intracellular bacterial communities (IBCs) (Figure 1D,E) [43–45]. In mice, type 1 pili are not only required for cellular adherence and invasion but also for the aggregation of bacteria into an IBC in the host cell cytoplasm [46]. Mouse studies have shown that invasion is a critical step in UPEC pathogenesis in naïve mice, allowing the bacteria to rapidly replicate in a niche protected from many innate immune defense mechanisms and antibiotics. UPEC that cannot invade the urothelium, like those lacking FimH, are quickly cleared from the bladder, emphasizing the importance of this intracellular stage to the success of the pathogen [46]. Mature IBCs contain approximately 10^4 bacteria. Upon maturation, bacteria

within the IBC adopt a filamentous morphology and disperse from the biomass, fluxing out of the cell and back into the bladder lumen where they can adhere to and/or invade adjacent facet cells or exposed transitional epithelial cells (Figure 1G,H) [43,44,47,48]. Importantly, evidence of IBCs and bacterial filaments have been observed in women suffering from acute UTI, one to two days post self-reported sexual intercourse, but not in healthy controls or infections caused by Gram-positive organisms, which do not form IBCs [49]. IBCs have also been observed in urine from children with an acute UTI and their presence was correlated with recurrent UTI, supporting the validity of their importance in pathogenesis and the ability of the mouse model to recapitulate human disease [50].

While the collection of tissue biopsies from women with UTI is generally contraindicated, one study of tissue biopsies demonstrated the presence of intracellular UPEC [51]. In urine from UTI patients and/or mice, the expression of type 1 pili has been reported to be variable [52–54]. Several studies, in mice and humans, have demonstrated that UPEC attached to shed epithelial cells in the urine express type 1 pili while planktonic UPEC found in the urine tend to be nonpiliated [54,55]. This suggests that the expression of type 1 pili is niche specific, with type 1 pili being expressed by UPEC that are attached to the epithelial surface.

In addition to type 1 pili, a mosaic of UPEC virulence factors including adhesins, toxins, capsule, siderophores, and flagella have been identified and characterized [39,56–61]; however the direct contribution of these putative urovirulence factors has not been exhaustively studied. In a recent comprehensive genomic analysis of 43 UPEC isolates, we found that “core” genes, defined as genes shared between all *E. coli*, constituted approximately 60% of each strain’s genome. Further, we were unable to find any single set of genes that accurately delineated UPEC from non-UPEC strains (Schreiber and Hultgren, personal communication). The lack of a strict

'genetic' definition of UPEC indicates that, in most cases, urovirulence in UPEC is more complicated than carriage of a set of virulence-associated genes that are missing in non-UPEC strains. Instead urovirulence in UPEC strains may be defined by alternative characteristics, like propensity to certain patterns of gene expression, as is seen with niche specific expression of type 1 pili in the bladder [54, 55], or the carriage of different alleles of core genes. There are a number of different alleles of FimH, described later in this review, that alter the affinity of the adhesin for its ligand and may be associated with more virulent strains. These alternative characteristics may explain how genes that are highly conserved in both UPEC and non-UPEC strains, like those that encode type 1 pili, contribute to pathogenesis during UTI.

The Host Response to Type 1 Piliated UPEC

The host has evolved several mechanisms to respond to type 1 pilus mediated binding in a manner that favors bacterial clearance or killing. Caspase-dependent apoptosis and exfoliation of superficial facet cells is observed within hours of type 1 pili binding and invasion in C57BL/6 mice [39,62,63]. This promotes the clearance of infected cells from the host during micturition (Figure 1F). In the absence of cell exfoliation, the host can expel UPEC directly from an invaded cell via a TLR-4 dependent mechanism, reducing the number of successful UPEC invasion events and decreasing the overall number of IBCs formed during acute infection (Figure 1C) [19]. UPEC interactions with the host also leads to the robust recruitment of immune cells, mainly neutrophils and inflammatory monocytes, to the urinary tract as well as the up regulation of pro-inflammatory cytokines which drive the mobilization of additional immune effectors [64–68]. Several natural allele variants of FimH exist. The residues in the mannose-binding pocket of FimH are invariant in all sequenced UPEC isolates [37,69], however there is diversity outside of

this pocket, including at a cluster of amino acids that are positively-selected in UPEC strains [69]. Interestingly, mutations in these positively selected residues results in distinct FimH alleles that are skewed into either elongated or compact conformations, which have been observed in several X-ray crystal structures of FimH [25,26,70]. The elongated conformation corresponds to the mannose binding conformation whereas the compact form binds mannose only weakly or not at all [69,71,72]. When FimH is bound to the FimC chaperone, it adopts an elongated conformation [26] however, upon its incorporation into the tip of the pilus, it can convert to a compact conformation with an altered mannose-binding pocket [25,70]. In the FimCH complex, all of the FimH allele variants tested have a high affinity for mannose. However, when incorporated into a tip-like state, following a DSE reaction with the FimG adaptor, FimH variants differ greatly in their mannose affinity suggesting that depending on the allele, FimH is skewed toward either an elongated or compact form after its incorporation into the tip [73]. Interestingly, UPEC strains containing distinct FimH alleles also display altered levels of pathogenicity during acute and chronic UTI in C57BL/6 [74] and C3H/HeN mice [73]. Of particular interest we found that specific mutations in two positively selected residues, A27 and V163, result in a FimH variant (FimH(A27V/V163A)) that resides within a tip-like complex predominantly in a high-affinity mannose binding conformation [73]. Surprisingly, this FimH allele is severely attenuated in a cystitis model [69,73]. These findings support the hypothesis that FimH resides in an equilibrium of mannose-binding and non-binding conformations, which are governed, in part, by the identity of select residues that are under positive selection in UPEC isolates. The inter-conversion between high and low mannose-binding conformations is likely important for tissue-binding and/or immune evasion, which may begin to explain why the FimH(A27V/V163A) variant, which appears to be “locked” in a high-affinity elongated state is

unable to cause infection *in vivo* despite its high-affinity for mannose. These findings may be related to the important observation made by others that FimH conformation is influenced by shear force leading to a "catch bond" model of FimH function [70–72,75,76]. Thus, the ability of FimH to be incorporated into a pilus tip to interconvert into different conformations affects virulence.

The Biophysics of FimH Structure and Function

Several natural allele variants of FimH exist. The residues in the mannose-binding pocket of FimH are invariant in all sequenced UPEC isolates [37,69], however there is diversity outside of this pocket, including at a cluster of amino acids that are positively-selected in UPEC strains [69]. Interestingly, mutations in these positively selected residues results in distinct FimH alleles that are skewed into either elongated or compact conformations, which have been observed in several X-ray crystal structures of FimH [25,26,70]. The elongated conformation corresponds to the mannose binding conformation whereas the compact form binds mannose only weakly or not at all [69,71,72]. When FimH is bound to the FimC chaperone, it adopts an elongated conformation [26] however, upon its incorporation into the tip of the pilus, it can convert to a compact conformation with an altered mannose-binding pocket [25,70]. In the FimCH complex, all of the FimH allele variants tested have a high affinity for mannose. However, when incorporated into a tip-like state, following a DSE reaction with the FimG adaptor, FimH variants differ greatly in their mannose affinity suggesting that depending on the allele, FimH is skewed toward either an elongated or compact form after its incorporation into the tip [73]. Interestingly, UPEC strains containing distinct FimH alleles also display altered levels of pathogenicity during acute and chronic UTI in C57BL/6 [74] and C3H/HeN mice [73]. Of

particular interest we found that specific mutations in two positively selected residues, A27 and V163, result in a FimH variant (FimH(A27V/V163A)) that resides within a tip-like complex predominantly in a high-affinity mannose binding conformation [73]. Surprisingly, this FimH allele is severely attenuated in a cystitis model [69,73]. These findings support the hypothesis that FimH resides in an equilibrium of mannose-binding and non-binding conformations, which are governed, in part, by the identity of select residues that are under positive selection in UPEC isolates. The inter-conversion between high and low mannose-binding conformations is likely important for tissue-binding and/or immune evasion, which may begin to explain why the FimH(A27V/V163A) variant, which appears to be "locked" in a high-affinity elongated state is unable to cause infection *in vivo* despite its high-affinity for mannose. These findings may be related to the important observation made by others that FimH conformation is influenced by shear force leading to a "catch bond" model of FimH function [70–72,75,76]. Thus, the ability of FimH to be incorporated into a pilus tip to interconvert into different conformations affects virulence.

The Role of P Pili in Pyelonephritis

The ability of UPEC to ascend from the bladder to the upper urinary tract likely involves many genetic and environmental factors, one of which is thought to be the up-regulation of P pili and corresponding down-regulation of type 1 pili [77]. P pili, which are encoded by the *pap* operon, mediate adhesion of UPEC to kidney tissue resulting in pyelonephritis [61,78–80]. This binding is dependent on the expression of the P pilus tip adhesin, PapG [56,81]. Three alleles of PapG exist (PapG-I, -II, and -III) and each allele shows a distinct affinity for a series of Galα1-4Gal containing glycolipid receptors, which are expressed to various degrees in the kidneys and

ureters of mammals [82]. Human kidneys, for example, abundantly express the ligands for PapG-II, globoside, and thus are colonized with UPEC that express PapG-II alleles. Conversely, PapG-III binds strongly to Forssman glycolipid, which is present in dog but not in human kidneys. Thus, different alleles of PapG mediate host tropisms [83–85].

Identifying Roles for Additional CUP Pilus Types during Disease

A recent analysis of 35 *Escherichia* spp. genomes and 132 plasmids identified a total of 458 CUP pili operons, representing 38 distinct CUP pilus types based on usher phylogeny [86,87]. CUP pili tipped with specific adhesins provides *E. coli* the ability to bind to distinct ligands with stereo-chemical specificity. Single UPEC strains were found to carry as many as 16 distinct, intact CUP pilus systems that likely aid UPEC strains in their colonization of many host niches, including the gut, vagina, urethra, bladder, and kidneys. Thus, it is likely that the retention of many distinct CUP pilus types reflects the adaptation to broad environmental and host niches and their function in facilitating the various tropisms of *E. coli* [88]. Aside from type 1 and P pili, UPEC strains encode a number of additional CUP pilus types for which a role in UPEC pathogenesis is minimally defined or completely undetermined. S pili are known to bind sialosyloligosaccaride residues in host cells and likely mediate infection of the ureters and kidneys [89]. Clinical isolates containing S pili are often associated with more severe outcomes in patients with UTI, including: pyelonephritis, sepsis, and meningitis. The Dr pili adhesin has been shown to bind type IV collagen and decay-accelerating factor (DAF), both of which are expressed in human kidneys. Dr pili enable UPEC colonization of the mouse renal interstitial basement membrane [90,91]. The roles for CUP pili, including F1C, F9, Ygi, Yad, and Auf, have been briefly explored and have been recently reviewed [92–94]. Identifying roles for additional

CUP pilus types will enhance our overall knowledge of UTI pathogenesis and may provide novel drug targets to treat patients with UTI.

Outcomes of UTI: Connecting Findings in Humans and Mice

Much of our understanding of UTI and rUTI pathogenesis comes from studies in mice. The development of murine models of acute and recurrent cystitis have allowed for many important advances in our understanding of UTI pathogenesis. However, it is also worth noting that the UTI mouse models, like all animal models, have limitations. Behavior, genetic, and environment differences between mice and humans make it challenging to translate all murine findings to humans [99]. Here we discuss advances in our understanding of UTI pathogenesis based on experiments performed in relevant mouse models and highlight how these findings have been recapitulated in clinical studies performed in women with UTI or rUTI.

For women with UTI, several disease outcomes are possible, including: asymptomatic bacteruria (ABU), acute self-limiting infection, or chronic/recurrent UTI [5]. Placebo studies in women have shown that approximately 50% of UTIs do not resolve in the absence of effective antibiotic treatment, implying that cystitis is not always self-limiting. These findings highlight the importance of clinical intervention to resolve UTI and the developing crisis of emerging multi-drug resistant uropathogens [95,96]. In naïve mice, there are two major outcomes of UTI: (i) self-limiting acute infection that resolves within days of the initiation of infection with or without the formation of quiescent intracellular reservoirs (QIR); or (ii) persistent, high-titer bacteruria concomitant with high bladder bacterial burden and severe bladder inflammation which, in the absence of antibiotic intervention, can last for the lifetime of the animal and is referred to as chronic cystitis [100] (Figure 1H). The resolution of infection in mice is often

accompanied by QIR formation [97] (Figure 1I). The exfoliation response results in the exposure of the underlying transitional cells, which allows the subsequent invasion of UPEC into these cells. However, unlike superficial facet cells, the underlying transitional cells do not support IBC formation; instead UPEC establish QIRs, which are comprised of 8–12 dormant bacteria in Lamp1+ vesicles [97]. The mechanism of QIR formation is unknown, however, these reservoirs are able to reactivate and release UPEC back into the bladder lumen to initiate a new infection cycle [97,98]. Interestingly, the fate of disease in mice is determined by whether an acute host-pathogen checkpoint, which is influenced by the genetic background of the mice, is triggered. C57BL/6 mice are resistant to chronic cystitis after a single infection; however, they can develop persistent bacteriuria and chronic cystitis when "superinfected", by multiple transurethral inoculations within a 24 hour period [74]. Elevated levels of interleukin-6 (IL-6), keratinocyte cytokine (KC/CXCL1), and granulocyte colony-stimulating factor (G-CSF) in the serum of C57BL/6 mice prior to the second infection predicted the development of chronic cystitis [74]. These same cytokines have been found to precede chronic cystitis in singly infected C3H/HeN mice, which are prone to the development of chronic cystitis [100]. Superinfection of C3H/HeN mice within a six-hour period doubles the proportion of mice that developed chronic cystitis. Intracellular bacterial replication, regulated hemolysin (HlyA) expression, and caspase 1/11 activation were essential for this increase [74]. The chronic bladder inflammation that accompanies chronic cystitis includes lymphonodular hyperplasia in the bladder submucosa and urothelial hyperplasia that results in the loss of superficial facet cells. Similar histological findings have been observed in humans suffering from persistent bacteriuria and rUTI [101,102].

Proteomic analysis of chronically infected bladders indicates that chronic inflammation also results in bladder epithelial remodeling, which may help to explain why mice that experience

chronic cystitis are more susceptible to rUTI upon further bacterial challenge weeks after antibiotic intervention and resolution of the initial infection [67]. Studies of mice with rUTI may also begin to explain why a history of UTI is a major risk factor for rUTI in women, highlighting the clinical relevance of this mouse model. Elevated soluble serum biomarkers that were predictive of rUTI were also detected in young women with UTI [67]. Interestingly, temperance of the neutrophil response during the first 24 hours of infection, by inhibition of cyclooxygenase-2 (COX 2), protected mice from chronic and recurrent cystitis [67]. These findings may help to explain the outcome of a small clinical trial that compared the outcomes of women with UPEC UTI after being given a three-day course of either ciprofloxacin or ibuprofen. The study found no difference in UTI outcome between these two groups at four or seven days post treatment [103]. Another study found that symptomatically treating women suffering from uncomplicated UTI with ibuprofen (without any antibiotics) resolved infection in two-thirds of the study group [104]. These results indicate that ibuprofen, which works by inhibiting COX 1 and 2, may act to decrease the severity of UTI in these patients. However, the second study also found that women in the ibuprofen treated group suffered from more UTI symptoms (abdominal pain, increased frequency of urination, dysuria) and were more likely to develop pyelonephritis [104].

The development of rUTI is likely a balance between bacterial factors and host genetics. Murine studies have indicated that the innate immune response is critical for combating UTI, which had been recapitulated in human clinical studies [105]. Therefore, mutations in the genes involved in this early immune response can greatly influence the susceptibility of a host to UTI. For example, certain polymorphisms and altered expression levels of innate immune genes, like Toll-like receptor 4 (TLR4) and CXCR1, have been associated with less severe symptomatic UTI but an increase in the development of ABU in women [105]. Alterations in the sequence or

expression of other innate immune genes, like IRF3 and CXCR1, have been associated with increased incidences of acute pyelonephritis [105].

Pili are Critical for the Establishment of UPEC and Enterococcus Mediated CAUTI

The introduction of a catheter into the urinary tract provides an additional surface on which bacteria can adhere and establish infection. Uropathogens that are commonly associated with CAUTI, like those belonging to the *Enterococcus* genus, also encode a number of distinct adhesive factors and pili that permit attachment within the host. Of these factors, the endocarditis- and biofilm-associated (Ebp) pilus has recently been identified to play an essential role in the establishment and persistence of UTI in a catheterized mouse model [106–110]. Upon catheterization, implanted catheters are coated with host-derived fibrinogen and are subsequently bound by Ebp expressing *Enterococcus faecalis* (*E. faecalis*), a common enterococcal uropathogen [109]. The Ebp pilus binds fibrinogen via its tip adhesin, EbpA, which contains an N-terminal fibrinogen-binding domain [109]. The mechanism(s) by which fibrinogen enters the bladder is still under investigation but is likely due to bladder damage that occurs during the catheterization process and subsequent infection. Mechanical stress induced by insertion of the catheter into the bladder results in the induction of a robust inflammatory response and severe bladder edema in humans and mice [107,111–113]. Bladder inflammation, including increases in serum cytokines IL-1α and IL-6, and edema, is elevated further upon introduction of *E. faecalis* into the catheterized mouse [107]. Increases in IL-1α and IL-6 have been previously shown to stimulate the release of fibrinogen from the liver into the bloodstream as a part of the pro-inflammatory response and circulating fibrinogen may then leak into the urinary tract via tissue damaged during catheterization. Once in the bladder, fibrinogen is deposited on the catheter,

providing a binding site for EbpA expressing *E. faecalis*. Catheterization and the subsequent inflammatory response are essential in mediating CAUTI, as mice infected with *E. faecalis* in the absence of a catheter are quickly cleared from the bladder [107]. Fibrinogen deposited onto the catheter surface not only enhances *E. faecalis* biofilm formation but also promotes growth, increasing the severity of the infection [109]. The ability to bind and utilize fibrinogen may be a general feature of infection in gram-positive bacteria, (as has been shown for *Staphylococcus aureus* (*S. aureus*), *Staphylococcus epidermidis* (*S. epidermidis*), and Group A streptococci) and potentially in some fungal pathogens (as was recently shown for *Candida albicans*) [114,115]. The Ebp pilus also plays a role in the transition of *E. faecalis* infection from the bladder to the kidneys. In *E. faecalis*, loss of the pilus reduces bacterial colonization of the kidneys and thus lowers the incidence of pyelonephritis in infected mice [110].

UPEC, the leading cause of complicated UTI, can also use CUP pili to colonize the bladder during catheterization [15,116]. However, unlike *Enterococcal* spp., UPEC does not rely on the presence of the catheter to propagate high levels of bacterial colonization. In a CAUTI mouse model, UPEC undergoes the same acute pathogenic lifecycle that is observed in cystitis models, including: invasion into the tissue, IBC formation and maturation, the formation of filaments, and the emergence of filamentous bacteria back into the bladder lumen [116]. However, in the presence of the catheter, UPEC does appear to have a more robust extracellular population during acute infection, which is likely due to UPEC colonization and subsequent biofilm formation on the surface of the catheter [116]. Interestingly, type 1 pili are required for biofilm formation and UPEC colonization of the catheter [116]. These studies continue to define the importance of type 1 pili as a virulence factor during uncomplicated and complicated UTI in mice.

Development of Pili-Based Alternative Treatments to Treat or Prevent UTI and CAUTI

Pili are potential drug targets due to the critical roles they play in UTI and CAUTI pathogenesis. Our understanding of the molecular mechanisms by which pili function and impact disease has permitted the development of novel therapeutics, such as vaccines and small molecule inhibitors, that target pili and block infection by preventing colonization. While a role for pili during intestinal colonization by uropathogens is currently unstudied, identifying and targeting pili that do permit intestinal colonization would provide a unique opportunity to target the source of uropathogens that lead to downstream infections.

Vaccines

A number of promising vaccines that target a wide-range of UPEC virulence factors are currently in development [117–121]. The FimCH vaccine, a subunit vaccine targeting the type 1 pilus adhesin FimH, is one such example. Significant protection was observed in subcutaneously vaccinated mice and cynomolgus monkeys given an intra-muscular vaccination, with the protected animals developing antigen-specific, long-lasting serum IgG antibodies [120,121]. Based on this data, it is presumed that the vaccine works by stimulating these FimH-specific IgG antibodies that block UPEC colonization of the bladder. Consistent with this, the polyclonal antibodies derived from vaccinated mice block FimH function and likely activate immune effector cells, like phagocytes and complement, for clearance of the infection [120,121]. The success of this vaccine in animal models highlights its potential as an alternative treatment to UTI in humans. A FimCH vaccine adjuvanted with PHAD (Avanti Polar Lipids, Alabaster, AL) is currently completing a Phase 1 human study. This study has enrolled about 67 women with and without a history of rUTI (personal communication, Gary Eldridge).

Other CUP pilus types are the focus of additional vaccine candidates. One such candidate is the PapDG subunit vaccine. P pili are strongly associated with pyelonephritis and as such have been designed to target UPEC and prevent complicated upper UTIs [61]. Intraperitoneal administration of the PapDG vaccine protects animals from infection and elicits a specific IgG antibody response in cynomolgus monkeys [118,122]. The Dr fimbriae represents another current vaccine target. Mice vaccinated with purified Dr fimbriae produce high titers of serum antibodies against the fimbriae but do not have lower colonization rates in either the bladder or kidneys [123].

Recent findings revealed an essential role for the Ebp pilus and its adhesin, EbpA, during *E. faecalis* mediated CAUTI in mice. Interestingly, vaccinating mice with EbpA results in significant protection against subsequent *E. faecalis* CAUTI compared to unvaccinated mice or mice vaccinated with other Ebp pilus protein subunits [109). Vaccinating mice with only the N-terminal portion of EbpA, which contains the fibrinogen-binding domain, is also sufficient to protect mice from subsequent infection and may provide a higher level of protection than vaccination with the entire adhesin.

Small Molecular Inhibitors

The importance of the FimH-mannose interaction during infection in mice has prompted studies that test the effects of oral treatment with D-mannose or mannose-analogs on UTI outcome. Oral D-mannose treatment has been shown in studies to work as well as antibiotics to prevent rUTI. One group found that women who received prophylaxis with D-mannose after an initial UTI had similar rates of rUTI as a group that received antibiotic prophylaxis, indicating that D-mannose may be useful to prevent rUTI [124]. Another strategy to prevent UPEC

pathogenesis has been the design of orally active, synthetic, small-molecule inhibitors of CUP pilus assembly or function. One such class of small molecule inhibitors are mannosides. Mannosides are mannose analogs that were rationally designed to bind within the mannose-binding pocket of FimH with a high affinity and thus block pilus binding of FimH to host receptors (Figure 2) [125,126]. Studies in mouse models have demonstrated that mannosides are potent, fast acting and highly efficacious in the treatment of UTI and CAUTI [116,127–129], highlighting their potential as a novel therapeutic strategy for UTI. Mannoside treatment is especially promising as a novel antibiotic sparing therapeutic because they are effective against multi-drug resistant uropathogens [128]. While D-mannose and mannosides both appear to effectively block FimH-mannose interactions, mannosides have approximately a 1,000,000-fold increase in potency for inhibiting FimH, making them promising antibiotic-sparing therapeutics [125,130].

Another class of compounds are pilicides, which are small, rationally designed 2-pyridinones that block pilus assembly (Figure 2) [131,132]. Pilicides block assembly by binding to the pilus chaperone, preventing chaperone-pilus subunit-usher interactions that are fundamental for pilus biogenesis [133]. While pilicides were originally designed to target type 1 pilus assembly, recent studies have found that pilicide treatment disrupts assembly of at least four-CUP pilus types (type 1-, P-, S-, and Dr- pili) as well as flagellar motility [134,135]. The ability of pilicides to target multiple pilus types makes it an extremely valuable treatment option.

Conclusions

Complicated and uncomplicated UTI are extremely common, affecting a large portion of the global population. The high rate of infection and recurrence of UTIs, their monetary cost, their physical burden, and the increasing occurrence of antibiotic resistant uropathogens emphasize

the need for effective treatments to combat the common causative agents of UTI and CAUTI, like UPEC and *Enterococcus* strains. Understanding the molecular mechanisms by which uropathogens are able to cause disease is the first step to identifying novel drug targets. Adhesive pili, like type 1, P, and Ebp, have been shown to play essential roles in UTI pathogenesis in mouse models and provide potential drug targets that may greatly reduce or prevent infection in patients. While the mouse models of uncomplicated UTI and CAUTI have been shown to mimic disease in human patients, the success of vaccine and small molecular inhibitor therapies against these pili in humans is dependent on determining the efficacy of these treatments in clinical trials.

Acknowledgments

We thank Karen Dodson, Ana Flores-Mireles, and Henry Schreiber for critical reading of this manuscript and helpful discussion. This work was supported by the National Institutes of Health and Office of Research on Women's Health Specialized Center of Research (DK64540, DK51406, AI48689, AI29549, AI49950 and AI95542 to Scott J. Hultgren).

Author Contributions

CNS is responsible for the design and content of this review. SJH contributed to the overall organization and content of this work.

Conflicts of Interest

CNS reported no potential conflicts of interest relevant to this article. SJH has intellectual property in the FimH vaccine and ownership interest in Fimbrion Therapeutics, and may benefit if the company is successful in marketing mannosides.

References

1. Nicolle, L.E. Catheter-related urinary tract infection. *Drugs Aging* **2005**, *22*, 627–639.
2. Stamm, W.E.; Norrby S.R. Urinary tract infections: disease panorama and challenges. *J. Infect. Dis.* **2001**, *183*, 1–4.
3. Harding, G.K.; Ronald A.R. The management of urinary tract infections: what we have learned in the past decade. *Int. J. Antimicrob. Agents* **1994**, *4*, 83–88.
4. Foxman, B. The epidemiology of urinary tract infection. *Nat. Rev. Urol.* **2010**, *7*, 653–660.
5. Foxman, B. Urinary tract infection syndromes: Occurrence, recurrence, bacteriology, risk factors, and disease burden. *Infect. Dis. Clin. N. Am.* **2014**, *28*, 1–13.
6. Hooton, T.M. Uncomplicated urinary tract infection. *N. Engl. J. Med.* **2012**, *366*, 1028–1037.
7. Lichtenberger, P.; Hooton, T.M. Complicated urinary tract infections. *Curr. Infect. Dis. Rep.* **2008**, *10*, 499–504.
8. Levison, M.E.; Kaye, D. Treatment of complicated urinary tract infections with an emphasis on drug-resistant gram-negative uropathogens. *Curr. Infect. Dis. Rep.* **2013**, *15*, 109–115.
9. Lo, E.; Nicolle, L.E.; Coffin, S.E.; Gould, C.; Maragakis, L.L.; Meddings, J.; Pegues, D.A.; Pettis, A.M.; Saint, S.; Yokoe, D.S. Strategies to prevent catheter-associated urinary tract

infections in acute care hospitals: 2014 update. *Infect. Control Hosp. Epidemiol.* **2014**, *35*, 32–47.

10. Foxman, B.; Brown, P. Epidemiology of urinary tract infections: Transmission and risk factors, incidence, and costs. *Infect. Dis. Clin. N. Am.* **2003**, *17*, 227–241.
11. Foxman, B. Epidemiology of urinary tract infections: Incidence, morbidity, and economic costs. *Am. J. Med.* **2002**, *113*, 5S–13S.
12. Ikaheimo, R.; Siitonen, A.; Heiskanen, T.; Karkkainen, U.; Kuosmanen, P.; Lipponen, P.; Makela, P.H. Recurrence of urinary tract infection in a primary care setting: Analysis of a 1-year follow-up of 179 women. *Clin. Infect. Dis.* **1996**, *22*, 91–99.
13. Al-Badr, A.; Al-Shaikh, G. Recurrent Urinary Tract Infections Management in Women: A review. *Sultan Qaboos Univ. Med. J.* **2013**, *13*, 359–367.
14. Griebling, T.L. Urinary tract infection in women. In *Urologic Diseases in Americ*a; Litwin, M.S., Saigal, C.S., Eds.; U.S. Government Printing Office: Washington, DC, USA, 2007; pp. 587–620.
15. Flores-Mireles, A.L.; Walker, J.N.; Caparon, M.; Hultgren, S.J. Urinary tract infections: epidemiology, mechanims of infection and treatment options. *Nat. Rev. Microbiol.* **2015**, *13*, 269–284.
16. Chen, S.L.; Wu, M.; Henderson, J.P.; Hooton, T.M.; Hibbing, M.E.; Hultgren, S.J.; Gordon, J.I. Genomic diversity and fitness of *E. coli* strains recovered from the intestinal and urinary tracts of women with recurrent urinary tract infection. *Sci. Transl. Med.* **2013**, doi:10.1126/scitranslmed.3005497.

17. Moreno, E.; Andreu, A.; Pigrau, C.; Kuskowski, M.A.; Johnson, J.R.; Prats, G. Relationship between *Escherichia coli* strains causing acute cystitis in women and the fecal *E. coli* population of the host. *J. Clin. Microbiol.* **2008**, *46*, 2529–2534.
18. Scholes, D.; Hooton, T.M.; Roberts, P.L.; Stapleton, A.E.; Gupta, K.; Stamm, W.E. Risk factors for recurrent urinary tract infection in young women. *J. Infect. Dis.* **2000**, *182*, 1177–1182.
19. Song, J.; Li, B.; Grady, R.; Stapleton, A.; Abraham, S. TLR4-mediated expulsion of bacteria from infected bladder epithelial cells. *Proc. Natl. Acad. Soc. USA* **2009**, *106*, 14966–14971.
20. Busch, A.; Waksman, G. Chaperone-usher pathways: Diversity and pilus assembly mechanism. *Philos. Trans. R. Soc. Lond. B Biol. Sci.* **2012**, *367*, 1112–1122.
21. Holmgren, A.; Brändén, C. Crystal structure of chaperone protein PapD reveals an immunoglobulin fold. *Nature* **1989**, *342*, 248–251.
22. Slonim, L.N.; Pinkner, J.S.; Branden, C.I.; Hultgren, S.J. Interactive surface in the PapD chaperone cleft is conserved in pilus chaperone superfamily and essential in subunit recognition and assembly. *EMBO* **1992**, *11*, 4747–4756.
23. Sauer, F.G.; Futterer, K.; Pinkner, J.S.; Dodson, K.W.; Hultgren, S.J.; Waksman, G. Structural basis of chaperone function and pilus biogenesis. *Science* **1999**, *285*, 1058–1061.
24. Barnhart, M.M.; Pinkner, J.S.; Soto, G.E.; Sauer, F.G.; Langermann, S.; Waksman, G.; Frieden, C.; Hultgren, S.J. PapD-like chaperones provide the missing information for folding of pilin proteins. *Proc. Natl. Acad. Soc. USA* **2000**, *97*, 7709–7714.
25. Geibel, S.; Procko, E.; Hultgren, S.J.; Baker, D.; Waksman, G. Structural and energetic basis of folded-protein transport by the FimD usher. *Nature* **2013**, *496*, 243–246.

26. Phan, G.; Remaut, H.; Wang, T.; Allen, W.J.; Pirker, K.F.; Lebedev, A.; Henderson, N.S.; Geibel, S.; Volkan, E.; Yan, J.; *et al*. Crystal structure of the FimD usher bound to its cognate FimC-FimH substrate. *Nature* **2011**, *474*, 49–53.

27. Remaut, H.; Tang, C.; Henderson, N.S.; Pinkner, J.S.; Wang, T.; Hultgren, S.J.; Thanassi, D.G.; Waksman, G.; Li, H. Fiber formation across the bacterial outer membrane by the chaperone/usher pathway. *Cell* **2008**, *133*, 640–652.

28. Thanassi, D.G.; Stathopoulos, C.; Dodson, K.; Geiger, D.; Hultgren, S.J. Bacterial outer membrane ushers contain distinct targeting and assembly domains for pilus biogenesis. *Bacteriology* **2002**, *184*, 6260–6269.

29. Nishiyama, M.; Vetsch, M.; Puorger, C.; Jelesarov, I.; Glockshuber, R. Identification and characterization of the chaperone-subunit complex-binding domain from the type 1 pilus assembly platform FimD. *Mol. Biol.* **2003**, *330*, 513–525.

30. Volkan, E.; Kalas, V.; Pinkner, J.S.; Dodson, K.W.; Henderson, N.S.; Pham, T.; Waksman, G.; Delcour, A.H.; Thanassi, D.G.; Hultgren, S.J. Molecular basis of usher pore gating in *Escherichia coli* pilus biogenesis. *Proc. Natl. Acad. Soc. USA* **2013**, *110*, 20741–20746.

31. Sauer, F.G.; Pinkner, J.S.; Waksman, G.; Hultgren, S.J. Chaperone priming of pilus subunits facilitates a topological transition that drives fiber formation. *Cell* **2002**, *111*, 543–551.

32. Barnhart, M.M.; Sauer, F.G.; Pinkner, J.S.; Hultgren, S.J. Chaperone-subunit-usher interactions required for donor strand exchange during bacterial pilus assembly. *Bacteriology* **2003**, *1985*, 2723–2730.

33. Remaut, H.; Rose, R.J.; Hannan, T.J.; Hultgren, S.J.; Radford, S.E.; Ashcroft, A.E.; Waksman, G. Donor-strand exchange in chaperone-assisted pilus assembly proceeds through a concerted beta strand displacement mechanism. *Mol. Cell* **2006**, *22*, 831–842.

34. Wu, X.R.; Sun, T.T.; Medina, J.J. *In vitro* binding of type 1-fimbriated *Escherichia coli* to uroplakins Ia and Ib: Relation to urinary tract infections. *Proc. Natl. Acad. Soc. USA* **1996**, *93*, 9630–9635.

35. Sun, T.T.; Zhao, H.; Provet, J.; Aebi, U.; Wu, X.R. Formation of asymmetric unit membrane during urothelial differentiation. *Mol. Biol. Rep.* **1996**, *23*, 3–11.

36. Zhou, G.; Mo, W.J.; Sebbel, P.; Min, G.; Neubert, T.A.; Glockshuber, R.; Wu, X.R.; Sun, T.T.; Kong, X.P. Uroplakin Ia is the urothelial receptor for uropathogenic *Escherichia coli*: Evidence from *in vitro* FimH binding. *J. Cell Sci.* **2001**, *114*, 4095–4103.

37. Hung, C.S.; Bouckaert, J.; Hung, D.; Pinkner, J.; Widberg, C.; De Fusco, A.; Auguste, C.G.; Strouse, B.; Langerman, S.; Waksman, G.; Hultgren, S.J. Structural basis of tropism of Escherichia coli to the bladder during urinary tract infection. *Mol. Microbiol.* **2002**, *44*, 903–915.

38. Eto, D.S.; Jones, T.A.; Sundsbak, J.L.; Mulvey, M.A. Integrin-mediated host cell invasion by type 1-piliated uropathogenic *Escherichia coli*. *PLoS Pathog.* **2007**, *3*, e100.

39. Mulvey, M.A.; Schilling, J.D.; Martinez, J.J.; Hultgren, S.J. Bad bugs and beleagured bladders: Interplay between uropathogenic *Escherichia coli* and innate host defenses. *Proc. Natl. Acad. Soc. USA* **2000**, *97*, 8829–8835.

40. Mulvey, M.A.; Lopez-Boado, Y.S.; Wilson, C.L.; Roth, R.; Parks, W.C.; Heuser, J.; Hultgren, S.J. Induction and Evasion of Host Defenses by Type 1-Piliated Uropathogenic *Escherichia coli*. *Science* **1998**, *282*, 1494–1497.

41. Martinez, J.J.; Mulvey, M.A.; Schilling, J.D.; Pinkner, J.S.; Hultgren, S.J. Type 1 pilus-mediated bacterial invasion of bladder epithelial cells. *EMBO* **2000**, *19*, 2803–2812.

42. Martinez, J.J.; Hultgren, S.J. Requirment of Rho-family GTPases in the invasion of Type-1 piliated uropathogenic *Escherichia coli*. *Cell. Microbiol*. **2002**, *4*, 19–28.

43. Anderson, G.G.; Palermo, J.J.; Schilling, J.D.; Roth, R.; Heuser, J.; Hultgren, S.J. Intracellular bacterial biofilm-like pods in urinary tract infections. *Science* **2003**, *301*, 105–107.

44. Justice, S.S.; Hung, C.; Theriot, J.A.; Fletcher, D.A.; Anderson, G.G.; Footer, M.J.; Hultgren, S.J. Differentiation and developmental pathways of uropathogenic *Escherichia coli* in urinary tract pathogenesis. *Proc. Natl. Acad. Soc. USA* **2004**, *101*, 1333–1338.

45. Hung, C.S.; Dodson, K.W.; Hultgren, S.J. A murine model of urinary tract infection. *Nat. Protoc.* **2009**, *4*, 1230–1243.

46. Wright, K.J.; Seed, P.C.; Hultgren, S.J. Development of intracellular bacterial communities of uropathogenic *Escherichia coli* depends on type 1 pili. *Cell. Microbiol.* **2007**, *9*, 2230–2241.

47. Mulvey, M.A.; Schilling, J.D.; Hultgren, S.J. Establishment of a persistent *Escherichia coli* reservoir during the acute phase of a bladder infection. *Infect. Immun.* **2001**, *69*, 4572–4579.

48. Justice, S.S.; Hunstad, D.A.; Seed, P.C.; Hultgren, S.J. Filamentation by *Escherichia coli* subverts innate defenses during urinary tract infection. *Proc. Natl. Acad. Soc. USA* **2006**, *103*, 19884–19889.

49. Rosen, D.A.; Hooton, T.M.; Stamm, W.E.; Humphrey, P.A.; Hultgren, S.J. Detection of intracellular bacterial communities in human urinary tract infection. *PLoS Med.* **2007**, *4*, e329.

50. Robino, L.; Scavone, P.; Araujo, L.; Algorta, G.; Zunino, P.; Vignoli, R. Detection of intracellular bacterial communities in a child with *Escherichia coli* recurrent urinary tract infections. *Pathog. Dis.* **2013**, *68*, 78–81.

51. Elliott, T.S.; Reed, L.; Slack, R.C.; Bishop, M.C. Bacteriology and ultrastructure of the bladder in patients with urinary tract infections. *J. Infect.* **1985**, *11*, 191–199.

52. Lim, J.K.; Gunther, N.W.; Zhao, H.; Johnson, D.E.; Keay, S.K.; Mobley, H.L. *In vivo* phase variation of *Escherichia coli* type 1 fimbrial genes in women with urinary tract infection. *Infect. Immun.* **1998**, *66*, 3303–3310.

53. Hagan, E.C.; Lloyd, A.L.; Rasko, D.A.; Faerber, G.J.; Mobley, H.L. *Escherichia coli* global gene expression in urine from women with urinary tract infection. *PLoS Pathog.* **2010**, *6*, e1001187.

54. Gunther, N.W.; Lockatell, V.; Johnson, D.E.; Mobley, H.L. *In vivo* dynamics of type 1 fimbria regulation in uropathogenic *Escherichia coli* during experimental urinary tract infection. *Infect. Immun.* **2001**, *69*, 2838–2846.

55. Hultgren, S.J.; Porter, T.N.; Schaeffer, A.J.; Duncan, J.L. Role of type 1 pili and effects of phase variation on lower urinary tract infections produced by *Escherichia coli*. *Infect. Immun.* **1985**, *50*, 370–377.

56. Dodson, K.W.; Pinkner, J.S.; Rose, T.; Magnusson, G.; Hultgren, S.J.; Waksman, G. Structural basis of the interaction of the pyelonephritic *E. coli* adhesin to its human kidney receptor. *Cell* **2001**, *105*, 733–743.

57. Guyer, D.M.; Radulovic, S.; Jones, F.E.; Mobley, H.L. Sat, the secreted autotransporter toxin of uropathogenic *Escherichia coli*, is a vacuolating cytotoxin for bladder and kidney epithelial cells. *Infect. Immun.* **2002**, *70*, 4539–4546.

58. Mills, M.; Meysick, K.C.; O'Brien, A.D. Cytotoxic necrotizing factor type 1 of uropathogenic *Escherichia coli* kills cultured human uroepithelial 5637 cells by an apoptotic mechanism. *Infect. Immun.* **2000**, *68*, 5869–5880.

59. Anderson, G.G.; Goller, C.C.; Justice, S.; Hultgren, S.J.; Seed, P.C. Polysaccharide capsule and sialic acid-mediated regulation promote biofilm-like intracellular bacterial communities during cystitis. *Infect. Immun.* **2010**, *78*, 963–975.

60. Henderson, J.P.; Crowley, J.R.; Pinkner, J.S.; Walker, J.N.; Tsukayama, P.; Stamm, W.E.; Hooton, T.M.; Hultgren, S.J. Quantitative metabolomics reveals an epigenetic blueprint for iron acquisition in uropathogenic *Escherichia coli*. *PLoS Pathog.* **2009**, *5*, e1000305.

61. Lane, M.C.; Mobley, H.L. Role of P-fimbrial-mediated adherence in pyelonephritis and persistence of uropathogenic *Escherichia coli* (UPEC) in the mammalian kidney. *Kidney Int.* **2007**, *72*, 19–25.

62. Klumpp, D.J.; Rycyk, M.T.; Chen, M.C.; Thumbikat, P.; Sengupta, S.; Schaeffer, A.J. Uropathogenic *Escherichia coli* induces extrinsic and intrinsic cascades to initiate urothelial apoptosis. *Infect. Immun.* **2006**, *74*, 5106–5113.

63. Thumbikat, P.; Berry, R.E.; Zhou, G.; Billips, B.; Yaggie, R.; Zaichuk, T.; Sun, T.; Schaeffer, A.J.; Klumpp, D.J. Bacteria-induced uroplakin signaling mediates bladder response to infection. *PLoS Pathog.* **2009**, *5*, e1000415.

64. Hirose, T.; Kumamoto, Y.; Matsukawa, M.; Yokoo, A.; Satoh, T.; Matsuura, A. Study on local immune response in *Escherichia coli*-induced experimental urinary tract infection in mice—Infiltration of Ia-positive cells, macrophages, neutrophils, T cells and B cells. *Jpn. Assoc. Infect. Dis.* **1992**, *66*, 964–973.

65. Hopkins, W.J.; James, L.J.; Balish, E.; Uehling, D.T. Congenital immunodeficiencies in mice increase susceptibility to urinary tract infection. *J. Urol.* **1993**, *149*, 922–925.

66. Godaly, G.; Bergsten, G.; Frendeus, B.; Hang, L.; Hedlund, M.; Karpman, D.; Samuelsson, P.; Svensson, M.; Otto, G.; Wullt, B.; *et al*. Innate defences and resistance to gram negative mucosal infection. *Adv. Exp. Med. Biol.* **2000**, *485*, 9–24.

67. Hannan, T.J.; Roberts, P.L.; Riehl, T.E., van der Post, S.; Binkley, J.M.; Schwartz, D.J.; Miyoshi, H.; Mack, M.; Schwendener, R.A.; Hooton, T.M.; *et al*. Inhibition of Cyclooxygenase-2 Prevents Chronic and Recurrent Cystitis. *EBioMedicine* **2014**, *1*, 46–57.

68. Godaly, G.; Ambite, I.; Svanborg, C. Innate immunity and genetic determinants of urinary tract infection susceptibility. *Curr. Opin. Infect. Dis.* **2015**, *28*, 88–96.

69. Chen, S.L.; Hung, C.S.; Pinkner, J.S.; Walker, J.N.; Cusumano, C.K.; Li, Z.; Bouckaert, J.; Gordon, J.I.; Hultgren, S.J. Positive selection identifies an *in vivo* role for FimH during urinary tract infection in addition to mannose binding. *Proc. Natl. Acad. Soc. USA* **2009**, *106*, 22439–22444.

70. Le Trong, I.; Aprikian, P.; Kidd, B.A.; Forero-Shelton, M.; Tchesnokova, V.; Rajagopal, P.; Rodriguez, V.; Interlandi, G.; Klevit, R.; Vogel, V.; *et al*. Structural basis for mechanical force regulation of the adhesin FimH via finger trap-like beta sheet twisting. *Cell* **2010**, *141*, 645–655.

71. Aprikian, P.; Tchesnokova, V.; Kidd, B.; Yakovenko, O.; Yarov-Yarovoy, V.; Trinchina, E.; Vogel, V.; Thomas, W.; Sokurenko, E. Interdomain interaction in the FimH adhesin of Escherichia coli regulates the affinity to mannose. *J. Biol. Chem*. **2007**, *282*, 23437–23440

72. Aprikian, P.; Interlandi, G.; Kidd, B.; LE Trong, I.; Tchesnokova, V.; Yakovenko, O.; Whitfield, M.J.; Bullitt, E.; Stenkamp, R.E.; Thomas, W.; Sokurenko, E. The bacterial fimbrial tip acts as a mechnical force sensor. *PLoS Biol*. **2011**, 9, e1000617.

73. Schwartz, D.J.; Kalas, V.; Pinkner, J.S.; Chen, S.L.; Spaulding, C.N.; Dodson, K.W.; Hultgren, S.J. Positively selected FimH residues enhance virulence during urinary tract infection by altering FimH conformation. *Proc. Natl. Acad. Soc. USA* **2013**, *110*, 15530–15537.

74. Schwartz, D.J.; Conover, M.S.; Hannan, T.J.; Hultgren, S.J. Uropathogenic *Escherichia coli* superinfection enhances the severity of mouse bladder infection. *PLoS Pathog.* **2015**, *11*, e1004599.

75. Sokurenko, E.V.; Vogel, V.; Thomas, W.E. Catch-bond mechanism of force-enhanced adhesion: Counterintuitive, elusive, but ... widespread? *Cell Host Microbe* **2008**, *4*, 314–323.

76. Rodriquez, V.B.; Kidd, B.A.; Interlandi, G.; Tchesnokova, V.; Sokurenko, E.; Thomas, W.E. Allosteric coupling in the bacteial adhesive protein FimH. *J. Biol. Chem*. **2013**, *288*, 24128–24139.

77. Schaeffer, A.J.; Schwan, W.R.; Hultgren, S.J.; Duncan, J.L. Relationship of type 1 pilus expression in *Escherichia coli* to ascending urinary tract infections in mice. *Infect. Immun.* **1987**, *55*, 373–380.

78. O'Hanley, P.; Low, D.; Romero, I.; Lark, D.; Vosti, K.; Falkow, S.; Schoolnik, G. Gal-Gal binding and hemolysin phenotypes and genotypes associated with uropathogenic *Escherichia coli*. *N. Engl. J. Med.* **1985**, *313*, 414–420.

79. Wullt, B.; Bergsten, G.; Connell. H.; Rullano, P.; Gebretsadik, N.; Hull, R.; Svanborg, C. P fimbriae enhance the early establishment of *Escherichia coli* in the human urinary tract. *Mol. Microbiol.* **2000**, *38*, 456–464.

80. Zhang, J.P.; Normark, S. Induction of gene expression in *Escherichia coli* after pilus-mediated adherence. *Science* **1996**, *273*, 1234–1236.

81. Lund, B.; Lindberg, F.; Marklund, B.I.; Normark, S. The PapG protein is the alpha-D-galactopyranosyl-(1----4)-beta-D-galactopyranose-binding adhesin of uropathogenic *Escherichia coli*. *Proc. Natl. Acad. Soc. USA* **1987**, *84*, 5898–5902.

82. Lanne, B.; Olsson, B.M.; Jovall, P.A.; Angstrum, J.; Linder, H.; Marklund, B.I.; Bergstrum, J.; Karlsson, K.A. Glycoconjugate receptors for P-fimbriated *Escherichia coli* in the mouse. An animal model of urinary tract infection. *J. Biol. Chem.* **1995**, *270*, 9017–9025.

83. Haslam, D.B.; Baenziger, J.U. Expression cloning of Forssman glycolipid synthetase: A novel member of the histo-blood group ABO gene family. *Proc. Natl. Acad. Soc. USA* **1996**, *93*, 10697–106702.

84. Breimer, M.E.; Karlsson, K.A. Chemical and immunological identification of glycolipid-based blood group ABH and Lewis antigens in human kidney. *Biochim. Biophys. Acta* **1983**, *75*, 170–177.

85. Breimer, M.E.; Hansson, G.C.; Leffler, H. The specific glycosphingolipid composition of human ureteral epithelial cells. *J. Biochem.* **1985**, *98*, 1169–1180.

86. Nuccio, S.; Baumler, A.J. Evolution of the chaperone/usher assembly pathway: Fimbrial classification goes Greek. *Microbiol. Mol. Biol. Rev.* **2007**, *71*, 551–575.

87. Wurpel, D.J.; Beatson, S.A.; Totsika, M.; Petty, N.K.; Schembri, M.A. Chaperone-usher fimbriae of *Escherichia coli*. *PLoS ONE* **2013**, *8*, e52835.

88. Lillington, J.; Geibel, S.; Waksman, G. Biogenesis and adhesion of type 1 and P pili. *Biochim. Biophys. Acta* **2014**, *1840*, 2783–2793.

89. Parkkinen, J.; Rogers, G.N.; Korhonen, T.; Dahr, W.; Finne, J. Identification of the O-linked sialyloligosaccharides of glycophorin A as the erythrocyte receptors for S-fimbriated *Escherichia coli*. *Infect. Immun.* **1986**, *54*, 37–42.

90. Nowicki, B.; Selvarangan, R.; Nowicki, S. Family of *Escherichia coli* Dr adhesins: Decay-accelerating factor receptor recognition and invasiveness. *J. Infect. Dis.* **2001**, *183*, 24–27.

91. Goluszko, P.; Popov, V.; Selvarangan, R.; Nowicki, S.; Pham, T.; Nowicki, B.J. Dr fimbriae operon of uropathogenic *Escherichia coli* mediate microtubule-dependent invasion to the HeLa epithelial cell line. *J. Infect. Dise.* **1997**, *176*, 158–167.

92. Spurbeck, R.R.; Stapleton, A.E.; Johnson, J.R.; Walk, S.T.; Hooton, T.M.; Mobley, H.L. Fimbrial Profiles Predict Virulence of Uropathogenic *E. coli* Strains: Contribution of Ygi and Yad Fimbriae. *Infect. Immun.* **2011**. 79, 4753–4763.

93. Wurpel, D.J.; Totsika, M.; Allsopp, L.P.; Hartley-Tassell, L.E.; Day, C.J.; Peters, K.M.; Sarkar, S.; Ulett, G.C.; Yang, J.; Tiralongo, J.; *et al*. F9 fimbriae of uropathogenic *Escherichia coli* are expressed at low temperature and recognise Galbeta1–3GlcNAc-containing glycans. *PLos ONE* **2014**, *9*, e93177.

94. Buckles, E.L.; Bahrani-Mougeot, F.K.; Molina, A.; Lockatell, C.V.; Johnson, D.E.; Drachenberg, C.B.; Burland, V.; Blattner, F.R.; Donnenberg, M.S. Identification and characterization of a novel uropathogenic *Escherichia coli*-associated fimbrial gene cluster. *Infect. Immun.* **2004**, *72*, 3890–3901.

95. Mabeck, C.E. Treatment of uncomplicated urinary tract infection in non-pregnant women. *Postgrad. Med. J.* **1972**, *48*, 69–75.

96. Ferry, S.; Holm, S.; Stenlund, H.; Lundholm, R.; Monsen, T. The natural course of uncomplicated lower urinary tract infection in women illustrated by a randomized placebo controlled study. *Scand. J. Infect. Dis.* **2004**, *36*, 296–301.

97. Mysorekar, I.U.; Hultgren, S.J. Mechanisms of uropathogenic *Escherichia coli* persistence and eradication from the urinary tract. *Proc. Natl. Acad. Soc. USA* **2006**, *103*, 14170–14175.

98. Schilling, J.D.; Hultgren, S.J. Recent advances into the pathogenesis of recurrent urinary tract infections: The bladder as a reservoir for uropathogenic *Escherichia coli*. *Int. J. Antimicrob. Agents* **2002**, *19*, 457–460.

99. Carey A.J.; Tan, C.K.; Ipe, D.S.; Sullivan, M.J.; Cripps, A.W.; Schembri, M.A.; Ulett, G.C. Urinary tract infection of mice to model human disease: practicalities, implications and limitations. *Crit. Rev. Microbiol*. **2015**, doi:10.3109/1040841X.2015.1028885.

100. Hannan, T.J.; Mysorekar, I.U.; Hung, C.S.; Isaacson-Schmid, M.L.; Hultgren, S.J. Early severe inflammatory responses to uropathogenic *E. coli* predispose to chronic and recurrent urinary tract infection. *PLoS Pathog.* **2010**, *6*, e1001042.

101. Schlager, T.A.; LeGallo, R.; Innes, D.; Hendley, J.O.; Peters, C.A. B cell infiltration and lymphonodular hyperplasia in bladder submucosa of patients with persistent bacteriuria and recurrent urinary tract infections. *J. Urol.* **2011**, *186*, 2359–2364.

102. Hansson, S.; Hanson, E.; Hjalmas, K.; Hultengren, M.; Jodal, U.; Olling, S.; Svanborg-Eden, C. Follicular cystitis in girls with untreated asymptomatic or covert bacteriuria. *J. Urol.* **1990**, *143*, 330–332.

103. Bleidorn, J.; Gagyor, I.; Kochen, M.M.; Wegscheider, K.; Hummers-Pradier, E. Symptomatic treatment (ibuprofen) or antibiotics (ciprofloxacin) for uncomplicated urinary tract inections? Results of a randomized contolled pilot trial. *BMC Med.* **2010**, *8*, 30.

104. Gagyor, I,; Bleidorn. J.; Kochen, M.M.; Schmiemann, G.; Wegscheider, K.; Hummers-Pradier, E. Ibuprofen versus fosfomycin for uncomplicated urinary tract infection in women: randomised controlled trial. *Br. Med. J.* **2015**, *351*, h6544.

105. Ragnarsdottir, B.; Lutay, N.; Gronberg-Hernandez, J.; Koves, B.; Svanborg, C. Genetics of innate immunity and UTI susceptibility. *Nat. Rev. Urol*. **2011**, *8*, 449–468.

106. Arias, C.A.; Murray, B.E. The rise of the *Enterococcus*: Beyond vancomycin resistance. *Nat. Rev. Microbiol.* **2012**, *10*, 266–278.

107. Guiton, P.S.; Hung, C.S.; Hancock, L.; Caparon, M.G.; Hultgren, S.J. Enterococcal biofilm formation and virulence in an optimized murine model of foreign body-associated urinary tract infections. *Infect. Immun.* **2010**, *78*, 4166–4175.

108. Nielsen, H.V.; Guiton, P.S.; Kline, K.A.; Port, G.C.; Pinkner, J.S.; Neiers, F.; Normark, S.; Henriques-Normark, B.; Caparon, M.G.; Hultgren, S.J. The metal ion-dependent adhesion site motif of the *Enterococcus* faecalis EbpA pilin mediates pilus function in catheter-associated urinary tract infection. *mBio* **2012**, doi:10.1128/mBio.00177-12.

109. Flores-Mireles, A.L.; Pinkner, J.S.; Caparon, M.G.; Hultgren, S.J. EbpA vaccine antibodies block binding of *Enterococcus* faecalis to fibrinogen to prevent catheter-associated bladder infection in mice. *Sci. Transl. Med.* **2014**, doi:10.1126/scitranslmed.3009384.

110. Singh, K.V.; Nallapareddy, S.R.; Murray, B.E. Importance of the ebp (endocarditis- and biofilm-associated pilus) locus in the pathogenesis of Enteroccous faecalis ascending urinary tract infection. *J. Infect. Dis*. **2007**, *195*, 1671–1677.

111. Goble, N.M.; Clarke, T.; Hammonds, J.C. Histological changes in the urinary bladder secondary to urethral catheterisation. *Br. J. Urol.* **1989**, *63*, 354–357.

112. Glahn, B.E.; Braendstrup, O.; Olesen, H.P. Influence of drainage conditions on mucosal bladder damage by indwelling catheters. II. Histological study. *Scand. J. Urol. Nephrol.* **1988**, *22*, 93–99.

113. Peychl, L.; Zalud, R. Changes in the urinary bladder caused by short-term permanent catheter insertion. *Cas. Lek. Cesk.* **2008**, *147*, 325–329.

114. Flores-Mireles, A.L.; Walker, J.N.; Bauman, T.M.; Potretzke, A.M.; Schreiber, H.L.; Park, A.M.; Pinkner, J.S.; Caparon, M.G.; Hultgren, S.J.; Desai, A. Fibrinogen release and deposition on urinary catheters placed during urologic procedures. *J. Urol.* **2016**, doi: http://dx.doi.org/10.1016/j.juro.2016.01.100.

115. Rivera, J.; Vannakambadi, G.; Hook, M.; Speziale, P. Fibrinogen-binding proteins of Gram-positive bacteria. *Thromb Haemostasis*. **2007**, *98*, 503–511.

116. Guiton, P.S.; Cusumano, C.K.; Kline, K.A.; Dodson, K.W.; Han, Z.; Janetka, J.W.; Henderson, J.P.; Caparon, M.G.; Hultgren, S.J. Combinatorial small-molecule therapy prevents uropathogenic *Escherichia coli* catheter-associated urinary tract infections in mice. *Antimicrob. Agents Chemother.* **2012**, *56*, 4738–4745.

117. Alteri, C.J.; Hagan, E.C.; Sivick, K.E.; Smith, S.N.; Mobley, H.L. Mucosal immunization with iron receptor antigens protects against urinary tract infection. *PLoS Pathog*. **2009**, *5*, e1000586.

118. Roberts, J.A.; Kaack, M.B.; Baskin, G.; Chapman, M.R.; Hunstad, D.A.; Pinkner, J.S.; Hultgren, S.J. Antibody responses and protection from pyelonephritis following vaccination with purified *Escherichia coli* PapDG protein. *J. Urol.* **2004**, *171*, 1682–1685.

119. Billips, B.K.; Yaggie, R.E.; Cashy, J.P.; Schaeffer, A.J.; Klumpp, D.J. A live-attenuated vaccine for the treatment of urinary tract infection by uropathogenic *Escherichia coli*. *J. Infect. Dis.* **2009**, *200*, 263–272.

120. Langermann, S.; Palaszynski, S.; Barnhart, M.; Auguste, G.; Pinkner, J.S.; Burlein, J.; Barren, P.; Koenig, S.; Leath, S.; Jones, C.H.; *et al*. Prevention of Mucosal *Escherichia coli* Infection by FimH-Adhesin-Based Systemic Vaccination. *Science* **1997**, *276*, 607–611.

121. Langermann, S.; Mollby, R.; Burlein, J.E.; Palaszynski, S.R.; Auguste, C.G.; DeFusco, A.; Strouse, R.; Schenerman, M.A.; Hultgren, S.J.; Pinkner, J.S; *et al*. Vaccination with FimH adhesin protects cynomolgus monkeys from colonization and infection by uropathogenic *Escherichia coli*. *J Infect. Dis*. **2000**, *181*, 774–778.

122. Roberts, J.A.; Hardaway, K.; Kaack, B.; Fussell, E.N.; Baskin, G. Prevention of pyelonephritis by immunizaiton with P-fimbriae. *J. Urol*. **1984**, *131*, 602–607.

123. Goluszko, P.; Goluszko, E.; Nowicki, B.; Nowicki, S.; Popov, V.; Wang, H.Q. Vaccination with purified Dr. Fimbriae reduces mortality associated with chronic urinary tract infection due to Escherichia coli bearing Dr. adhesin. *Infect Immun.* **2005**, *73*, 627–631.

124. Kranjcec, B.; Papes, D.; Altarac, S. D-mannose powder for prophylaxis of recurrent urinary tract infections in women: a randomized clinical trial. *World J. Urol.* **2014**, *32*, 79–84.

125. Han, Z.; Pinkner, J.S.; Ford, B.; Obermann, R.; Nolan, W.; Wildman, S.A.; Hobbs, D.; Ellenberger, T.; Cusumano, C.K.; Hultgren, S.J.; *et al*. Structure-based drug design and optimization of mannoside bacterial FimH antagonists. *J. Med. Chem.* **2010**, *53*, 4779–4792.

126. Kleeb, S; Pang, L.; Mayer, K.; Eris, D.; Sigl, A.; Preston, R.C.; Zihlmann, P.; Sharpe, T.; Jakob, R.P.; Abgottspon, D.; Hutter, A.S.; Scharenberg, M.; Jiang, X.; Navarra, G.; Rabbani, S.; Smiesko, M.; Ludin, N.; Bezencon, J.; Schwardt, O.; Maier, T.; Ernst, B. FimH

antagonists: bioisosteres to improve the in vitro and in vivo PK/PD profile. *J. Med. Chem*. **2015**, *58*, 2221–2239.

127. Cusumano, C.K.; Pinkner, J.S.; Han, Z.; Greene, S.A.; Ford, B.A.; Crowley, J.R.; Henderson, J.P.; Janetka, J.W.; Hultgren, S.J. Treatment and prevention of urinary tract infection with orally active FimH inhibitors. *Sci. Transl. Med.* **2011**, *3*, 109–115.
128. Totsika, M.; Kostakioti, M.; Hannan, T.J.; Upton, M.; Beatson, S.A.; Janetka, J.W.; Hultgren, S.J.; Schembri, M.A. A FimH inhibitor prevents acute bladder infection and treats chronic cystitis caused by multidrug-resistant uropathogenic *Escherichia coli* ST131. *J. Infect. Dis.* **2013**, *208*, 921–928.
129. Klein, T.; Abgottspon, D.; Wittwer, M.; Rabbani, S.; Herold, J.; Jiang, X.; Kleeb, S.; Luthi, C.; Scharenberg, M.; Bezenuon, J.; *et al*. FimH antagonists for the oral treatment of urinary tract infections: From design and synthesis to *in vitro* and *in vivo* evaluation. *J. Med. Chem.* **2010**, *53*, 8627–8641.
130. Bouckaert, J.; Berglund, J.; Schembri, M.; De Genst, E.; Cools, L.; Wuhrer, M.; Hung, C.S.; Pinkner, J.; Slattegard, R.; Zavialov, A.; Choudhury, D.; Langermann, S.; Hultgren, S.J.; Wyns, L.; Klemm, P.; Oscarson, S.; Knight, S.D.; De Greve, H. Receptor binding studies disclose a novel class of high-affinity inhibitors of the Escherichia coli FimH adhesin. *Mol. Microbiol*. **2005**, *55*, 441–455.
131. Aberg, V.; Almqvist, F. Pilicides-small molecules targeting bacterial virulence. *Org. Biomol. Chem.* **2007**, *5*, 1827–1834.
132. Aberg, V.; Fallman, E.; Axner, O.; Uhlin, B.E.; Hultgren, S.J.; Almqvist, F. Pilicides regulate pili expression in E. coli without affecting the functional properties of the pilus rod. *Mol. bioSyst.* **2007**, *3*, 214–218.

133. Pinkner, J.S.; Remaut, H.; Buelens, F.; Miller, E.; Aberg, V.; Pemberton, N.; Hedenstrom, M,; Larsson, A.; Seed, P.; Waksman, G.; Hultgren, S.J.; Almqvist, F. Rationally designed small compounds inhibit pilus biogenesis in uropathogenic bacteria. *Proc. Natl. Acad. Soc. USA* **2006**, *103*, 17897–17902.

134. Piatek, R.; Zalewska-Piatek, B.; Dzierzbicka, K.; Makowiec, S.; Pilipczuk, J.; Szemiako, K.; Cyranka-Czaja, A.; Wojciechowski, M. Pilicides inhibit the FGL chaperone/usher assisted biogenesis of the Dr fimbrial polyadhesin from uropathogenic *Escherichia coli*. *BMC Microbiol.* **2013**, doi:10.1186/1471-2180-13-131.

135. Greene, S.E.; Pinkner, J.S.; Chorell, E.; Dodson, K.W.; Shaffer, C.L.; Conover, M.S.; Livny, J.; Hadjifrangiskou, M.; Almqvist, F.; Hultgren, S.J. Pilicide ec240 disrupts virulence circuits in uropathogenic *Escherichia coli*. *mBio.* **2014**, *5*, e02038.

Figures

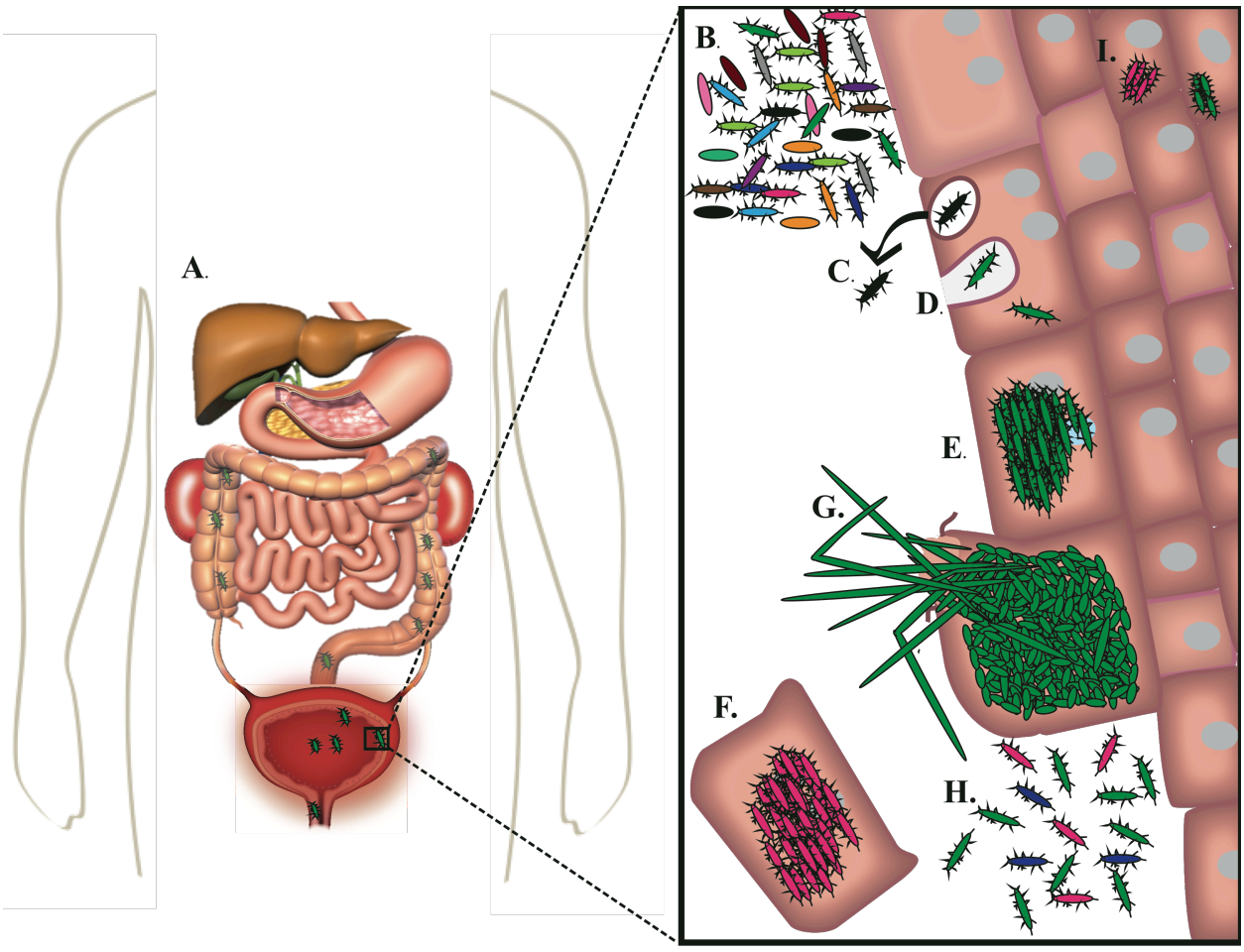

Figure 1. Uropathogenic *E. coli* (UPEC) pathogenic cascade during cystitis. (**A**) UPEC residing in the gut are shed in the feces and colonize the peri-urethral and vaginal areas before ascending into the bladder. Upon accessing the bladder, UPEC adhere to the surface of superficial facet cells that line the bladder lumen in a type 1 pili dependent manner (**B**). Adherent bacteria invade into the facet cells and are either expelled back into the lumen by the cell in a TLR-4 dependent manner [19] (**C**) or escape from the endocytic vesicle into the cytoplasm (**D**). Upon invasion, bacteria replicate in the cytoplasm forming intracellular bacterial communities (IBCs) (**E**). One host mechanism of defense against intracellular UPEC is the shedding of urothelial cells into the urine (**F**), which reduces the overall

number of UPEC in the bladder. During the late stages of IBC formation, filamentous bacteria dissociate from the IBC, burst out of the cell and back into the bladder lumen where they remain or can invade an adjacent facet cell (**G**). There are two potential outcomes of infection: chronic cystitis or resolution of infection. Uncontrolled bacterial replication in the urine occurs in mice that develop chronic cystitis (**H**). In mice that resolve infection, small pockets of bacteria, termed quiescent intracellular reservoirs (QIRs), form and reside in the underlying urothelium and may seed future rUTI (**I**).

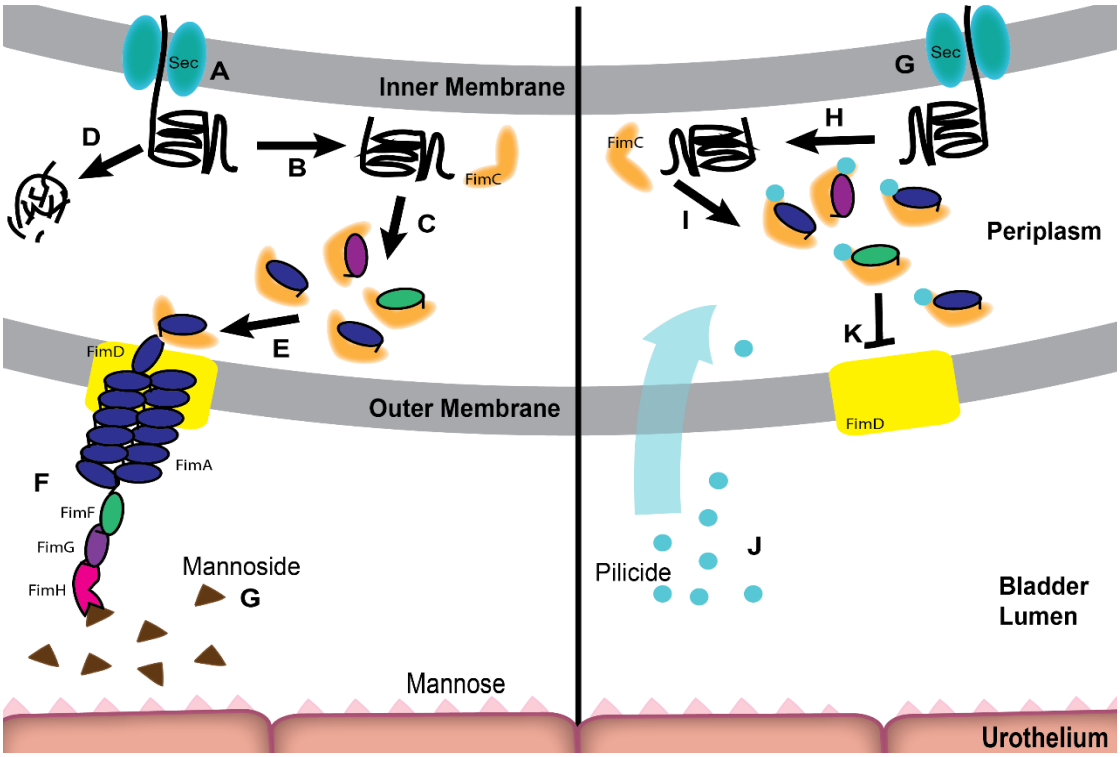

Figure 2. Mannosides and Pilicides prevent *uropathogenic E. coli* (UPEC) urinary tract infections (UTI) by targeting the function or formation of type 1 pili. (**A,G**) Unfolded pilus subunits are secreted to the periplasm by the Sec apparatus. (**B,H**) Upon entering the periplasm, unfolded subunits immediately interact with the cognate chaperone (FimC). Subunits have an incomplete Ig-like fold which must be completed in order to properly fold. In a process called donor strand complementation (DSC) FimC donates its G1 β-stand to the subunit, stabilizing it (**C,I**). Subunits that do not interact with FimC are unable to fold correctly and are degraded (**D**). The chaperone then delivers the subunit to the outer member usher, FimD (**E**). Upon reaching FimD the subunit is assembled into the maturing pilus via donor stand exchange (DSE) with the adjacent pilus subunit (**F**). Mannosides prevent type 1 pilus function by binding, in an irreversible manner, to FimH and therefore prevent the interaction of FimH and mannose on the bladder surface (**G**). Pilicide works by halting pilus

assembly. These molecules enter the periplasm (**J**) and bind to the pilus chaperone, halting assembly (**K**).

Chapter 2: Type 1 and F17-like Pili Promote UPEC Intestinal Colonization

Adapted from:

Selective depletion of uropathogenic *E. coli* from the gut by a FimH antagonist

Caitlin N. Spaulding, Roger D. Klein, Ségolène Ruer, Andrew L. Kau, Henry L. Schreiber IV, Zachary T. Cusumano, Karen W. Dodson, Jerome S. Pinkner, Daved H. Fremont, James W. Janetka, Han Remaut, Jeffrey I. Gordon, Scott J. Hultgren

Nature 2017 Jun 22; 546(7659) 528-532. doi: 10.1038/nature22972.

Abstract

Uropathogenic *E. coli* (UPEC) are responsible for 80% of community-acquired and 65% of nosocomial urinary tract infections (UTI)[1,2], which together affect 150 million people annually[3]. Despite effective antibiotic therapy, 30-50% of patients experience recurrent UTI (rUTI)[3]. In addition, the growing prevalence of UPEC strains resistant to last-line antibiotic treatments like fluoroquinolones, and more recently carbapenems and colistin, make UTIs a prime example of the current antibiotic-resistance crisis and emphasize the dire need to develop new approaches for treatment and prevention of bacterial infections[4,5]. It is widely accepted that

UPEC: i) establish reservoirs in the gut; ii) are shed in the feces; iii) are then able to colonize the peri-urethral area or vagina and subsequently ascend through the urethra to the bladder and/or kidneys, where they cause cystitis and/or pyelonephritis, respectively[6]. Chaperone-usher pathway (CUP) pili such as the mannose-binding type 1 pilus mediate colonization of the bladder, but little is known regarding the mechanisms underlying UPEC persistence in the intestinal tract. Single UPEC isolates can encode up to 16 distinct CUP pilus operons and each pilus type is thought to enable colonization of a microhabitat within a host or the environment[7]. In the present study, we use a mouse model to examine the ability of a human UPEC strain harboring nine different CUP operon mutants to colonize the gut. We found that both F17-like and type 1 pili promote intestinal colonization and show distinct binding to epithelial cells distributed along colonic crypts. Phylogenomic and structural analyses reveal that F17-like pili are closely related to pilus types carried by intestinal pathogens, but are restricted to extra-intestinal pathogenic *E. coli* (ExPEC), and have a distinct ligand specificity.

Main Text

Type 1 and F17-like pili promote UPEC intestinal colonization

To examine the role of CUP pili in colonization of the gut by human UPEC strains, we developed a streptomycin mouse model of UPEC intestinal colonization[8]. We pretreated 6-week old female C3H/HeN and C57BL/6 mice with an oral dose of streptomycin, followed 1 day (d) later by an oral gavage (10^8 CFU) of a well-characterized human cystitis UPEC strain (UTI89) containing engineered chromosomal kanamycin or chloramphenicol antibiotic resistance markers. Sampling of feces collected 1-21 d following oral inoculation, plus surveys along the length of the gut conducted at the time of sacrifice, revealed that stable colonization was

achieved in both mouse backgrounds when they had been pretreated with streptomycin, in contrast to controls that did not receive antibiotic (**Figure 3**).

The UTI89 genome contains 11 distinct CUP operons, 9 of which include all of the genes necessary to assemble a full, functional pilus. To determine if any of the 9 intact CUP operons promote intestinal colonization, C3H/HeN mice were co-colonized with wildtype (WT) UTI89 and one of 9 different mutant strains, each lacking a single CUP operon. Individual deletion of 7 CUP pilus operons *yfc, yeh, yad, pap, sfa, yqi,* and *mat* had no effect on the fitness of UTI89 in the gut compared to the isogenic WT strain **(Figure 4a-g)**. However, deletion of the *fim* or *ucl* pilus operons, which encode type 1 and F17-like pili, respectively, resulted in significant colonization defects (up to 100- and 1000-fold, respectively; **Figure 4h,i)**. Deletion of the gene encoding the type 1 pilus adhesin, *fimH,* mirrored the intestinal defect caused by deletion of the full type 1 pilus operon **(Figure 5a)**. Deletion of both pilus types in a single strain produced a fitness defect greater than either individual deletion alone, suggesting that these two pilus types do not have redundant roles **(Figure 4j,k)**.

F17-like pili do not contribute to UTI in a mouse model of UTI

In a mouse model, type 1-mediated binding to mannose is indispensible for bladder colonization and for invasion of the urothelial cells that line the bladder on its luminal side[1,2]. Once inside urothelial cells, a single bacterium can rapidly divide to form an intracellular bacterial community (IBC) containing 10^4-10^5 organisms[1,2]. Additionally, in mice that spontaneously resolve bacteriuria, small collections of bacteria can remain in quiescent intracellular reservoirs (QIRs) located within transitional bladder cells underlying the urothelium[1,2]. Bacteria from QIRs can serve to seed rUTI[1,2]. Numerous studies have shown

that mutations in *fimH* abolish the ability of UPEC to colonize the bladder, form IBCs and QIRs[1,2,9]. In contrast, we found no role for the F17-like pilus in bladder colonization (**Figure 6)**. Both the WT and UTI89Δ*ucl* strains (i) produced similar numbers of IBCs 6 hours post infection (**Figure 6e**), (ii) had similar CFUs 28 days post infection in the urine, bladder, and kidneys (**Figure 6b,d**) and (iii) were capable of maintaining bladder-associated CFUs after resolution of bacteriuria, suggesting that UTI89 and UTI89Δ*ucl* are similarly capable of forming QIRs (**Figure 6c,d)**. Paradoxically, one study found that genetically engineered *E. coli* strains overexpressing the *ucl* operon *in vitro* bind to desquamated epithelial cells harvested from human urine[10]. It is possible that this paradox is explained by differences between mouse and human bladders or that over-expression of F17-like pili *in vitro* may promote binding to cells from a habitat where the F17-like pilus is not normally expressed *in vivo*. Thus, in contrast to the significant reduction in intestinal colonization seen for both type 1 and F17-like mutants, no role was observed for the F17-like pilus in the rate or severity of bladder infection in individual or concurrent transurethral inoculations of UTI89 and isogenic UTI89Δ*ucl* strains into the bladders of C3H/HeN mice.

Type 1 and F17-like pili bind to distinct micro-habitats in the mouse colon

Type 1 and F17-like operons each encode a two-domain tip adhesin, FimH and UclD, respectively. The N-terminal lectin domain of the adhesin is responsible for recognition and attachment to specific ligands, while the C-terminal pilin domain connects the adhesin to the bulk of the pilus[2]. We cloned and purified the lectin domains of FimH and UclD and tested their ability to bind to sections of mouse colon. Purified FimH lectin domain ($FimH^{LD}$) bound to more differentiated epithelial cells located in the upper portion of crypts and in ‘surface epithelial

cuffs' (the colonic homologs of small intestinal villi) (**Fig. 4l**). FimH binding was prevented by pretreatment of the tissue sections with PNGase, which cleaves N-linked oligosaccharides. This is consistent with known FimH specificity for mannosylated ligands since mannose is a major constituent of N-linked oligosaccharides (**Fig 4l)**. $FimH^{LD}$ also bound to Caco-2 cells (an immortalized human enterocyte-like cell line derived from colorectal carcinoma) and binding was inhibited by both D-mannose and a high affinity mannose-analog (mannoside), M4284[11] **(Figure 5b)**. The UclD lectin domain, $UclD^{LD}$, also bound to colonic epithelial cells in tissue sections. Binding was inhibited by pretreatment of the tissue sections with O-glycosidase, an enzyme that cleaves O-linked oligosaccharides, suggesting that the UclD ligand is contained within an O-glycan **(Fig. 4m)**. Interestingly, $FimH^{LD}$ and $UclD^{LD}$ appeared to bind at distinct locations within the mouse colon; while $FimH^{LD}$ bound to the upper region of the crypts, $UclD^{LD}$ binding was restricted to the lower portion of crypts, suggesting that these pilus types promote colonization of specific niches due to binding of different carbohydrate structures expressed by epithelial cells at different stages of their differentiation **(Fig 4l-m).**

F17-like pili are closely related to pilus types used for intestinal colonization and pathogenesis

CUP pili are highly conserved throughout Proteobacteria and are assembled by dedicated chaperone-usher assembly machines encoded by each respective CUP operon along with the various subunit types comprising the pilus fiber[2,7]. The sequence identity between usher genes of distinct CUP pilus types is greater than the identity of genes that encode other CUP pilus proteins and thus can be compared to elucidate the evolutionary relationship of CUP pili amongst all proteobacterial strains[7,12]. Using this type of usher analysis, six large clades of pili have been

described. The γ clade, which is the largest, has been divided into subclades, including the γ_1 subclade containing the *fim* operon of *E. coli*, *Klebsiella,* and *Salmonella* and the γ_4 clade containing the *ucl* operon[7,12]. To examine the evolutionary origin of F17-like pili, we performed a homology search of a database of γ-Proteobacterial genomes and found that the UTI89 F17-like usher gene sequence (*uclC*) shared highest identity with other *E. coli uclC* sequences and with orthologous usher sequences of *P. mirabilis,* a bacterium that can colonize the gut*,* and *S. enterica,* an intestinal pathogen (**Table 1**). The *uclC* usher gene was also closely related to the gene encoding the F17 pilus usher (thus the derivation of the name, F17-like), as well as two ushers for uncharacterized pilus types, *pVir99* and *ECs1278* (**Table 1**). A phylogenetic analysis showed clustering of these *E. coli* and *Proteus* species' ushers into a distinct sub-branch within the broader F17 group usher phylogeny, suggesting that they share a common ancestor (**Figure 7**). *E. coli* are categorized into six distinct groups or clades of genetically related strains (clades A-E)[10,13]. F17-like pili are encoded by genes present in only 10% of all *E. coli* strains; these strains are almost exclusively in the B2 clade that harbors the majority of extraintestinal pathogenic *E. coli* (ExPEC)[10]. In contrast, F17 and ECs1278 pilus operons are found in the intestinal pathogens, enterotoxigenic *E. coli* (ETEC) and enterohemorrhagic *E. coli* (EHEC), respectively, which are specific to clades E, B1, and occasionally A[14,15]. These findings suggest that UPEC strains in clade B2 may have acquired the *ucl* operon from a different species and retained this factor to facilitate its residency in the gut. A number of genetic variants of the *E. coli* F17 adhesin, F17G, have evolved that bind different ligand variants, all containing a core N-acetylglucosamine (GlcNAc) moiety[16]. No binding of $UclD^{LD}$ was observed to GlcNAc, either with the Center for Functional Glycomics glycan array or via differential scanning fluorimetry, indicating that the F17-like pilus binds a ligand distinct from that of the F17 pilus (**Fig. 4n**).

Interestingly, although the amino acid sequence of the full length UclD adhesin has diverged from that of the F17 adhesin F17G, it is virtually invariant across all strains encoding it (>99%), suggesting that there is a single, distinct ligand for UclD adhesins[10].

Structural analysis of the F17-like adhesin, UclD

To examine the distribution of F17-like pili specifically in UTI isolates, a comparative genomic analysis was performed on 43 strains isolated from a cohort of 14 women at the time of initial presentation with acute UTI, or during subsequent recurrent UTIs[17]. Fourteen of the rUTI events were caused by B2 strains, which encompass the majority of *E. coli* strains that cause UTI[10,13]. Of these 14 strains, 13 encoded F17-like pili (~93%) **(Figure 8)**. In contrast, F17-like pili have been found in less than 50% of all B2 strains[10] (*E. coli* reference collection (ECOR)). We concluded that F17-like pili are enriched in B2 isolates associated with rUTI episodes in women from this cohort. This data, along with our findings that F17-like pili promote UPEC intestinal colonization, suggest that F17-like pili might be associated with UPEC persistence in women with rUTI due to their ability to promote maintenance of a UPEC intestinal reservoir.

To better understand the role of the F17-like pilus in gut colonization, we solved two high resolution X-ray crystal structures of $UclD^{LD}$. Overlay of the structures in the $P2_1$ (green) and $P2_12_12_1$ (gray) space groups resolved to 1.05 Å and 1.6 Å, respectively **(Table S2)** reveals they are nearly identical (**Figure 9a-1)**. These structures show that nine β-strands within $UclD^{LD}$ coalesce to form an elongated β-barrel structure. Seven additional β-strands, one α-helix and two short 3/10 helices, that are located within inter-strand loops, comprise the remainder of the protein (**Figure 9a-1)**. Comparison of the $P2_1$ $UclD^{LD}$ structure with the previously solved lectin domain structure of an F17 adhesin, $F17G^{LD}$ (**Figure 9a-2**), (PDB 1OIO[18]) indicates that, despite

a sequence identity of only 25%, the overall secondary structure characteristics are remarkably conserved between these two pilus types as seen when the structures are overlayed **(Figure 9a-3**). Nevertheless, a structural alignment of the two lectin domains reveals two large insertions in UclD relative to the F17G sequence (**Figure 9b;** highlighted in orange and yellow). The first insertion is an elongation of the loop located between strands 4 and 5 and is highlighted in orange in **Figure 9b**,**c**. The second insertion is located between strands 8 and 9 (highlighted in yellow in **Figure 9b**,**c**), and contains a short 3/10 helix. Previous studies have demonstrated that the GlcNAc receptor binding site for the F17G adhesin is located on the side of the lectin domain (**Figure 9a,d)**[16]. Comparison of the $UclD^{LD}$ and $F17G^{LD}$ structures suggests the presence of a transverse binding site along the surface of $UclD^{LD}$ located in a similar position to the GlcNAc binding site on F17G (**Figure 9a,d**). This binding site, highlighted in purple in **Figure 9c** and by purple residues and stars in **Figure 9b** is directly adjacent to the helix-containing insertion located between strands 8 and 9 (colored yellow in **Figure 9b,c**), and located slightly above the elongated loop between strands 4 and 5 (colored orange in **Figure 9b,c**). The proximity of the putative binding pocket to both insertions suggests that these regions may be involved in creating UclD's unique receptor binding specificity.

The proposed UclD binding pocket is comprised of residues found in the loops connecting strands 6 and 7, strands 8 and 9, and within strands 2b and 9. Six key residues (Q43, W103, D119, N131, T134, and S136) within this pocket are denoted with stars in **Figure 9b** and shown as sticks in **Figure 9d**). The corresponding residues in the F17G binding site are chemically distinct from their UclD counterparts, (**Figure 9b,d**) providing further evidence to support our observation that UclD does not share a molecular ligand with F17G.

Comparison of residue positioning and electrostatic surface potential of the putative binding site between both $UclD^{LD}$ structures suggests that W103 may play a key role in the coordination of a sugar residue within the binding pocket, as tryptophan residues have an established role in aromatic-sugar stacking interactions in bacterial carbohydrate binding proteins[19]. In the $P2_1$ space group, W103 is positioned adjacent to a putative binding pocket that is 11 Å wide and 7 Å deep. In contrast, the $P2_12_12_1$ structure shows well-resolved density indicating that the W103 side chain is flipped approximately 120 degrees, partially occluding the proposed binding pocket (**Figure 9d**). These differences may arise from differences in crystal packing, but may also indicate flexibility in the W103 residue that may play a regulatory role in ligand binding.

Conclusions

Identifying the role of novel UPEC virulence factors, like type 1 and F17-like pili in gut colonization, revealed new mechanisms of UPEC association with its host. Specifically, identification of the role of F17-like pili in intestinal colonization and its relatedness to homologs in other bacteria that inhabit the gut provides new insights into a previously uncharacterized CUP pilus type. Further examination of the ligands and micro-evolution of this pilus type is needed to dissect the specifics of its role in gut colonization. In addition, identification of genes involved in UPEC colonization of the gut may also provide a method by which UTI patients could be stratified for epidemiologic studies of disease recurrence risk as well as for proof of concept clinical studies of the efficacy of CUP-directed treatment regimens.

Acknowledgments

We thank: Ashlee Earl, Abigail Manson for assistance in acquiring genomic data, Jay Nix and Molecular Biology Consortium (Beamline 4.2.2) for collection/processing crystallographic data, Lars Vereecke and Amanda Goncalves at VIB Bio Imaging Core for support with tissue sectioning/microscopy, Zhenfu Han for synthesizing M4284, Kevin Tamadonfar for assistance with tissue binding studies, and Magdalena Lukaszczyk with protein production. This work was supported by grants from the NIH [K08AI113184 (ALK), R01AI048689 (SJH), P50DK064540 (SJH), RC1DK086378 (SJH), R01DK051406 (SJH), DK30292 (JIG) and 1F31DK107057 (CNS)], FWO-Flanders (G030411N), Hercules Foundation (UABR/09/005) and VIB PRJ9.

Materials and Methods

Ethics statement

The Washington University Animal Studies Committee approved all procedures used for the mouse experiments described in the present study. Overall care of the animals was consistent with *The Guide for the Care and Use of Laboratory Animals* from the National Research Council and the USDA *Animal Care Resource Guide*. For collection of colonic tissues for adhesion binding studies, mice were sacrificed according to institutional, national and European animal regulations, using protocols that were also approved by the animal ethics committee of Ghent University.

Bacterial strains

CUP operon and adhesin deletions in UTI89 were engineered by replacing the gene(s) of interest with antibiotic-resistance markers using the λ Red Recombinase system[20]. Earlier reports

described WT UTI89 and its isogenic *fim* and *fimH* mutants[21,22] as well as EC958[23], 41.4p[24] and CFT073[25].

Colonization of mice with UPEC strains

6-week old female C3H/HeN mice were obtained from Envigo or Charles Rivers Labs (CRL). 6-week old female C57BL/6 mice were also obtained from Envigo. Animals were maintained in a single room in our vivarium for no more than 2 days prior to treatment. Prior to and after treatment all animals received PicoLab Rodent Diet 20 (Purina) *ad libitum*. All animals were maintained under a strict light cycle (lights on at 0600h, off at 1800h). For competitive infections, if a phenotype was observed after testing five mice (1 biological replicate), the experiment was repeated 1-2 times (total of n=10-16 mice, 2-3 biological replicates). For 16S rRNA analyses, 4-5 mice were examined (1 biological replicate). For all other experiments, 9-16 mice were tested and the experiment was repeated 2-3 times (2-3 biological replicates). Exclusion criteria for mice were pre-established; (i) both introduced strains in competitive infections became undetectable during the course of a 14 day experiment, and (ii) mice died or lost > 20% of their body weight. No mice in this study met these criteria. Mice were acquired from indicated vendors and randomly placed into cages (n=5 mice/cage) by employees of Washington University's Division of Comparative Medicine (DCM); no additional methods for randomization were used to determine how animals were allocated to experimental groups. Investigators were not blinded to group allocation during experiments.

Animals received a single dose of streptomycin (1000mg/kg in 100 µL water by oral gavage (PO)) followed 24 h later by an oral gavage of ~10^8 CFU UPEC in 100 µl phosphate-buffered saline (PBS). Bladder infections were performed via transurethral inoculation[26]. UPEC

strains were prepared for inoculation as described previously[26]. Briefly, a single UTI89 colony was inoculated in 20 mL of Luria Broth (LB) and incubated at 37°C under static conditions for 24 h. Bacteria were then diluted (1:1000) into fresh LB and incubated at 37°C under static conditions for 18-24 h. Bacteria were subsequently washed three times with PBS and then concentrated to ~$1x10^8$ CFU per 100 μL for intestinal infections and ~$1x10^8$ CFU per 50 μL for bladder infections.

In all cases, fecal and urine samples were collected directly from each animal at the indicated time points. Fecal samples were immediately weighed and homogenized in 1 mL PBS. Urine samples were immediately diluted 1:10 prior to plating. Mice were sacrificed via cervical dislocation under isofluorane anesthesia and their organs were removed and processed under aseptic conditions. Intestinal segments (cecum and colon) were weighed prior to homogenization and plating on LB supplemented with the appropriate antibiotic.

Enumeration of bladder intracellular bacterial communities (IBCs)

6 week old C3H/HeN mice were given a single oral dose of either M4284 (100mg/kg) or vehicle control (10% cyclodextrin) 30 min before transurethral inoculation with UTI89. To accurately count the number of IBCs, mice were sacrificed 6 hours after infection. Bladders were removed aseptically, bi-sected, splayed on silicone plates and fixed in 4% (v/v) paraformaldehyde. IBCs, readily discernable as punctate violet spots, were quantified by LacZ staining of bladder wholemounts[27,28].

Immunofluorescence Studies

The protocols used for immunohistochemical analysis are based on a previous study[29].

Following sacrifice of 6 week old, female C57BL/6 mice (supplied by VIB-Ghent University breeding program, Belgium), segments of colon were fixed in methanol-Carnoy for a minimum of 3 hours at room temperature. The fixed tissues were then embedded in paraffin and 4-μm-thick sections were cut and placed on glass slides. Slides were de-paraffinized and re-hydrated by incubating them in xylene, isopropanol, 100% ethanol and finally 70% ethanol (each step involving a 3 min incubation in the reagent followed by another 3 min incubation in fresh reagent). Slides were subsequently rinsed in tap water and PBS, placed in blocking buffer (5% fecal calf serum prepared in PBS) at room temperature for 30 min, and then incubated with rabbit polyclonal antibodies to Muc2 [1/2000; Mucin 2 (H-300), Santa Cruz Biotechnology] for 2 h. After three washes with PBS, slides were incubated with a goat anti-rabbit Dylight-488 labeled secondary antibody (1/1000 dilution, ThermoFisher Cat No. 35553) in blocking buffer for 1 h at room temperature. Slides were washed three times with PBS before counterstaining with bis-benzimide (Hoechst dye) (1/1000 in PBS) for 10 min at room temperature. Finally, slides were incubated with $FimH^{LD}$ or $UclD^{LD}$ ($P2_1$) protein, labeled with NHS 650nm Dylight, in blocking buffer at 4°C overnight. Prior to staining, sections were treated with O-glycosidase (NEB) or PNGaseF (SIGMA) at 37°C using buffers and protocols supplied by manufacturer . Slides were washed subsequently with PBS before treatment with fluoro mounting medium (n-propyl gallate in glycerol) and viewing under a confocal microscope (Leica Microsystems LAS-AF-TCS SP5) using a 20x125 objective.

Carriage of F17-like pili

We examined 43 available UPEC isolates (**Table 2**). These isolates originated from a clinical study of 14 women who experienced at least two episodes of UTI (an initial UTI and one or

more rUTI) during the 90 day study window[17]. The isolates used in this work were sequenced in a previous study[24] (Bioproject ID: PRJNA269984) and include (i) 14 isolates collected at enrollment, (ii) 18 isolates collected during rUTI (10 women experienced a single rUTI while four women experienced two rUTI events), and (iii) 11 isolates collected in the days leading up to an rUTI.

The distribution of the F17-like operon in these clinical *E. coli* isolates was determined using BLAST and the F17-like operon from UTI89 as the query sequence. A "hit" was considered as any genome sequence that matched the entire length of the query sequence with >75% identity. As a control to prevent false negatives in the BLAST search of draft genomes, DNA sequencing reads from each clinical UPEC isolate were mapped against a reference sequence constructed by concatenating all the *ucl* genes with 100 N's separators using Geneious v6.1.7[30].

Phylogenetic Analyses and Sequence Alignments

Amino acid alignments of full-length UTI89 UclD, *P. mirabilis* UcaD, *S. enterica* UclH, and ETEC F17G were conducted using the MAFFT L-INS-i iterative refinement method and the default BLOSUM62 scoring matrix (**Table 1**)[31]. MAFFT collected up to 100 homologs with E values of less than 1e-10 to each sequence from the SwissProt database to improve alignment accuracy. Homologs are automatically removed from the final alignment. The alignment was visualized using Geneious[30]. A homology search of the coding sequence database of the European Nucleotide Archive (ENA) was conducted using the Basic Local Alignment Search Tool (BLAST)[32] using the UTI89 *uclC* (ENA accession: ABE10308) and EDL933 *ECs1278* (ENA accession: AIG67653) as queries. Sequences that matched either gene sequence with

>50% identity were downloaded and then filtered to remove partial hits (<80% length of query sequence) and sequences with nonsense mutations, which resulted in a total of 659 sequences (**Supplementary table 1**). Duplicate sequences were then removed, resulting in a list of 122 unique, representative sequences. These sequences were then aligned with the UTI89 *fimD* usher sequence (ENA accession: ABE10417) as an outgroup using the MAFFT MAFFT L-INS-i alignment method and the 200PAM scoring matrix[31]: The phylogenetic relationship between gene sequences was then estimated using RAxML v8.1.3 with the GTRCAT model and supported with 1000 bootstrap replicates; the tree was visualized using the tool interactive Tree of Life (iTOL) v3[33].

Enzyme-linked immunosorbent assay (ELISA) targeting FimH

Caco-2 cells (ATCC Number HTB-37) were cultured in minimum essential medium (MEM) supplemented with 20% fetal bovine serum (FBS). Cell cultures tested negative for mycoplasma. Cells were split into 48-well plates, grown to 100% confluence and then fixed with paraformeldahyde for 15 min followed by treatment with blocking buffer (1x PBS containing 2% BSA) for 2h. A truncated FimH, corresponding to residues 1-178 of the mature FimH adhesin ($FimH^{LD}$), expressed in *E. coli* and purified as described previously[34], was serially diluted in blocking buffer and incubated with the fixed CaCo-2 cells for 1h at room temperature. To test the effect of D-mannose or M4284 on FimH binding, 0.2 mg/mL $FimH^{LD}$ was pre-incubated for 5 min in the presence or absence of 1 mM D-mannose (Sigma-Aldrich) or 1mM M4828 (in 20 mM Tris pH 8.0 or 20 mM Tris plus water or 10% cyclodextrin, respectively) before serial dilution and incubation. Wells were washed four times with PBS/0.05% Tween 20 (PBST) prior to incubation with a polyclonal rabbit anti-T3 antibody against $FimH^{LD}$ (generated against FimH

residues 1-165; ref. 39) for one hour at room temperature. Following another series of four washes, secondary antibody (goat anti-rabbit Ig conjugated to horse radish peroxidase; ThermoFisher, Catalog Number 32460) was incubated with the cells for 1 h at room temperature (24^{o}C) before washing in PBST. Plates were developed with the BD OptEIA TMB substrate reagent kit for 5 min at room temperature (24^{o}C) before quenching with 1 M H_2SO_4. Binding was assessed by measuring the absorbance at 450 nM on a TECAN infinite 2 PRO plate reader. Wells lacking protein were used as control. All conditions were examined in quadruplicate.

F17-Like Constructs and Purification

For the $P2_1$ $UclD^{LD}$ construct, the first 197 amino acids of the mature UclD adhesin protein were cloned into pDEST14 using Gateway® technology (Invitrogen), resulting in plasmid $pUclD^{AD}$. Expression was induced with 1mM IPTG. Periplasmic extracts were prepared by resuspending bacterial pellets in 20mM Tris/20% sucrose (pH 8) (4 ml/per gram of pellet). Subsequently, 40µl of 0.5M EDTA and 10mg/ml lysozyme were added per gram of pellet and the suspension was incubated on ice for 30 min. This step was followed by addition of 40 µl of 2.5M $MgCl_2$ per gram of cell pellet and incubation on ice for 5 min. Cells were spun at 15,000 x g and the supernatant was saved as the periplasmic extract. The extract containing the UclD lectin domain was dialyzed against 20mM HEPES pH 7, passed over a SP FF cation exchange column (GE) and bound material eluted with 20mM HEPES pH7/ 1M NaCl. Pooled fractions containing UclD lectin domain were then applied to a Phenyl Hi Trap column (GE) after addition of 1M ammonium sulfate. Elution was performed using 20mM HEPES pH 7.

To generate purified $UclD^{LD}$ for the $P2_12_12_1$ space group, DNA from the UTI89 *uclD* gene encoding the N-terminal 217 amino acids of the protein were cloned into pTRC99a with a

C-terminal 6-His tag. This construct was expressed in the periplasm of *E. coli* DL41(DE3), a methionine auxotroph strain suitable for expression of native or selenomethionine-labeled protein. Periplasmic extracts were first dialyzed against PBS supplemented with 250 mM NaCl, then bound to a Cobalt (Goldbio) column; bound proteins were eluted with PBS containing 250 mM NaCl, and 250 mM imidazole. Pooled fractions were dialyzed into 20 mM MES (pH 5.8), bound to an HR16/10 Mono S cation exchange column (GE Healthcare), and eluted with 300 mM NaCl. Following cleavage of the periplasmic localization sequence, the mature form of $UclD^{LD}$-6xHis contained 203 amino acids.

Selenomethionine-labeled protein was purified using the same protocol, but all buffers were supplemented with 2 mM β-mercaptoethanol and 1 mM EDTA to prevent oxidation. EDTA was omitted from the periplasmic dialysis buffer to prevent chelation of immobilized cobalt.

Crystallization and Structure Determination

For the $P2_1$ $UclD^{LD}$ structure solved in the $P2_1$ space group, $UclD^{LD}$ (15mg/ml) was crystallized using sitting drop vapor diffusion against a solution containing 16% PEG 4000, 0.1M Tris HCl pH 8.5, 0.2M magnesium chloride. UclD crystals were flash cooled to 100^{o}K in a solution containing 16% PEG 4000, 0.1M Tris HCl pH 8.5, 0.2M magnesium chloride and 30% glycerol. Data were collected at beamline ID29 (ESRF, Grenoble, France) to 1.05 Å resolution. Data were indexed and processed with XDS[35], scaled and merged using SCALA in the CCP4 suite[36]. Data and refinement statistics can be found in **Table 3**.

For the $UclD^{LD}$ structure solved in the $P2_12_12_1$ space group, $UclD^{LD}$ (10 mg/ml 10 mM MES 5.8) was crystallized by the hanging drop vapor diffusion method against a well solution

containing 0.1 M potassium phosphate (monobasic), 0.2 M potassium iodide and 20% PEG 3350. One microliter of the protein solution was mixed with 1 μL well solution and incubated at 18 °C. Crystals were harvested and transferred to a solution containing 0.1 M KH_2PO_4, 0.2 M KI and 20% PEG 3350 supplemented with 20% glycerol before being flash-frozen in a bath of liquid N_2. Data were collected at beamline 4.2.2 (ALS Berkeley) to 1.6 Å resolution. Data were indexed and processed with XDS[35], scaled and merged AIMLESS in the CCP4 suite[36] and phased with the Single anomalous dispersion (SAD) method using phenix.autosol, and refined with phenix.refine[37]. Data and refinement statistics can be found in **Table 3**. RMSD values were calculating using the DALI server[38]. Structural alignments were performed in Promal's 3D using the default settings. Secondary structure assignments for $UclD^{LD}$ were completed using DSSP.

Differential Scanning Fluorimetry

Purified $UclD^{LD}$ (1.4 mg/well) was incubated with 5x Sypro orange fluorescent dye in 20 mM Tris (pH 8.0) with or without 10 mM monosaccharide in a total volume of 70 μL. Samples were heated from 20 °C to 100 °C in 30-second/0.5 °C increments using a Bio-rad C1000 thermocycler with CFX96 RT-PCR attachment. The reported melting temperatures were determined by the inflection point of the sigmoidal graph.

Data Availability

Sequences used to examine the carriage of F17-like pili in clinical rUTI isolates were previously published[24] and are deposited in the NCBI under the Bioproject ID: PRJNA269984. Crystallography data have been deposited in the PDB under accession codes: 5NWP ($P2_1$) and 5VQ5 ($P2_12_12_1$).

Statistical Analysis

The statistical significance of differences between groups in experiments (excluding competitive infections) was determined by a Mann Whitney U test. Competitive Index (CI) was defined as (CFU output strain A/CFU output strain B)/(CFU input strain A/CFU input strain B). For competitive infections, statistical significance was determined by a Wilcoxon Signed Ranked test. Statistical analyses were performed using Graphpad Prism 7.

References

1 Flores-Mireles, A. L., Walker, J. N., Caparon, M. & Hultgren, S. J. Urinary tract infections: epidemiology, mechanisms of infection and treatment options. *Nature Reviews Microbiology* **13**, 269-284, doi:10.1038/nrmicro3432 (2015).

2 Spaulding, C. N. & Hultgren, S. J. Adhesive Pili in UTI Pathogenesis and Drug Development. *Pathogens* **5**, doi:10.3390/pathogens5010030 (2016).

3 Foxman, B. Urinary tract infection syndromes: occurrence, recurrence, bacteriology, risk factors, and disease burden. *Infect Dis Clin North Am* **28**, 1-13, doi:10.1016/j.idc.2013.09.003 (2014).

4 Zowawi, H. M. *et al.* The emerging threat of multidrug-resistant Gram-negative bacteria in urology. *Nature Reviews Urology* **12**, 570-584, doi:10.1038/nrurol.2015.199 (2015).

5 Mediavilla, J. R. *et al.* Colistin- and Carbapenem-Resistant Escherichia coli Harboring mcr-1 and blaNDM-5, Causing a Complicated Urinary Tract Infection in a Patient from the United States. *mBio* **7**, doi:10.1128/mBio.01191-16 (2016).

6 Yamamoto, S. *et al.* Genetic evidence supporting the fecal-perineal-urethral hypothesis in cystitis caused by Escherichia coli. *J Urology* **157**, 1127-1129 (1997).

7 Wurpel, D. J., Beatson, S. A., Totsika, M., Petty, N. K. & Schembri, M. A. Chaperone-usher fimbriae of Escherichia coli. *PloS One* **8**, e52835, doi:10.1371/journal.pone.0052835 (2013).

8 Kaiser, P., Diard, M., Stecher, B. & Hardt, W. D. The streptomycin mouse model for Salmonella diarrhea: functional analysis of the microbiota, the pathogen's virulence factors, and the host's mucosal immune response. *Immunological Reviews* **245**, 56-83, doi:10.1111/j.1600-065X.2011.01070.x (2012).

9 Wright, K. J., Seed, P. C. & Hultgren, S. J. Development of intracellular bacterial communities of uropathogenic Escherichia coli depends on type 1 pili. *Cellular Microbiology* **9**, 2230-2241, doi:10.1111/j.1462-5822.2007.00952.x (2007).

10 Wurpel, D. J. *et al.* Comparative proteomics of uropathogenic Escherichia coli during growth in human urine identify UCA-like (UCL) fimbriae as an adherence factor involved in biofilm formation and binding to uroepithelial cells. *J Proteomics* **131**, 177-189, doi:10.1016/j.jprot.2015.11.001 (2016).

11 Jarvis, C. *et al.* Antivirulence Isoquinolone Mannosides: Optimization of the Biaryl Aglycone for FimH Lectin Binding Affinity and Efficacy in the Treatment of Chronic UTI. *ChemMedChem* **11**, 367-373, doi:10.1002/cmdc.201600006 (2016).

12 Nuccio, S. & B√§umler, A. J. Evolution of the chaperone/usher assembly pathway: fimbrial classification goes Greek. *Microbiol Molec Biology Reviews* **71**, 551-575 (2007).

13 Zhang, L., Foxman, B. & Marrs, C. Both urinary and rectal Escherichia coli isolates are dominated by strains of phylogenetic group B2. *J Clinical Microbiology* **40**, 3951-3955 (2002).

14 Richards, V. P. *et al.* Genome based phylogeny and comparative genomic analysis of intra-mammary pathogenic Escherichia coli. *PloS One* **10**, e0119799, doi:10.1371/journal.pone.0119799 (2015).

15 Low, A. S. *et al.* Analysis of fimbrial gene clusters and their expression in enterohaemorrhagic Escherichia coli O157:H7. *Environ Microbiol* **8**, 1033-1047, doi:10.1111/j.1462-2920.2006.00995.x (2006).

16 Buts, L. *et al.* The fimbrial adhesin F17-G of enterotoxigenic Escherichia coli has an immunoglobulin-like lectin domain that binds N-acetylglucosamine. *Molecular Microbiology* **49**, 705-715 (2003).

17 Czaja, C. A. *et al.* Prospective cohort study of microbial and inflammatory events immediately preceding Escherichia coli recurrent urinary tract infection in women. *J Infectious Diseases* **200**, 528-536, doi:10.1086/600385 (2009).

18 Merckel, M. C. *et al.* The structural basis of receptor-binding by Escherichia coli associated with diarrhea and septicemia. *J Molecular Biology* **331**, 897-905 (2003).

19 Hudson, K. L. *et al.* Carbohydrate-Aromatic Interactions in Proteins. *J American Chemical Society* **137**, 15152-15160, doi:10.1021/jacs.5b08424 (2015).

20 Datsenko, K. A. & Wanner, B. L. One-step inactivation of chromosomal genes in Escherichia coli K-12 using PCR products. *Proc Natl Acad Sci USA* **97**, 6640-6645, doi:10.1073/pnas.120163297 (2000).

21 Wright, K. J., Seed, P. C. & Hultgren, S. J. Development of intracellular bacterial communities of uropathogenic Escherichia coli depends on type 1 pili. *Cellular Microbiology* **9**, 2230-2241, doi:10.1111/j.1462-5822.2007.00952.x (2007).

22 Rosen, D. A., Hung, C. S., Kline, K. A. & Hultgren, S. J. Streptozocin-induced diabetic mouse model of urinary tract infection. *Infection and Immunity* **76**, 4290-4298 (2008).

23 Totsika, M. *et al.* Insights into a multidrug resistant Escherichia coli pathogen of the globally disseminated ST131 lineage: genome analysis and virulence mechanisms. *PloS One* **6**, e26578, doi:10.1371/journal.pone.0026578 (2011).

24 Schreiber, H. L. t. *et al.* Bacterial virulence phenotypes of Escherichia coli and host susceptibility determine risk for urinary tract infections. *Science Translational Med* **9**, doi:10.1126/scitranslmed.aaf1283 (2017).

25 Welch, R. A. *et al.* Extensive mosaic structure revealed by the complete genome sequence of uropathogenic Escherichia coli. *Proc Natl Acad Sci USA* **99**, 17020-17024, doi:10.1073/pnas.25252979952529799 [pii] (2002).

26 Hung, C. S., Dodson, K. W. & Hultgren, S. J. A murine model of urinary tract infection. *Nature Protocols* **4**, 1230-1243, doi:10.1038/nprot.2009.116 (2009).

27 Justice, S. S., Lauer, S. R., Hultgren, S. J. & Hunstad, D. A. Maturation of intracellular Escherichia coli communities requires SurA. *Infection and Immunity* **74**, 4793-4800, doi:10.1128/IAI.00355-06 (2006).

28 Cusumano, C. K. *et al.* Treatment and prevention of urinary tract infection with orally active FimH inhibitors. *Science Translational Med* **3**, 109-115 (2011).

29 Johansson, M. E. & Hansson, G. C. Preservation of mucus in histological sections, immunostaining of mucins in fixed tissue, and localization of bacteria with FISH. *Methods Molecular Biology* **842**, 229-235, doi:10.1007/978-1-61779-513-8_13 (2012).

30 Kearse, M. *et al.* Geneious Basic: an integrated and extendable desktop software platform for the organization and analysis of sequence data. *Bioinformatics* **28**, 1647-1649, doi:10.1093/bioinformatics/bts199 (2012).

31 Katoh, K., Kuma, K., Toh, H. & Miyata, T. MAFFT version 5: improvement in accuracy of multiple sequence alignment. *Nucleic Acids Res* **33**, 511-518, doi:10.1093/nar/gki198 (2005).

32 Altschul, S. F., Gish, W., Miller, W., Myers, E. W. & Lipman, D. J. Basic local alignment search tool. *J Molecular Biology* **215**, 403-410, doi:10.1016/S0022-2836(05)80360-2 (1990).

33 Letunic, I. & Bork, P. Interactive tree of life (iTOL) v3: an online tool for the display and annotation of phylogenetic and other trees. *Nucleic Acids Res* **44**, W242-245, doi:10.1093/nar/gkw290 (2016).

34 Kalas, V. *et al.* Evolutionary fine-tuning of conformational ensembles in FimH during host-pathogen interactions. *Sci Adv* **3**, e1601944, doi:10.1126/sciadv.1601944 (2017).

35 Kabsch, W. Xds. *Acta Crystallographica* **66**, 125-132, doi:10.1107/S0907444909047337 (2010).

36 Evans, P. R. & Murshudov, G. N. How good are my data and what is the resolution? *Acta Crystallographica* **69**, 1204-1214 doi:10.1107/S0907444913000061 (2013).

37 Adams, P. D. *et al.* PHENIX: a comprehensive Python-based system for macromolecular structure solution. *Acta Crystallographica.* **66**, 213-221, doi:10.1107/S0907444909052925 (2010).

38 Holm, L. & Rosenstrom, P. Dali server: conservation mapping in 3D. *Nucleic Acids Res* **38**, W545-549, doi:10.1093/nar/gkq366 (2010).

39 Stamatakis, A. RAxML version 8: a tool for phylogenetic analysis and post-analysis of large phylogenies. *Bioinformatics* **30**, 1312-1313, doi:10.1093/bioinformatics/btu033 (2014).

40 Joosten, R. P. *et al.* A series of PDB related databases for everyday needs. *Nucleic Acids Res* **39**, D411-419, doi:10.1093/nar/gkq1105 (2011).

Figures

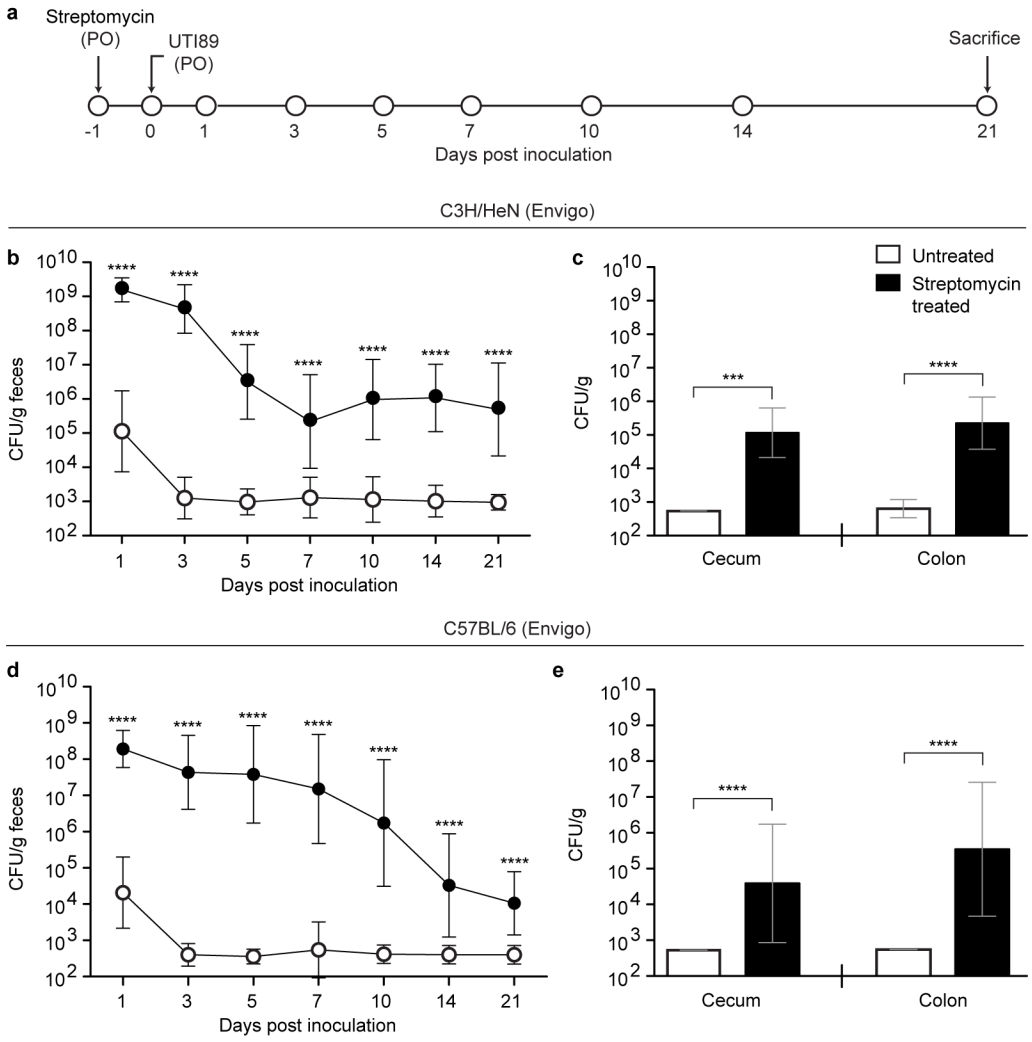

Figure 3. Streptomycin treatment allows for persistent UTI89 colonization of the intestine in female C3H/HeN and C57BL/6 mice. (a) Mice were pretreated with streptomycin and subsequently colonized via oral gavage (PO) with UTI89, a prototypical human UPEC cystitis isolate. (b-e) Colonization of UTI89 in C3H/HeN mice from Envigo (panels b,c) or C57BL/6 mice from Envigo (panels d,e) was assessed by quantifying colony forming units (CFU) in fecal samples collected over the course of 21 days from mice who did not receive streptomycin (white circles) or mice pretreated with the antibiotic (black circles). CFU analysis of levels of

colonization in the cecum and colon were defined by analyzing tissue homogenates prepared 21 days post colonization. Symbols represent geometric means ± SD, *p<0.05, **p<0.01, ***p<0.001, ****p<0.0001 (Mann Whitney U test). n=15 mice, 3 replicates (panels b-e).

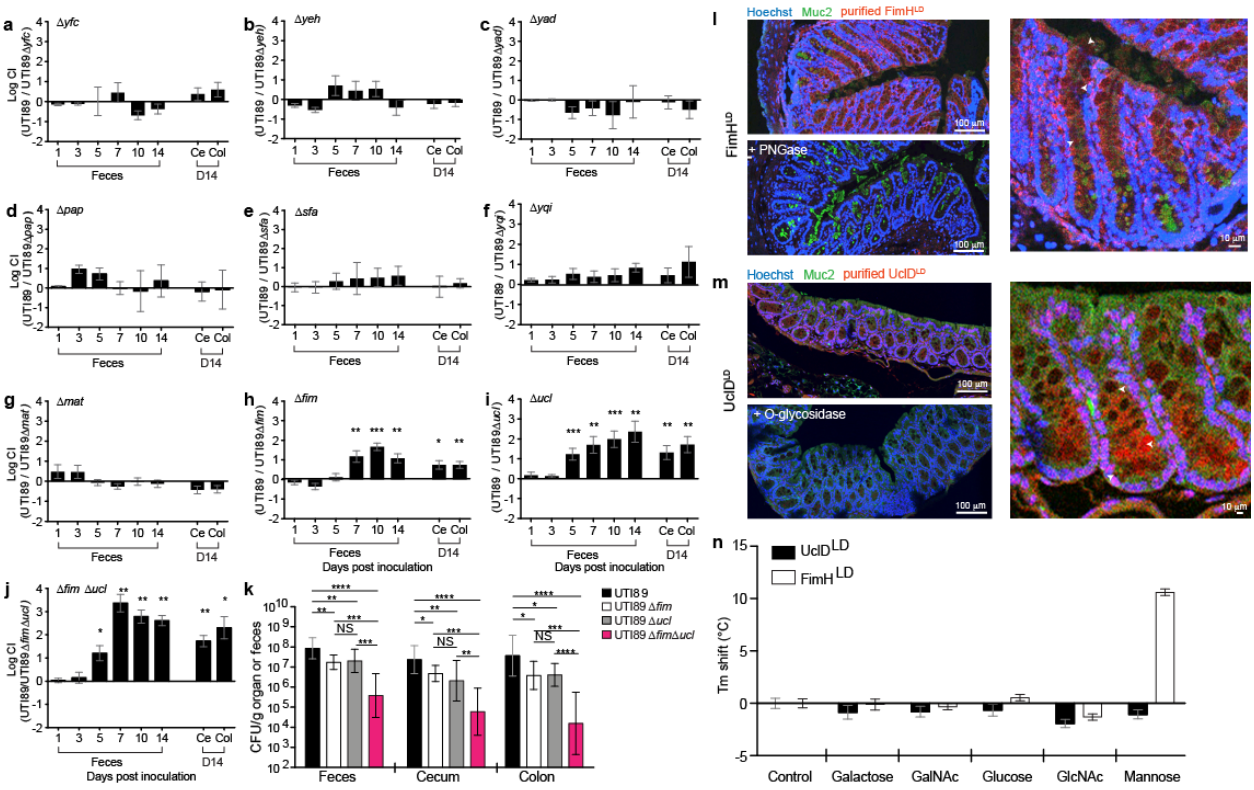

Figure 4. Type 1 and F17-like pili promote UPEC intestinal colonization. (a-i) C3H/HeN mice were treated with streptomycin and concurrently colonized with $1x10^8$ CFU of Wildtype (WT) UTI89 and one of 9 CUP operon knockout strains. (a-g) Deletion of 7 CUP operons had no impact on the fitness of UTI89. (h,i) Loss of operons that encode type 1 and F17-like pili (*fim* and *ucl* operons, respectively) decreased fitness compared to the WT strain. (j) Deletion of the *fim* and *ucl* operons in a single strain produced a fitness defect greater than deletion of each pilus alone. (k) Strains lacking either or both pilus operons also had fitness defects at 4 days post

gavage when singly-colonized. (l,m) Purified adhesin lectin domains for the type 1 and F17-like pilus ($FimH^{LD}$ and $UclD^{LD}$, respectively) were tested for binding to mouse colonic sections. Sections were stained with Hoechst (blue) and rabbit antibodies to Muc2, a prominent mucus-associated glycoprotein (green). Purified $FimH^{LD}$ binds to epithelial cells positioned in the upper half of crypts and surface epithelial cuffs. $FimH^{LD}$ binding is lost by pre-treatment of sections with PNGase (compare top and bottom images in panel l). $UclD^{LD}$ binds to epithelial cells located in the lower half of crypts. Binding is inhibited by pretreatment of sections with O-glycosidase (compare top and bottom images in panel m). To the right of the overview images in panels l and m, we show higher power views of individual crypts. Arrowheads point to examples of sites of binding of the purified adhesins. (n) The absence of a shift in the melting temperature of $UclD^{LD}$ in the presence of five monosaccharides tested using differential scanning fluorimnetry suggests that none of these sugars bind $UclD^{LD}$ in solution. In contrast, $FimH^{LD}$ binds monomannose with high affinity, resulting in a mean melting temperature shift of ~11°C. Abbreviations. Ce= cecum, Col= colon. CI= competitive index. Bars represent mean values ± SEM in panels a-j, n and geometric means ± SD in panel k. *$p<0.05$, **$p<0.01$, ***$p<0.001$ by Wilcoxon Signed Ranked test (panels a-j) or Mann Whitney U test (panel k). n=5 mice, 1 replicate (panels a, d-g), n=6 mice, 1 replicate (panel c); n=9, 2 replicates (panel j); n= 10 mice, 2 replicates (panels b,h) n=15 mice, 3 replicates (panels i,k).

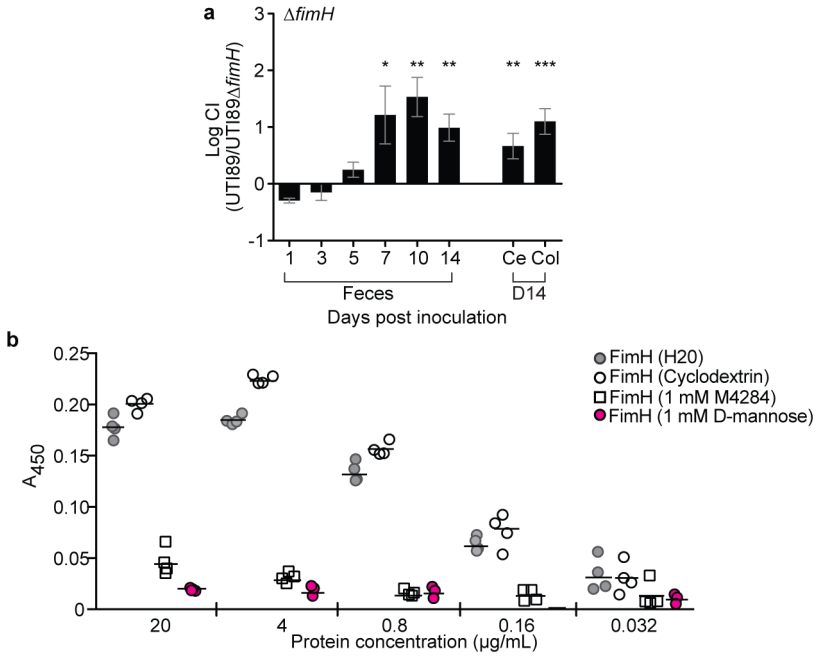

Figure 5. The FimH adhesin is required for type 1 pilus-dependent colonization of the mouse gut and for binding to human intestinal epithelial cells. (a) C3H/HeN mice from Envigo were pretreated with streptomycin and colonized with $1x10^8$ CFU of WT UTI89 and UTI89Δ*fimH*. The WT strain is able to outcompete the strain lacking the FimH adhesin. (b) The ability of purified FimH lectin domain ($FimH^{LD}$) to bind to Caco-2 cells was assessed by FimH-ELISA. Pre-incubation of $FimH^{LD}$ with a 50-fold excess of D-mannose (5mM) or M4284 (5mM) results in significant reductions in FimH binding to the Caco-2 cells while 10% cyclodextrin (M4284 vehicle) alone had no significant effect. All data shown are normalized to wells that were not exposed to the purified adhesin. Abbreviations CI= competitive index. Ce= cecum, Col= colon. Bars represent mean values ± SEM, *p<0.05, **p<0.01, ***p<0.001 (Wilcoxon Signed Ranked test) in panel a. Bars represent mean ± SEM, *p<0.05 (Mann Whitney U test) in panel b. n=14 mice, 3 replicates (panel a); n=4 replicates/treatment (panel b).

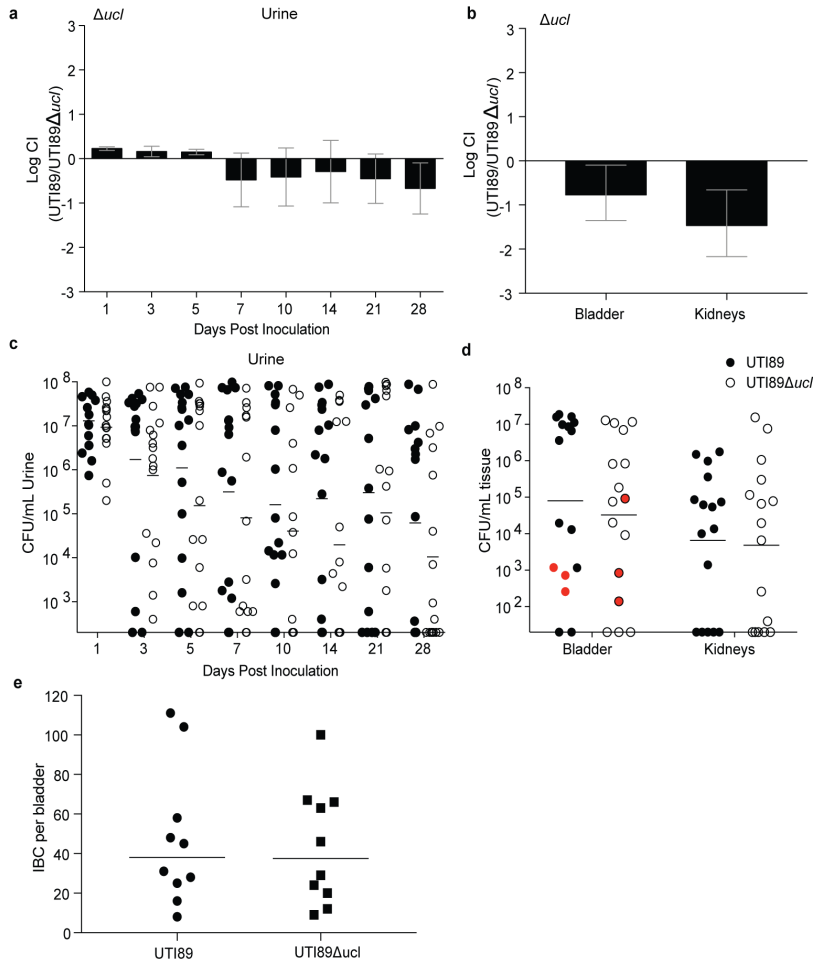

Figure 6. F17-like pili are not required for UTI in mice. C3H/HeN mice received a transurethral inoculation of UTI89 (WT) and UTI89Δ*ucl*, concurrently (a, b), or individually (c-e). (a) UTI89Δ*ucl* and WT strains persist at similar levels in the urine over 28 d in competitive infections. (b) The two strains are also present at equal levels in the bladder and kidney at the time of sacrifice 28 days post infection. (c) Single infection with the WT strain (black circles) or the F17-like mutant strain (white circles) produces similar levels of bacteruria over 28 days. (d) Single strain infection also produces similar levels of viable cells in homogenates of whole bladder or kidneys harvested at the time of sacrifice (28dpi). There was no statistically

significant difference in the number of mice that resolved bacteriuria while maintaining bladder-associated CFUs after transurethral infection with either WT or UTI89Δ*ucl* (highlighted in red in panel d), suggesting that both of these strains are capable of forming similar numbers of QIRs. (e) Mice infected transurethrally with WT or UTI89Δ*ucl* formed a similar number of intracellular bacterial communities (IBCs) at 6 hours in the bladder, indicating that loss of the *ucl* operon does not alter UTI89's ability to form IBCs. CI= competitive index. Bars represent mean ± SEM (panels a,b), geometric mean (panels c,d) or median (e). No significant difference was detected between any samples by Wilcoxon Signed Ranked test (panels a,b) or Mann Whitney U test (panels c-e). n=10 mice, 2 replicates (panels a-b, e). n=16 mice, 3 replicates (panels c-d).

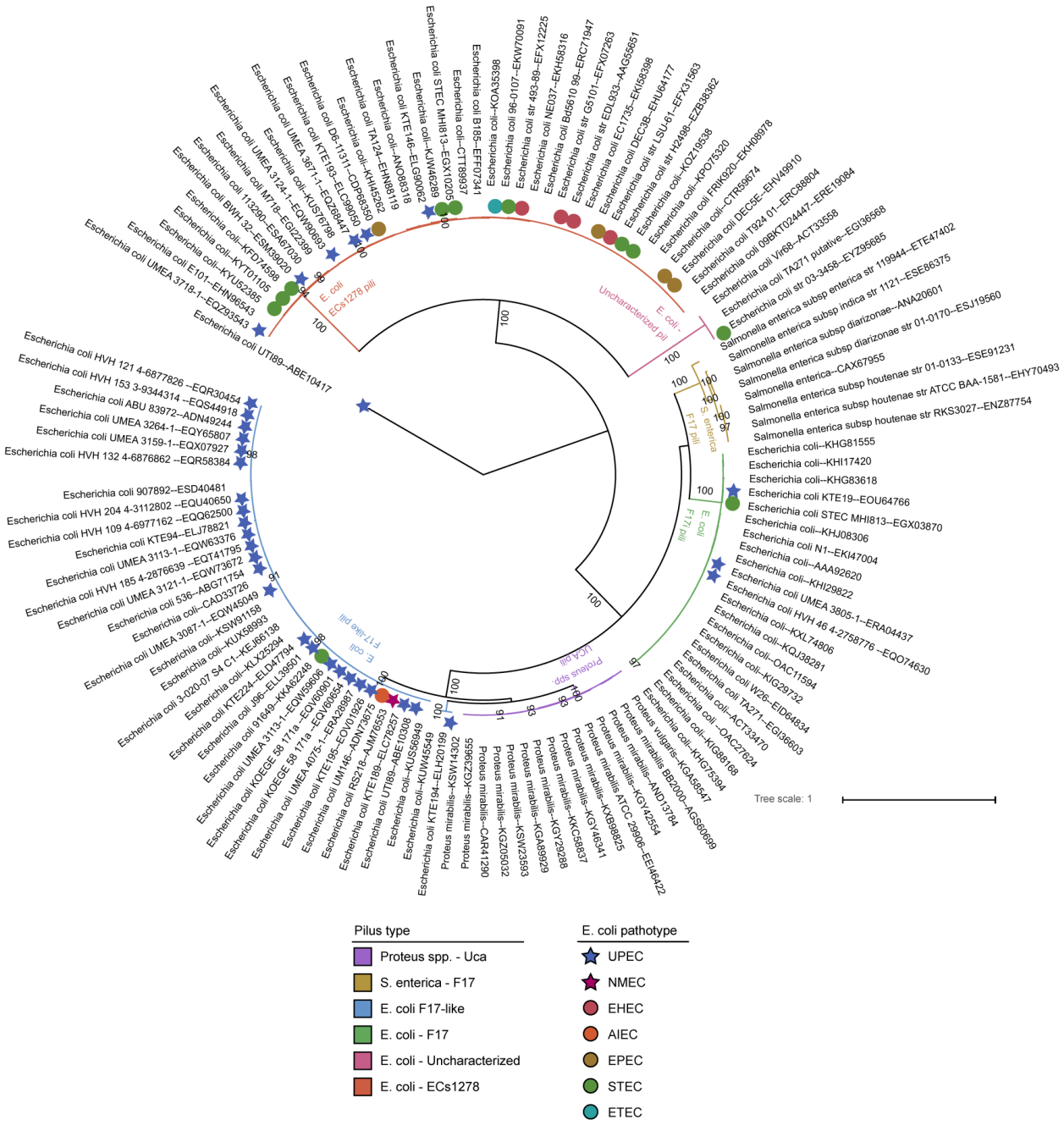
Escherichia coli STEC MHI813--EGX10205
Escherichia coli B185--EFF07341
Escherichia coli--KOA3536398
Escherichia coli 96-0107--EKW70091
Escherichia coli str 493-89--EFX12225
Escherichia coli NE037--EKH58316
Escherichia coli Bd5610 99--ERC71947
Escherichia coli str G5101--EFX07263
Escherichia coli str EDL933--AAG55651
Escherichia coli EC1735--EHI58398
Escherichia coli DEC3B--EHU64177
Escherichia coli str LSU-61--EFX31563
Escherichia coli str H2498--EZB38362
Escherichia coli--KOZ19538
Escherichia coli--KPO75320
Escherichia coli FRIK920--EKH08978
Escherichia coli--CTR59674
Escherichia coli DEC5E--EHV49910
Escherichia coli T924 01--ERC88804
Escherichia coli 09BKT024447--ERE19084
Escherichia coli Vir68--ACT33556
Escherichia coli TA271 putative--EGI36568
Escherichia coli str 03-3458--EYZ95685
Escherichia coli str 119944--ETE47402
Salmonella enterica subsp enterica str 1121--ESE86375
Salmonella enterica subsp indica str 1121--ANA20601
Salmonella enterica subsp diarizonae str 01-0170--ESJ19560
Salmonella enterica subsp diarizonae--CAX67955
Salmonella enterica subsp houtenae str 01-0133--ESE91231
Salmonella enterica subsp houtenae str ATCC BAA-1581--EHY70493
Salmonella enterica subsp houtenae str RKS3027--ENZ87754
Escherichia coli--KHG81555
Escherichia coli--KHI17420
Escherichia coli--KHG83618
Escherichia coli KTE19--EOU64766
Escherichia coli STEC MHI813--EGX03870
Escherichia coli--KHJ08306
Escherichia coli N1--EKI47004
Escherichia coli--AAA92620
Escherichia coli--KHI29822
Escherichia coli UMEA 3805-1--ERA04437
Escherichia coli HVH 46 4-2758776--EQO74630
Escherichia coli--KXL74806
Escherichia coli--KQJ38281
Escherichia coli--OAC11594
Escherichia coli--KIG29732
Escherichia coli W26--EID64834
Escherichia coli TA271--EGI36603
Escherichia coli--ACT33470
Escherichia coli--OAC27924
Escherichia coli--KHG75394
Escherichia coli--KIG98168
Escherichia coli--KGA58547
Proteus vulgaris--AGS60699
Proteus mirabilis BB2000--AND13784
Proteus mirabilis ATCC 29906--EEI46422
Proteus mirabilis--KGY42554
Proteus mirabilis--KXB98825
Proteus mirabilis--KGY46341
Proteus mirabilis--KKC58637
Proteus mirabilis--KGA89929
Proteus mirabilis--KGY29288
Proteus mirabilis--KSW23593
Proteus mirabilis--KGZ05032
Proteus mirabilis--CAR41290
Proteus mirabilis--KGZ39595
Escherichia coli--KUW45549
Escherichia coli KTE194--ELH20199
Proteus mirabilis--KSW14302
Escherichia coli--KUS56949
Escherichia coli UT189--ABE10308
Escherichia coli KTE189--ELC78257
Escherichia coli--KUW59606
Escherichia coli RS218--ADN73675
Escherichia coli UM146--ADN01926
Escherichia coli KTE195--EQV60901
Escherichia coli UMEA 4075-1--ERA28987
Escherichia coli UMEA 3113-1--EQW59606
Escherichia coli KOEGE 58 171a--EQV60554
Escherichia coli KOEGE 58 171a--EQV60901
Escherichia coli--KUX25294
Escherichia coli--KEJ66138
Escherichia coli--KUX58893
Escherichia coli--KSW91158
Escherichia coli UMEA 3087-1--EQW45049
Escherichia coli--CAD33726
Escherichia coli 536--ABG71754
Escherichia coli UMEA 3121-1--EQW73672
Escherichia coli HVH 185 4-2876639--EQT41795
Escherichia coli UMEA 3113-1--EQW63376
Escherichia coli KTE94--ELJ78821
Escherichia coli HVH 109 4-6977162--EQQ62500
Escherichia coli HVH 204 4-3112802--EQU40650
Escherichia coli 907892--ESD40481
Escherichia coli HVH 132 4-6876862--EQR58384
Escherichia coli UMEA 3159-1--EQX07927
Escherichia coli UMEA 3264-1--EQY65807
Escherichia coli ABU 83972--ADN49244
Escherichia coli HVH 153 3-9344314--EQS44918
Escherichia coli HVH 121 4-6877826--EQR30454
Escherichia coli UT189--ABE10417
Escherichia coli UMEA 3718-1--EQZ93543
Escherichia coli E101--EHN96543
Escherichia coli--KYU52385
Escherichia coli--KYT01105
Escherichia coli--KFD74598
Escherichia coli BWH 32--ESM39020
Escherichia coli 113290--ESA67030
Escherichia coli MT18--EGU22399
Escherichia coli UMEA 3124-1--EQW90893
Escherichia coli--KUS76798
Escherichia coli KTE193--ELC98447
Escherichia coli DE-11311--CDP68350
Escherichia coli--KHI45262
Escherichia coli TA124--EHN88119
Escherichia coli KTE146--ELG90062
Escherichia coli--KJW46289
Escherichia coli--ANO88318
E. coli ECs1278 pili
E. coli - Uncharacterized pili
S. enterica F17 pili
E. coli F17 pili
Proteus spp. UCA pili
E. coli F17-like pili
Tree scale: 1
Pilus type
Proteus spp. - Uca
S. enterica - F17
E. coli F17-like
E. coli - F17
E. coli - Uncharacterized
E. coli - ECs1278
E. coli pathotype
UPEC
NMEC
EHEC
AIEC
EPEC
STEC
ETEC

Figure 7. Distribution of F17 usher homologs in Enterobacteriaceae. The phylogenetic relationships between F17 homologs was estimated using the sequence of the usher genes. Branch colors indicate host strain and pilus identity, while colored symbols indicate the annotated pathotype of the *E. coli* strain for each sequence as determined by publically available annotations. Stars indicate extraintestinal pathogenic *E. coli* (ExPEC) strains while circles indicate intestinal pathogenic *E. coli* strains. Carriage of F17-like pili is enriched in UPEC strains while F17 and ECs1278 pili are more common in intestinal pathogens such as EHEC. The strain names for each sequence and ENA accession IDs are given. Numbers beneath the branches indicate the percentage of support from 1000 bootstrap replicates (numbers greater than 80% are shown).

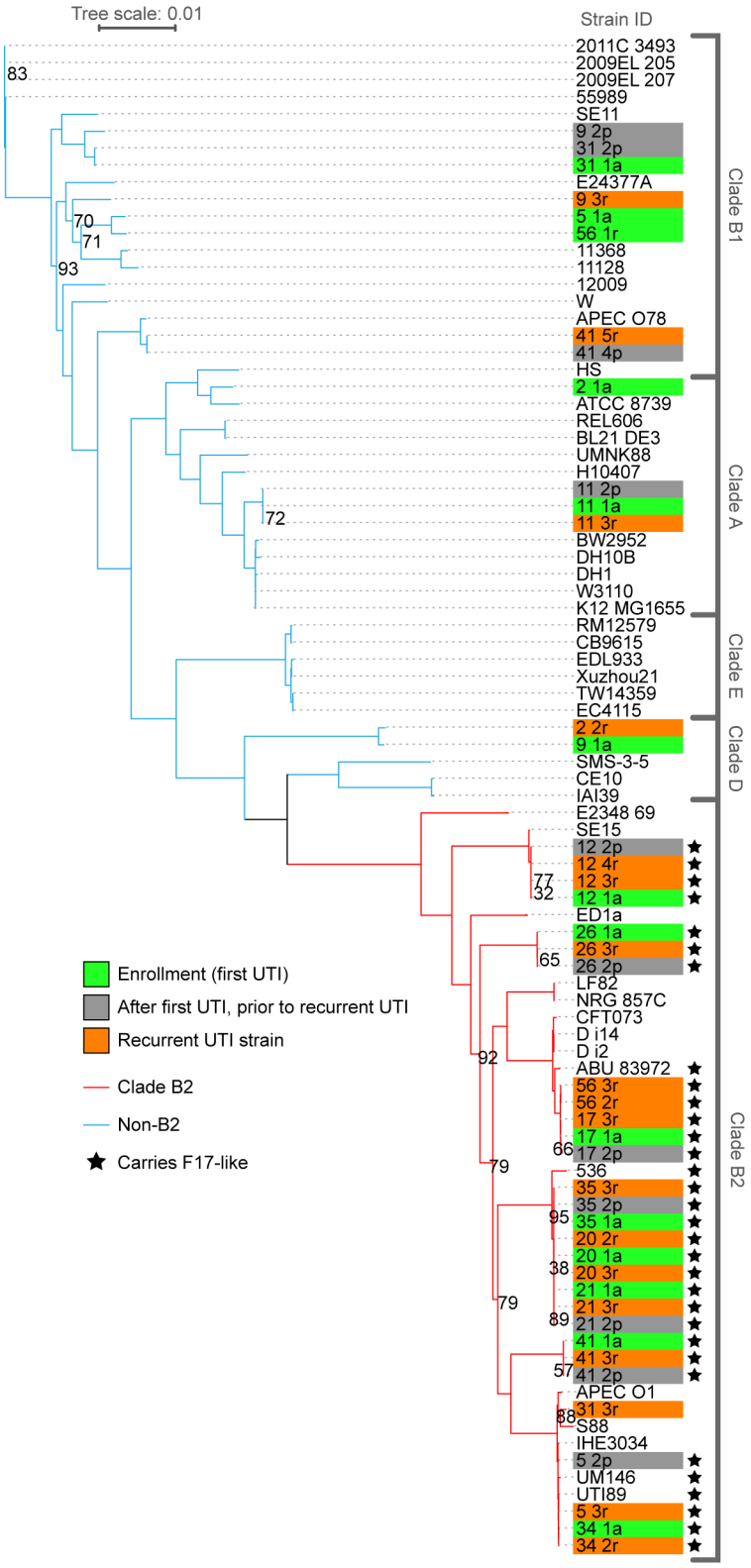
Tree scale: 0.01
Strain ID
2011C 3493
2009EL 205
2009EL 207
55989
SE11
9 2p
31 2p
31 1a
E24377A
9 3r
5 1a
56 1r
11368
11128
12009
W
APEC O78
41 5r
41 4p
HS
2 1a
ATCC 8739
REL606
BL21 DE3
UMNK88
H10407
11 2p
11 1a
11 3r
BW2952
DH10B
DH1
W3110
K12 MG1655
RM12579
CB9615
EDL933
Xuzhou21
TW14359
EC4115
2 2r
9 1a
SMS-3-5
CE10
IAI39
E2348 69
SE15
12 2p
12 4r
12 3r
12 1a
ED1a
26 1a
26 3r
26 2p
LF82
NRG 857C
CFT073
D i14
D i2
ABU 83972
56 3r
56 2r
17 3r
17 1a
17 2p
536
35 3r
35 2p
35 1a
20 2r
20 1a
20 3r
21 1a
21 3r
21 2p
41 1a
41 3r
41 2p
APEC O1
31 3r
S88
IHE3034
5 2p
UM146
UTI89
5 3r
34 1a
34 2r
Clade B1
Clade A
Clade E
Clade D
Clade B2
83
70
71
93
72
77
32
65
92
66
79
95
38
79
89
57
88
Enrollment (first UTI)
After first UTI, prior to recurrent UTI
Recurrent UTI strain
Clade B2
Non-B2
Carries F17-like

Figure 8. Phylogenetic distribution of F17-like carriage in UPEC from patients with rUTI. The phylogeny of a set of clinical UPEC strains (n=43 with taxon labels highlighted in green, orange, or grey) was contextualized with reference *E. coli* strains (n=46, unhighlighted taxon labels) by comparing the concatenated single-copy, core genes of the strains using the RAxML algorithm and the GTRCAT model[39]. Highlighted taxon labels indicate UPEC isolates collected at enrollment (green) and during recurrent UTI (orange). In all cases, patients cleared each infection prior to recurrence, no patient exhibited signs of asymptomatic bacteriuria. The study design also allowed for the collection, from cohort participants, of *E. coli* isolates present in the urine in the days leading up to their clinical visit and rUTI diagnosis (highlighted in grey), as described previously[17]. Branch lines indicate phylogenetic background for strains from clade B2 (red branch lines) and non-B2 clades (blue branch lines). Carriage of F17-like pili (black stars) was limited to the B2 clade and enriched within rUTI UPEC isolates. Bootstrap supports are indicated at internal nodes. Bootstrap values >95 have been removed. The clade to which each strain belongs is indicated in brackets to the right.

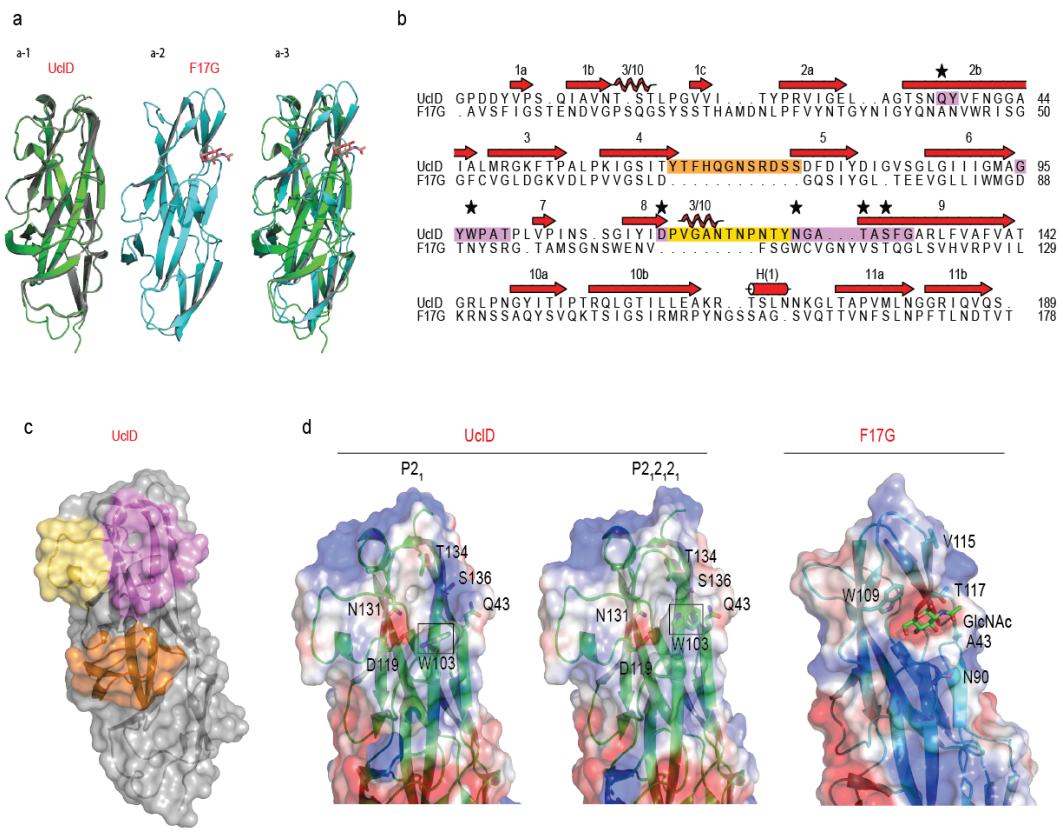

Figure 9. Structural analysis of UclD^{LD}. (a) Comparison of the structures of UclD^{LD} and F17G^{LD}. Superposition of the P2$_1$ UclD^{LD} (green) P2$_1$2$_1$2$_1$ UclD^{LD} (grey) crystal structures (a-1). Crystal structure of the F17G adhesin (PDB 1OIO[18]) (a-2). Superposition of the P2$_1$ UclD^{LD} (green) and F17G^{LD} (cyan) crystal structures (a-3). Despite a primary sequence identity of only 25%, the structures superimpose with an Cα root mean square deviation of of 2.7 Å. (b) Structural alignment of the UclD^{LD} and F17G^{LD} amino acid sequences using the PROMALS3D server. All 16 regions assigned as β-strands by the Dictionary of Secondary Structure of Proteins (DSSP)[40] are conserved in both proteins despite low sequence identities. UclD residues highlighted in purple are postulated to contribute to binding of a small core ligand, while surrounding residues highlighted in yellow and orange may bind to different moieties on a larger molecular receptor. Starred residues are represented as sticks in panel d. (c) Surface

representation of the UclD^{LD} structure, with key regions of divergence highlighted in yellow, orange, and purple according to the representation in panel b. (d) Comparison of residue positioning and electrostatic surface potential of the putative binding site between the two UclD^{LD} structures and the known binding site of the F17G^{LD} structure. We believe that the side chain and/or backbone positions of Q43, W103, D119, N131, T134, and S136, shown here in the stick representation, likely coordinate binding to a glycan-containing sugar residue in the putative binding pocket. The residues occupying the analogous positions on F17G are also shown as sticks.

Chapter 3: Selective depletion of uropathogenic *E. coli* from the gut by a FimH antagonist

Adapted from:

Selective depletion of uropathogenic *E. coli* from the gut by a FimH antagonist

Caitlin N. Spaulding, Roger D. Klein, Ségolène Ruer, Andrew L. Kau, Henry L. Schreiber IV, Zachary T. Cusumano, Karen W. Dodson, Jerome S. Pinkner, Daved H. Fremont, James W. Janetka, Han Remaut, Jeffrey I. Gordon, Scott J. Hultgren

Nature 2017 Jun 22; 546(7659) 528-532. doi: 10.1038/nature22972.

Abstract

UTIs are a major contributor to global antibiotic use. In the United States alone, 9% of all antibiotics prescribed in a year are for the treatment of UTIs [1]. The global prevalence of single and multi-drug resistant UPEC isolates highlights our reliance on antibiotics to treat these infections and stresses the need to develop alternative treatments to combat resistant pathogens. However, the development and spread of antibiotic resistance is not the only issue with our current method of treatment. An increasing number of published papers are finding that disruption of the gut microbiota by orally administered antibiotics, especially during childhood,

may affect its functional properties in ways that are deleterious to the host, not only in the short term but for more protracted periods of time if the antibiotic perturbation is not followed by adequate restoration of the community [2,3]. Therefore, developing treatments for pathogens, like UPEC, that can specifically target a pathogen without damaging the remainder of the microbial community is important. This 'molecular-scalpel' approach to drug development is increasing in scope. Treatment with mannoside has recently been shown to target the intestinal population of AIEC in a transgenic mouse model [4]. The identification of a selective therapy that is designed to target staphylococci spp. but has minimal other effects on the microbiota has shown that this type of treatment is possible [5]. Another study found that a cocktail of bacteriophages could target UPEC in the gut with minimal impact on the overall composition of the microbiota; however, the translatability of these types treatment to a wide-range of uropathogens and in hosts with different genetics and microbial compositions is unknown [6].

My finding that type 1 pili promote UPEC intestinal colonization, outlined in Chapter 2, provided an exciting and unique opportunity determine if an anti-adhesive therapeutic could provide an alternative, and potentially antibiotic sparing, method to removing UPEC from the host. The essentiality of the FimH-mannose interaction during UTI prompted the design and development of orally active, synthetic, small-molecule inhibitors of FimH called mannosides, which are mannose analogs that are rationally designed to bind within the mannose-binding pocket of FimH with a high affinity [7]. Therefore, I tested the ability of oral mannoside treatment to target UPEC in both the gut and bladder. My findings show that mannoside treatment successfully targets a pilus type that is importance for intestinal colonization in mice and humans. This treatment targets a range of UPEC strains and is successful regardless of host genetics or microbiota composition. This treatment specifically targets UPEC while leaving the

surrounding microbiota uninjured and can simultaneously target UPEC in the gut reservoir and at the site of infection.

Aside from providing a much-needed method to treat individuals infected with drug resistant uropathogens, a selective treatment, like mannosides, would also reduce the exposure of entire gut microbiota to antibiotics and thus could curb the development of antibiotic resistant pathogens. Due to their prevalence worldwide, UTIs are and will continue to be a major contributor to antibiotic use and resistance. Unfortunately, high rates of UTI and rUTI worldwide have provided almost persistent exposure of uropathogens to antibiotics, resulting in the development and swift expansion of UPEC strains encoding resistance genes to one or more classes of antibiotics. Without effective antibiotics active against uropathogens, UTIs, which are typically considered low risk infections, will become life threatening and many urological procedures will carry excessive risk. The need to develop alternative, antibiotic-sparing therapies to treat individuals with UTI is obvious and pressing.

Main Text

Mannosides target and reduce type 1-expressing UPEC in the gut reservoir

As outlined in Chapter 2, FimH and UclD promote gut colonization and epithelial cell binding by UTI89. Therefore I conducted a proof-of-concept study designed to eliminate the UPEC intestinal reservoir in this mouse model using a candidate adhesin-directed therapeutic. M4284 is a high affinity biphenyl mannoside that inhibits FimH binding to Caco-2 cells (**Figure 5**). M4284 has a binding affinity for FimH that is ~100,000-fold higher than the natural sugar D-mannose[7,8]. Pharmacokinetic (PK) analysis showed that after a single oral gavage, M4284 remains present at high concentration in the feces of recipient mice for up to 8 hours (h) **(Figure**

10a). In a follow-up experiment, mice were treated with streptomycin, orally gavaged with UTI89 24 h later, and 3 d later given 3 doses of M4284 (100mg/kg) over a 24 h period **(Figure 10b**). This dosing regimen was previously used to successfully treat UPEC infection of the mouse bladder with mannoside[9-11]. Treatment with M4284 significantly reduced levels of UTI89 in feces as well as cecum and colon by up to 1.5 logs (98% reduction) **(Figure 10c)**. Treating mice with up to 5 oral doses of M4284 (3 doses administered over 24 h followed by two additional doses given over the remaining 48 h) reduced the UTI89 population to an even greater extent (up to 1000-fold) **(Figure 11a,b)**. Moreover, the overall number of UPEC continued to be lower in mannoside-treated mice up to 5 days after termination of treatment **(Figure 11c,d).** While D-mannose blocks FimH binding *in vitro* at high concentrations **(Figure 5)**, treating mice with D-mannose had no effect on UTI89 titers in the cecum, colon, and feces **(Figure 10d).** Thus, unlike D-mannose, M4284 can effectively compete with the natural receptor at nanomolar concentrations and prevent FimH-mediated host-pathogen interactions.

Mannosides simultaneously target UPEC in the gut and bladder

There is no mouse model of spontaneous UTI. Moreover, the proximity of the mouse urethra to soiled bedding and the coprophagic behavior of these animals make creating such a model challenging. Thus, there is no direct way to test how reducing the UPEC intestinal reservoir would alter the rate of UTI. However, the established ID_{50}, or minimum number of UPEC that result in a 50% infection rate in the mouse model of UTI, is 10^5 CFU[12]. Decreasing the inoculation dose of UPEC introduced into the bladder from 10^8 to 10^6 CFU resulted in significantly reduced rates of UTI (**Figure 12**) suggesting that the 1-1.5 log (or 90-95%)

mannoside-driven reduction in fecal UPEC levels would reduce the numbers of bacteria available to be inoculated into the urinary tract and likely reduce the rate of UTI and/or rUTI.

M4284 has low oral bioavailability (<2 %). Thus, >98% of the drug is not absorbed into the systemic circulation, allowing the compound to exert its effects on type 1-expressing UPEC in the gut but potentially limiting its effectiveness in the bladder[7]. To assess whether M4284 could treat an active infection in the bladder while simultaneously reducing the intestinal UPEC reservoir, mice were orally gavaged with UTI89 and 24 h later given a UTI via transurethral inoculation. Two days after inoculation of UTI89, 3 doses of M4284 were administered orally over a 24 h period. Animals were sacrificed 8 h after the last dose and colonization was assessed **(Figure 10e).** M4284 significantly reduced UTI89 titers throughout the length of the distal gut (up to 98%) and in the urinary tract (96-99%) **(Figure 10f,g),** demonstrating that this mannoside has sufficient oral absorption to exert its effect in the bladder.

Oral mannoside treatment has minimal effects of the structure of the gut microbiota

To determine whether mannoside treatment affects the gut microbiota structure, we treated C3H/HeN mice that had not been given streptomycin or infected with UPEC with 3 doses of M4284 or vehicle alone (10% cyclodextrin). Sequencing bacterial 16S rRNA gene amplicons generated from fecal samples collected 24 h after cessation of treatment revealed that M4284 produced no significant changes in the overall phylogenetic configuration of the microbiota as judged by the unweighted UniFrac dissimilarity metric, in contrast to the significant perturbations produced by treatment with ciprofloxacin, a fluoroquinolone antibiotic **(Figure 13a,b, Figure 14a,b)**. Using this same metric, we found that M4284 treatment did not produce significant perturbations in bacterial community structure in mice pretreated with streptomycin

and then colonized with UTI89 **(Figure 15).** We concluded that M4284 can function to selectively extirpate UPEC from the gut in our preclinical model. Interestingly, the operon encoding type 1 pili is carried by nearly every sequenced *E. coli* strain[13] and is highly conserved throughout the family Enterobacteriaceae[14]. However, we found that M4284 treatment has no significant effect on the abundance of Enterobacteriaceae (**Figure 14a,b**), suggesting that these bacteria may not be expressing type 1 pili during M4284 exposure or that they reside within inaccessible intestinal habitats, like biofilms, and are therefore not greatly affected by mannoside treatment. Further examination of the effects of M4284 treatment on gut colonization by different species/strains of Enterobacteriaceae is needed to more fully interpret the significance of these findings.

Mannoside treatment decreases gut colonization by genetically diverse UPEC clinical isolates

Clinical isolates of UPEC strains are genetically diverse, differing significantly in their carriage of different pathogenicity associated islands, CUP pili, and resistances to commonly-used antibiotics. Only 60-75% of each UPEC strain's genome is comprised of a set of shared genes; *fimH* is part of this core genome. Therefore, we examined the efficacy of M4284 against a panel of four diverse UPEC clinical isolates, UTI89, CFT073, EC958, and 41.4p. These isolates reflect some of the genetic diversity of UPEC; UTI89, EC958, and CFT073 belong to clade B2, while 41.4p is a member of clade B1. UTI89, EC958, and 41.4p are cystitis isolates, while CFT073 is a urosepsis isolate. EC958 also encodes resistance genes to a number of clinically relevant antibiotics. We were able to establish and maintain intestinal colonization of our mouse model with each isolate tested, and found that M4284 treatment produced similar, statistically

significant reductions in the levels of each UPEC strain in the cecum, colon, and feces **(Figure 13b-f)**. In each case, the percent reduction in feces or cecum/colon was similar **(Figure 16a)**.

Mannoside treatment reduces UTI89 intestinal colonization in mice of different genetic backgrounds with diverse gut microbiota communities

Since UTI and rUTI occur in individuals of diverse genetic backgrounds and varied gut microbiota configurations, we also tested the efficacy of M4284 in both C3H/HeN and C57Bl/6 mice, each from different vendors with different gut microbial community configurations (e.g. **Figure 14c)**. We found that this treatment reduced the UTI89 intestinal reservoir in each case tested, with the percentage of UPEC removed from the feces, cecum, and colon not varying significantly between the three groups of mice (**Figure 14f-h, Figure 16b**). From these results, we concluded that M4284 treatment has activity against different UPEC strains in different host genetic backgrounds and gut microbial community contexts.

Conclusions

As the prevalence of antibiotic-resistant pathogens continues to rise, the need to develop highly targeted/specific therapeutic approaches has gained increased urgency[5,6]. Additionally, an increasing number of studies are finding that disruption of the gut microbiota by orally administered antibiotics, especially during childhood, may affect its functional properties in ways that are deleterious to the host, not only in the short term but for more protracted periods of time[2,3]. Therefore, developing therapeutic agents, like mannosides, that can specifically target a pathogen without disrupting the remainder of a microbial community has important ramifications

not only for UPEC but potentially for other infections, including those caused by enteropathogens.

Acknowledgments

This work was supported by grants from the NIH [K08AI113184 (ALK), R01AI048689 (SJH), P50DK064540 (SJH), RC1DK086378 (SJH), R01DK051406 (SJH), DK30292 (JIG) and 1F31DK107057 (CNS)], FWO-Flanders (G030411N), Hercules Foundation (UABR/09/005) and VIB PRJ9.

Competing Financial Interests (CFI)

JWJ and SJH are inventors on patent application US8937167, which covers the use of mannoside-based FimH ligand antagonists for the treatment of disease. JWJ and SJH have ownership interest in Fimbrion Therapeutics, and may benefit if the company is successful in marketing mannosides.

Materials and Methods

Ethics statement

The Washington University Animal Studies Committee approved all procedures used for the mouse experiments described in the present study. Overall care of the animals was consistent with *The Guide for the Care and Use of Laboratory Animals* from the National Research Council and the USDA *Animal Care Resource Guide*. For collection of colonic tissues for adhesion binding studies, mice were sacrificed according to institutional, national and European animal regulations, using protocols that were also approved by the animal ethics committee of Ghent

University.

Bacterial strains

CUP operon and adhesin deletions in UTI89 were engineered by replacing the gene(s) of interest with antibiotic-resistance markers using the λ Red Recombinase system[15]. Earlier reports described WT UTI89 and its isogenic *fim* and *fimH* mutants[12,16] as well as EC958[17], 41.4p[18] and CFT073[19].

Colonization of mice with UPEC strains

6-week old female C3H/HeN mice were obtained from Envigo or Charles Rivers Labs (CRL). 6-week old female C57BL/6 mice were also obtained from Envigo. Animals were maintained in a single room in our vivarium for no more than 2 days prior to treatment. Prior to and after treatment all animals received PicoLab Rodent Diet 20 (Purina) *ad libitum*. All animals were maintained under a strict light cycle (lights on at 0600h, off at 1800h). For competitive infections, if a phenotype was observed after testing five mice (1 biological replicate), the experiment was repeated 1-2 times (total of n=10-16 mice, 2-3 biological replicates). For 16S rRNA analyses, 4-5 mice were examined (1 biological replicate). For all other experiments, 9-16 mice were tested and the experiment was repeated 2-3 times (2-3 biological replicates). Exclusion criteria for mice were pre-established; (i) both introduced strains in competitive infections became undetectable during the course of a 14 day experiment, and (ii) mice died or lost > 20% of their body weight. No mice in this study met these criteria. Mice were acquired from indicated vendors and randomly placed into cages (n=5 mice/cage) by employees of Washington University's Division of Comparative Medicine (DCM); no additional methods for

randomization were used to determine how animals were allocated to experimental groups. Investigators were not blinded to group allocation during experiments.

Animals received a single dose of streptomycin (1000mg/kg in 100 μL water by oral gavage (PO)) followed 24 h later by an oral gavage of ~10^8 CFU UPEC in 100 μl phosphate-buffered saline (PBS). Bladder infections were performed via transurethral inoculation[20]. UPEC strains were prepared for inoculation as described previously[20]. Briefly, a single UTI89 colony was inoculated in 20 mL of Luria Broth (LB) and incubated at 37°C under static conditions for 24 h. Bacteria were then diluted (1:1000) into fresh LB and incubated at 37°C under static conditions for 18-24 h. Bacteria were subsequently washed three times with PBS and then concentrated to ~1x10^8 CFU per 100 μL for intestinal infections and ~1x10^8 CFU per 50 μL for bladder infections.

In all cases, fecal and urine samples were collected directly from each animal at the indicated time points. Fecal samples were immediately weighed and homogenized in 1 mL PBS. Urine samples were immediately diluted 1:10 prior to plating. Mice were sacrificed via cervical dislocation under isofluorane anesthesia and their organs were removed and processed under aseptic conditions. Intestinal segments (cecum and colon) were weighed prior to homogenization and plating on LB supplemented with the appropriate antibiotic.

Mannoside Treatment

D-mannose or the mannoside M4284 (which has been characterized in a prior published study[11]), were diluted in vehicle (water and 10% cyclodextrin, respectively) and administered to 6 week old C3H/HeN mice at a dose of 100mg/kg. Control animals were treated with water or 10% cyclodextrin alone. Unless stated otherwise, three doses of M4284, cyclodextrin, or D-mannose

were given via oral gavage over 24 hours, with doses administered 8 h apart. Mice were sacrificed and intestinal tissues were processed for analysis of viable bacteria (CFU) 8 h after the last dose, unless otherwise noted. To test the effect of M4284 on intestinal UPEC titers after treatment was terminated, mice were sacrificed 5 days after the last dose of mannoside. To test the effect of additional doses on M4284 treatment on UPEC titers, mice were given 5 doses of mannoside; the first 3 doses were administered 8 h apart, followed 12h later by the 4^{th} dose, and 24h later by the 5^{th} dose. Mice were sacrificed 24h after the 5^{th} dose.

Effect of antibiotic exposure on the microbiota

Six week old female C3H/HeN mice from Envigo and CRL were subjected to the following treatments: (i) none (naïve control mice, Untreated), (ii) three doses of M4284 (100mg/kg; in 10% cyclodextrin) or 10% cyclodextrin given 8 h apart, or (iii) ciprofloxacin (two doses of 15mg/kg given 12 h apart). All doses were given via oral gavage. Five mice were included for each treatment type (1 biological replicate) and fecal samples were collected prior to treatment and 24 hours after the last dose of each treatment. Another group of four C3H/HeN mice from Envigo (1 biological replicate) were pretreated with streptomycin and colonized with UTI89 before recieving treatment with either three doses of M4284 (100mg/kg; in 10% cyclodextrin) or with 10% cyclodextrin alone; fecal samples were collected prior to treatment but after exposure to streptomycin and UTI89 and 24 hours after the last dose of each treatment.

Bacterial 16S rRNA sequencing

DNA was extracted by bead beating in extraction buffer [200 mM Tris (pH 8.0), 200 mM NaCl, 20 mM EDTA], 210µL of 20% SDS and 500µL phenol:chloroform:isoamyl alcohol (pH 7.9,

25:24:1). This crude DNA extract was purified (Qiaquick PCR purification kit) and PCR used to generate amplicons from the V4 region of bacterial 16S rRNA genes using primers and cycling conditions described previously[21]. Amplicons were pooled in equimolar ratios and sequenced on an Illumina MiSeq instrument (paired end 250 nt reads). Paired V4-16S rRNA sequences were merged using FLASH software[22], demultiplexed, and reads clustered into 97%ID OTUs (2013 Greengenes OTU reference database; QIIME version 1.9.0[23]). A custom database using modified NCBI bacterial taxonomy was used to train the Ribosomal Database Project (RDP) version 2.4 classifier and assign taxonomy to picked OTUs[24]. The resulting OTU table was filtered to include only OTUs found in at least two samples at greater than or equal to 0.1% relative abundance.

Data Availability

Bacterial V4-16S rRNA datasets have been deposited in the European Nucleotide Archive (ENA) under accession number PRJEB19121.

Code Availability

No new code was generated for this study. All software was obtained from publicly available sources; papers describing the software are cited in the text.

Statistical Analysis

The statistical significance of differences between groups in experiments (excluding competitive infections) was determined by a Mann Whitney U test. Competitive Index (CI) was defined as (CFU output strain A/CFU output strain B)/(CFU input strain A/CFU input strain B). For

competitive infections, statistical significance was determined by a Wilcoxon Signed Ranked test. Statistical analyses were performed using Graphpad Prism 7.

References

1 Shapiro, D. J., Hicks, L. A., Pavia, A. T. & Hersh, A. L. Antibiotic prescribing for adults in ambulatory care in the USA, 2007-09. *J Antimicrobial Chemotherapy* **69**, 234-240, doi:10.1093/jac/dkt301 (2014).

2 Cox, L. M. *et al.* Altering the intestinal microbiota during a critical developmental window has lasting metabolic consequences. *Cell* **158**, 705-721, doi:10.1016/j.cell.2014.05.052 (2014).

3 Dethlefsen, L. & Relman, D. A. Incomplete recovery and individualized responses of the human distal gut microbiota to repeated antibiotic perturbation. *Proc Natl Acad Sci USA* **108 Suppl 1**, 4554-4561, doi:10.1073/pnas.1000087107 (2011).

4 Alvarez Dorta, D. *et al.* The Antiadhesive Strategy in Crohn's Disease: Orally Active Mannosides to Decolonize Pathogenic Escherichia coli from the Gut. *Chembiochem* **17**, 936-952, doi:10.1002/cbic.201600018 (2016).

5 Yao, J. *et al.* A Pathogen-Selective Antibiotic Minimizes Disturbance to the Microbiome. *Antimicrobial Agents and Chemotherapy*, doi:10.1128/AAC.00535-16 (2016).

6 Galtier, M. *et al.* Bacteriophages to reduce gut carriage of antibiotic resistant uropathogens with low impact on microbiota composition. *Environ Microbiol*, doi:10.1111/1462-2920.13284 (2016).

7 Jarvis, C. *et al.* Antivirulence Isoquinolone Mannosides: Optimization of the Biaryl Aglycone for FimH Lectin Binding Affinity and Efficacy in the Treatment of Chronic UTI. *ChemMedChem* **11**, 367-373, doi:10.1002/cmdc.201600006 (2016).

8 Han, Z. *et al.* Lead optimization studies on FimH antagonists: discovery of potent and orally bioavailable ortho-substituted biphenyl mannosides. *J Medicinal Chemistry* **55**, 3945-3959, doi:10.1021/jm300165m (2012).

9 Cusumano, C. K. *et al.* Treatment and prevention of urinary tract infection with orally active FimH inhibitors. *Science Translational Med* **3**, 109-115 (2011).

10 Flores-Mireles, A. L., Walker, J. N., Caparon, M. & Hultgren, S. J. Urinary tract infections: epidemiology, mechanisms of infection and treatment options. *Nature Reviews Microbiology* **13**, 269-284, doi:10.1038/nrmicro3432 (2015).

11 Spaulding, C. N. & Hultgren, S. J. Adhesive Pili in UTI Pathogenesis and Drug Development. *Pathogens* **5**, doi:10.3390/pathogens5010030 (2016).

12 Rosen, D. A., Hung, C. S., Kline, K. A. & Hultgren, S. J. Streptozocin-induced diabetic mouse model of urinary tract infection. *Infection and Immunity* **76**, 4290-4298 (2008).

13 Wurpel, D. J., Beatson, S. A., Totsika, M., Petty, N. K. & Schembri, M. A. Chaperone-usher fimbriae of Escherichia coli. *PloS One* **8**, e52835, doi:10.1371/journal.pone.0052835 (2013).

14 Jones, C. H. *et al.* FimH adhesin of type 1 pili is assembled into a fibrillar tip structure in the Enterobacteriaceae. *Proc Natl Acad Sci USA* **92**, 2081-2085 (1995).

15 Datsenko, K. A. & Wanner, B. L. One-step inactivation of chromosomal genes in Escherichia coli K-12 using PCR products. *Proc Natl Acad Sci USA* **97**, 6640-6645, doi:10.1073/pnas.120163297 (2000).

16 Wright, K. J., Seed, P. C. & Hultgren, S. J. Development of intracellular bacterial communities of uropathogenic Escherichia coli depends on type 1 pili. *Cellular Microbiology* **9**, 2230-2241, doi:10.1111/j.1462-5822.2007.00952.x (2007).

17 Totsika, M. *et al.* Insights into a multidrug resistant Escherichia coli pathogen of the globally disseminated ST131 lineage: genome analysis and virulence mechanisms. *PloS One* **6**, e26578, doi:10.1371/journal.pone.0026578 (2011).

18 Schreiber, H. L. t. *et al.* Bacterial virulence phenotypes of Escherichia coli and host susceptibility determine risk for urinary tract infections. *Science Translational Medicine* **9**, doi:10.1126/scitranslmed.aaf1283 (2017).

19 Welch, R. A. *et al.* Extensive mosaic structure revealed by the complete genome sequence of uropathogenic Escherichia coli. *Proc Natl Acad Sci USA* **99**, 17020-17024, doi:10.1073/pnas.252529799 [pii] (2002).

20 Hung, C. S., Dodson, K. W. & Hultgren, S. J. A murine model of urinary tract infection. *Nature Protocols* **4**, 1230-1243, doi:10.1038/nprot.2009.116 (2009).

21 Caporaso, J. G. *et al.* Global patterns of 16S rRNA diversity at a depth of millions of sequences per sample. *Proc Natl Acad Sci USA* **108 Suppl 1**, 4516-4522, doi:10.1073/pnas.1000080107 (2011).

22 Magoc, T. & Salzberg, S. L. FLASH: fast length adjustment of short reads to improve genome assemblies. *Bioinformatics* **27**, 2957-2963, doi:10.1093/bioinformatics/btr507 (2011).

23 Rideout, J. R. *et al.* Subsampled open-reference clustering creates consistent, comprehensive OTU definitions and scales to billions of sequences. *PeerJ* **2**, e545, doi:10.7717/peerj.545 (2014).

24 Kau, A. L. *et al.* Functional characterization of IgA-targeted bacterial taxa from undernourished Malawian children that produce diet-dependent enteropathy. *Science Translational Medicine* **7**, 276ra224, doi:10.1126/scitranslmed.aaa4877 (2015).

Figures

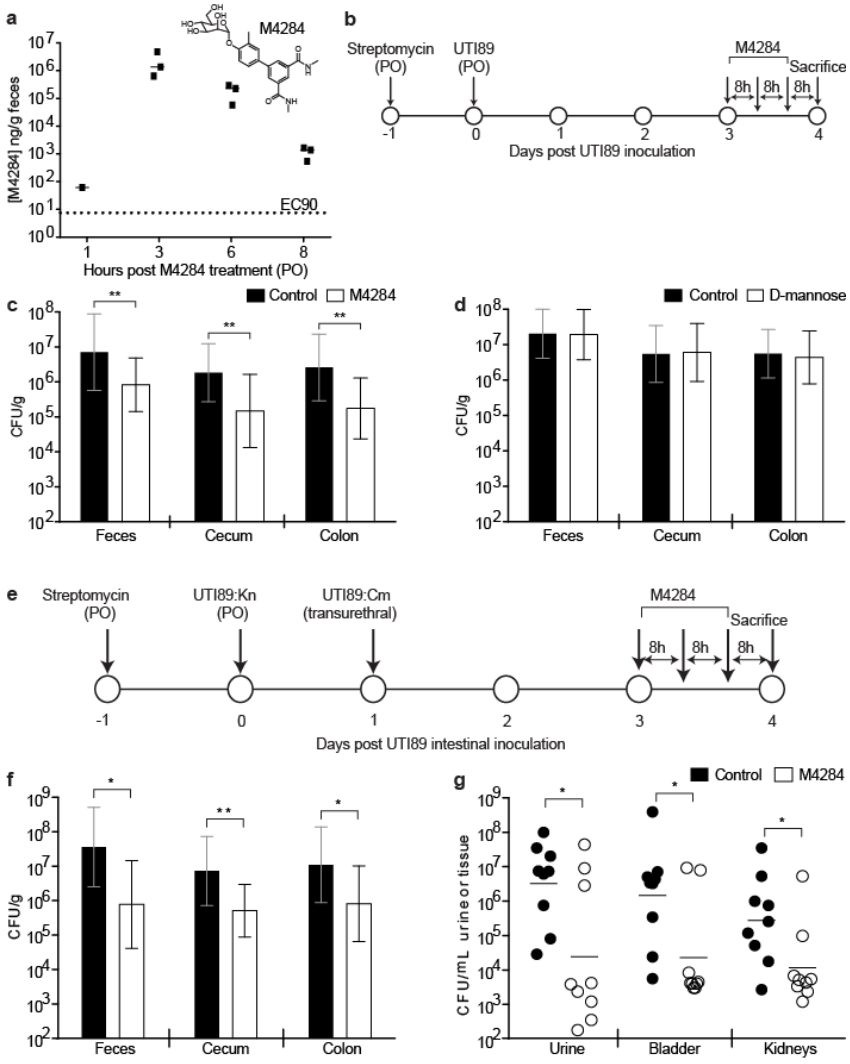

Figure 10. Mannoside simultaneously reduces the UPEC intestinal reservoir and treats UTI. (a) The concentration of M4284 in the feces of mice remains higher than the EC90 of the drug after a single, oral dose of 100mg/kg. (b) To test the efficacy of M4284 to target UTI89 in

the mouse intestine, mice were pretreated with streptomycin and colonized with UTI89. Starting at 3 days post colonization (dpc), mice were given 3 oral doses of M4284 (100mg/kg) or 10% cyclodextrin (control). (c) UTI89 levels in the feces and intestinal segments were assessed 8 h after the last dose of mannoside. (d) While mannoside treatment reduced the UTI89 intestinal load, treatment with D-mannose did not. (e) To determine if M4284 treatment can simultaneously treat an active UTI and target UPEC in the gut, mice were pretreated with streptomycin and then received an oral gavage of UTI89. One day later, they were given a UTI via a transurethral inoculation of this uropathogen. Two days later, they received 3 oral doses of M4284 (100mg/kg). M4284 reduces UTI89 titers in the gut (f) and urinary tract (g). Bars represent mean± SEM (a), geometric means ± SD (c,d,f), geometric mean (g) *$p<0.05$, **$p<0.01$ by Mann Whitney U test. n=9 mice, 2 replicates (panels f, g), n= 10 mice, 2 replicates (panel d)

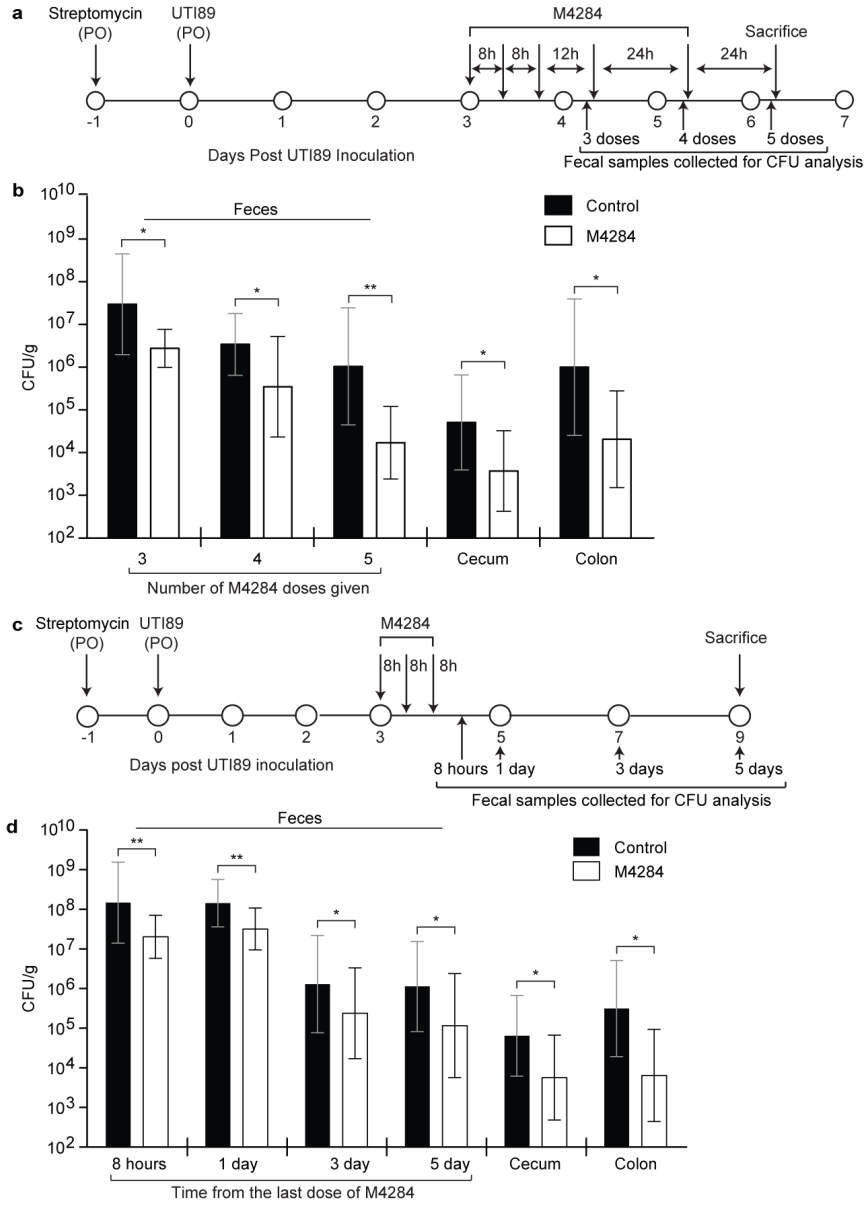

Figure 11. Testing the effects of more prolonged dosing of M4284 and analysis of the duration of its effects. (a) C3H/HeN mice from Envigo were given two additional doses of M4284 (5 doses total). (b) Animals treated as in panel (a) show a continued decrease in UTI89 levels in their feces (fecal samples were processed after 3, 4, and 5 doses of M4284), and at the time of sacrifice in the cecum and colon, compared to control mice treated with vehicle alone

(10% cyclodextrin). (c,d) The effects of mannoside treatment persist out to 5 days post M4284 exposure. Bars represent geometric mean ± SD, *p<0.05, **p<0.01 by Mann Whitney, n=9-10, 2 replicates (panel b), n=16 mice, 3 replicates (panel d).

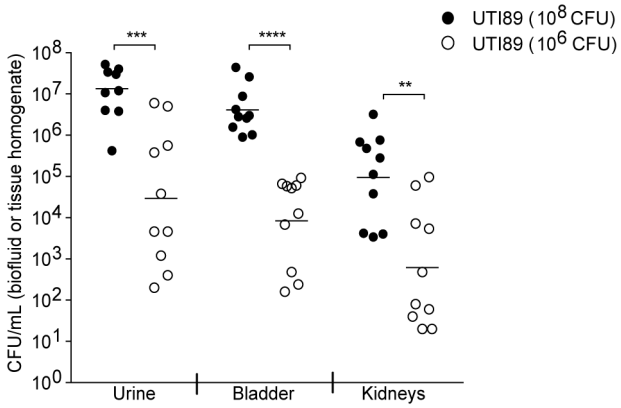

Figure 12. The severity of UTI outcome is directly linked to the dose of UTI89 inoculated into the urinary tract. C3H/HeN mice (Envigo) were given an experimental UTI via transurethral inoculation of either 10^8 or 10^6 CFU of UTI89. The doses were chosen to represent the reduction observed in intestinal UTI89 titers before and after treatment with the M4284 mannoside. Mice were sacrificed 24 hours after inoculation and UTI89 titers in urine, bladder, and kidneys were defined by quantifying CFU. Mice receiving the 10^6 dose of UTI89 had significantly fewer bacteria in all three biospecimen types, indicating an important relationship between the number of bacteria introduced into the urinary tract and the severity of UTI outcome. Bars represent geometric means, **p<0.01, ***p<0.001, ****p<0.0001 by Mann Whitney U test. n=10 mice, 2 replicates.

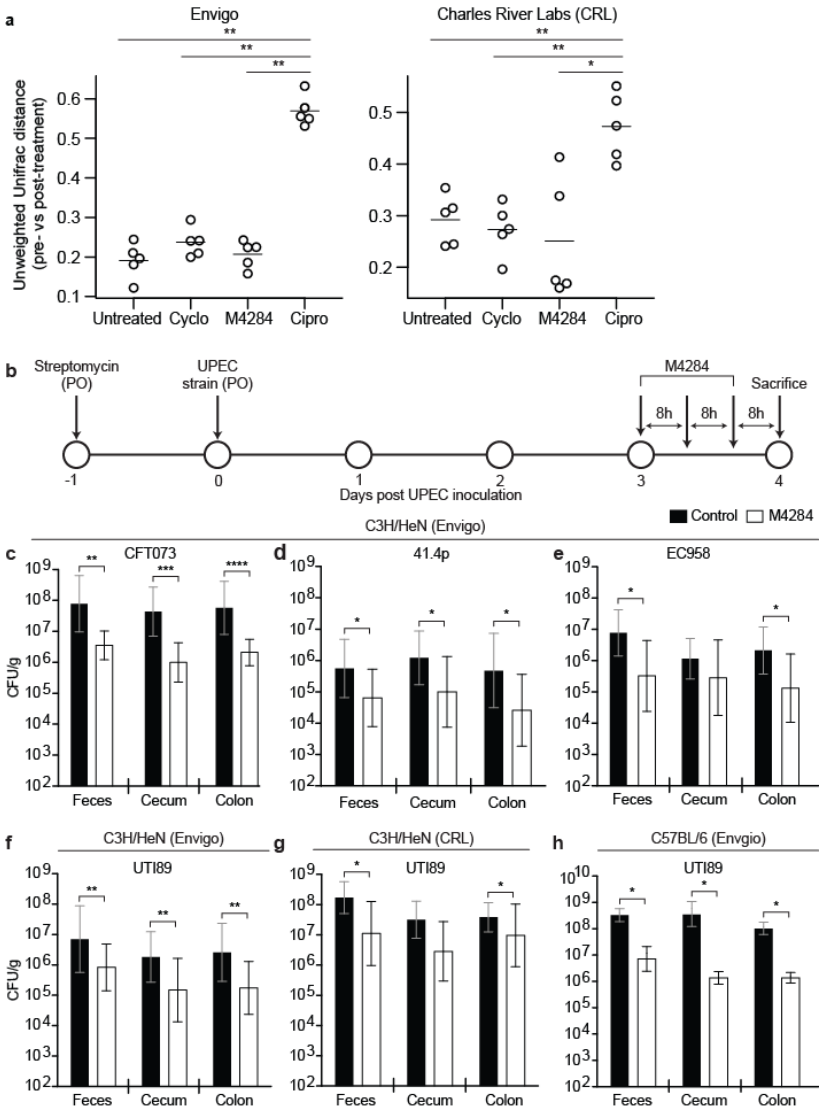

Figure 13. Mannoside treatment has minimal effect on the overall configuration of the fecal microbiota and targets different human UPEC isolates in mice with different genetic backgrounds. Mice were given one of the following treatments: (i) M4284 (100mg/kg; 3 doses over 24 h), (ii) cyclodextrin (10%, Cyclo; 3 doses over 24 h); or (iii) ciprofloxacin (Cipro; 15mg/kg; 2 doses over 24 h). Naïve, untreated mice served as controls (Untreated). Fecal community structure was defined by sequencing bacterial 16S rRNA gene amplicons. (a) For

each treatment performed on C3H/HeN mice obtained from Envigo and Charles Rivers Labs, the change in microbiota configuration was determined by measuring the unweighted UniFrac distance between samples obtained from each mouse before treatment and 24 h after they received their last dose (larger UniFrac distance equates to a larger shift in community structure (beta diversity)). (b) Mice of different genetic backgrounds were colonized by oral gavage with one of 4 different UPEC strains. At 3 dpc, mice were given 3 doses of M4284 and sacrificed 8 h after the last dose. (c-f) The intestinal tracts of C3H/HeN mice from Envigo labs were colonized by each of the genetically diverse human UPEC isolates. (g,h) The ability of M4284 to target UTI89 in C3H/HeN mice from Charles Rivers Labs (CRL) (panel g) and C57BL/6 mice from Envigo Labs (panel h) was also assessed. bar = median value. *$p<0.05$, **$p<0.01$ (Mann Whitney U test). n=5 mice, 1 replicate (panel a). Bars represent geometric means ± SD, *$p<0.05$, **$p<0.01$, ***$p<0.001$, ****$p<0.0001$ (Mann Whitney U test) (panels c-h). n=9-10 animals, 2 replicates (panels c-e, g-h); n=14-15 mice, 3 replicates (panel f)

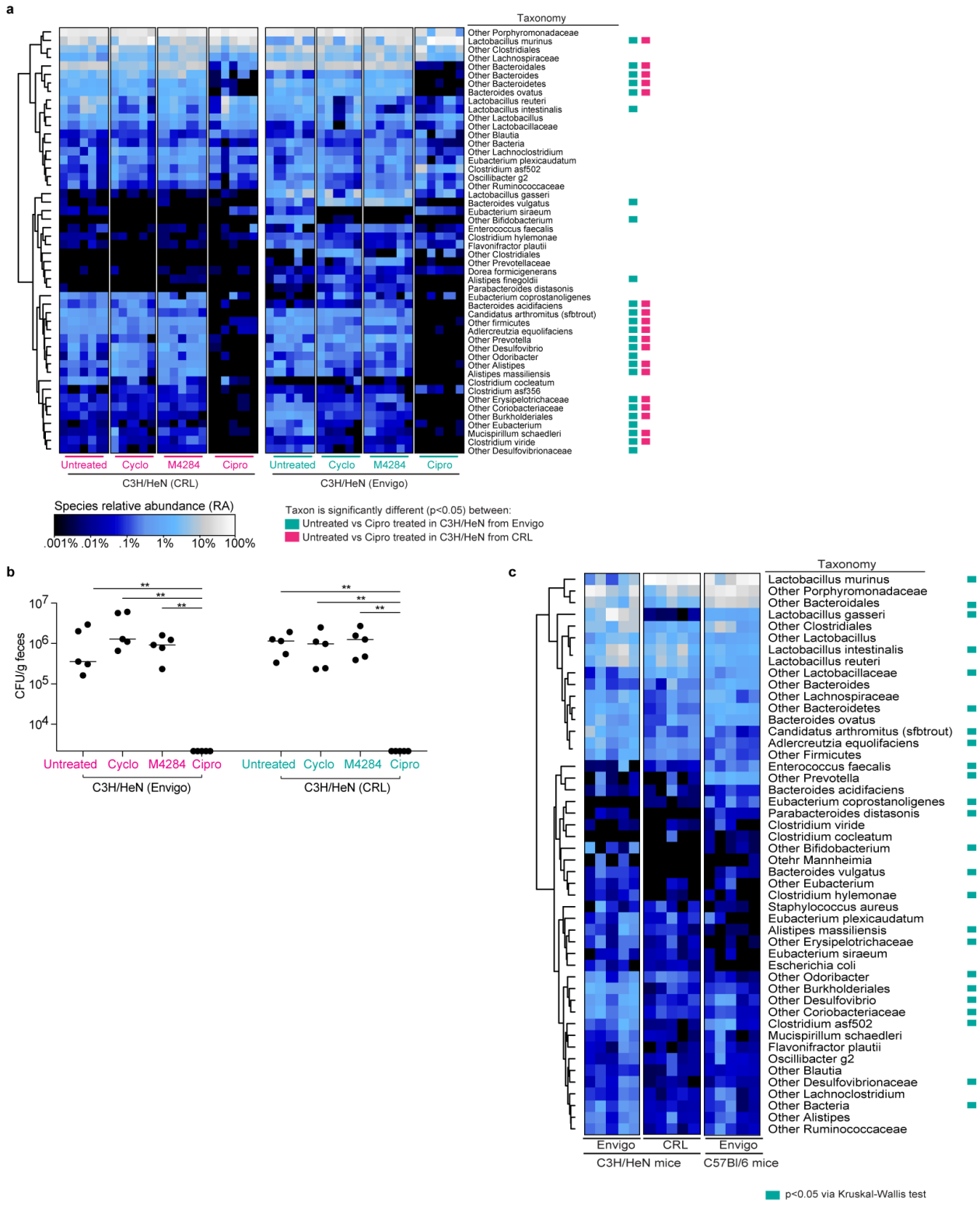
a
Taxonomy
Other Porphyromonadaceae
Lactobacillus murinus
Other Clostridiales
Other Lachnospiraceae
Other Bacteroidales
Other Bacteroides
Other Bacteroidetes
Bacteroides ovatus
Lactobacillus reuteri
Lactobacillus intestinalis
Other Lactobacillus
Other Lactobacillaceae
Other Blautia
Other Bacteria
Other Lachnoclostridium
Eubacterium plexicaudatum
Clostridium asf502
Oscillibacter g2
Other Ruminococcaceae
Lactobacillus gasseri
Bacteroides vulgatus
Eubacterium siraeum
Other Bifidobacterium
Enterococcus faecalis
Clostridium hylemonae
Flavonifractor plautii
Other Clostridiales
Other Prevotellaceae
Dorea formicigenerans
Alistipes finegoldii
Parabacteroides distasonis
Eubacterium coprostanoligenes
Bacteroides acidifaciens
Candidatus arthromitus (sfbtrout)
Other firmicutes
Adlercreutzia equolifaciens
Other Prevotella
Other Desulfovibrio
Other Odoribacter
Other Alistipes
Alistipes massiliensis
Clostridium cocleatum
Clostridium asf356
Other Erysipelotrichaceae
Other Coriobacteriaceae
Other Burkholderiales
Other Eubacterium
Mucispirillum schaedleri
Clostridium viride
Other Desulfovibrionaceae
Untreated
Cyclo
M4284
Cipro
C3H/HeN (CRL)
C3H/HeN (Envigo)
Species relative abundance (RA)
.001% .01% .1% 1% 10% 100%
Taxon is significantly different (p<0.05) between:
Untreated vs Cipro treated in C3H/HeN from Envigo
Untreated vs Cipro treated in C3H/HeN from CRL
b
CFU/g feces
Untreated
Cyclo
M4284
Cipro
C3H/HeN (Envigo)
C3H/HeN (CRL)
c
Taxonomy
Lactobacillus murinus
Other Porphyromonadaceae
Other Bacteroidales
Lactobacillus gasseri
Other Clostridiales
Other Lactobacillus
Lactobacillus intestinalis
Lactobacillus reuteri
Other Lactobacillaceae
Other Bacteroides
Other Lachnospiraceae
Other Bacteroidetes
Bacteroides ovatus
Candidatus arthromitus (sfbtrout)
Adlercreutzia equolifaciens
Other Firmicutes
Enterococcus faecalis
Other Prevotella
Bacteroides acidifaciens
Eubacterium coprostanoligenes
Parabacteroides distasonis
Clostridium viride
Clostridium cocleatum
Other Bifidobacterium
Otehr Mannheimia
Bacteroides vulgatus
Other Eubacterium
Clostridium hylemonae
Staphylococcus aureus
Eubacterium plexicaudatum
Alistipes massiliensis
Other Erysipelotrichaceae
Eubacterium siraeum
Escherichia coli
Other Odoribacter
Other Burkholderiales
Other Desulfovibrio
Other Coriobacteriaceae
Clostridium asf502
Mucispirillum schaedleri
Flavonifractor plautii
Oscillibacter g2
Other Blautia
Other Desulfovibrionaceae
Other Lachnoclostridium
Other Bacteria
Other Alistipes
Other Ruminococcaceae
Envigo
CRL
Envigo
C3H/HeN mice
C57Bl/6 mice
p<0.05 via Kruskal-Wallis test

Figure 14. 16S rRNA-based comparison of fecal bacterial communities in mice obtained from Envigo and Charles Rivers Labs and mice of different genetic backgrounds from a common vendor. (a) C3H/HeN mice were treated with M4284 (100mg/kg, 3 doses over 24 h), vehicle alone (10% cyclodextrin (Cyclo), 3 doses over 24 h), or ciprofloxacin (Cipro; 15mg/kg, 2 doses over 24 h). Untreated mice served as reference controls. Heatmaps show the effect of each of the treatments on animals from Charles Rivers Labs (CRL) and Envigo Labs (Envigo). Each row represents a species-level bacterial taxon, while each column represents a mouse sampled 24 hours after the termination of the indicated treatment. Colored boxes next to the taxon names indicate species whose relative abundance was significantly changed by Cipro treatment ($p<0.05$;Wilcoxon Signed Rank test with FDR correction). Individual comparisons between untreated and other treatment types did not disclose changes that were statistically significant by Wilcoxon Signed Rank test with FDR correction. (b) Corresponding fecal samples collected 24 h after treatments (as shown in Extended Data **Figure 8a**) were homogenized, diluted serially, and plated on MacConkey medium. The abundance of bacteria capable of growing on the selective medium was similar between fecal samples taken from untreated mice and those collected 24 hours after treatment with cyclodextrin and M4284. No colonies were detected from fecal samples collected 24 hours after ciprofloxacin treatment. n=5 mice, 1 replicate. Bars= median value, $^{**}p<0.001$ (Mann Whitney U test). (c) Comparison of the representation of bacterial taxa in the fecal microbiota of untreated mice obtained from different vendors or representing different genetic backgrounds. Each row in the heatmap represents a species-level taxon, while each column represents a mouse of the indicated genetic background from the indicated vendor. Colored boxes indicate species whose relative abundances were significantly different ($p<0.05$)

between all three groups of animals (Kruskal-Wallis test with FDR correction). Rows of each heatmap were hierarchically clustered according to pair-wise distances using Pearson correlation.

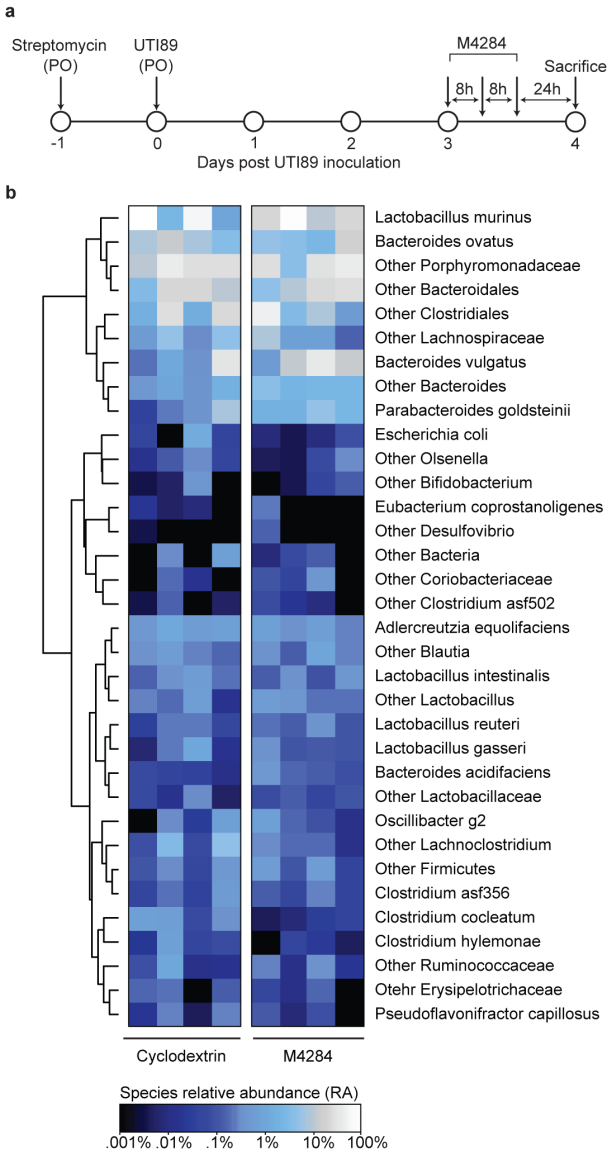

Figure 15. Bacterial 16S rRNA-based analysis showing that the fecal microbiota of C3H/HeN mice pretreated with streptomycin and colonized with UTI89 is minimally altered by M4284 treatment. (a) C3H/HeN mice from Envigo were pretreated with streptomycin and 24 h later colonized with UTI89 by oral gavage. Three days after inoculation, mice were treated with 3 doses of M4284 (100mg/kg, 3 doses over 24 h) or vehicle alone (10% cyclodextrin (Cyclo), 3 doses over 24 h). Fecal samples were collected 24 h after the last dose of M4284 or vehicle. (b) Heatmap showing the effect of each treatment type. Each row represents a

bacterial species-level taxon, while each column represents a mouse 24 h after the indicated treatment. Rows of the heatmap were hierarchically clustered according to pair-wise distances using Pearson correlation. No treatments produced changes that were statistically significant, as judged by Wilcoxon Signed Rank test with FDR correction.

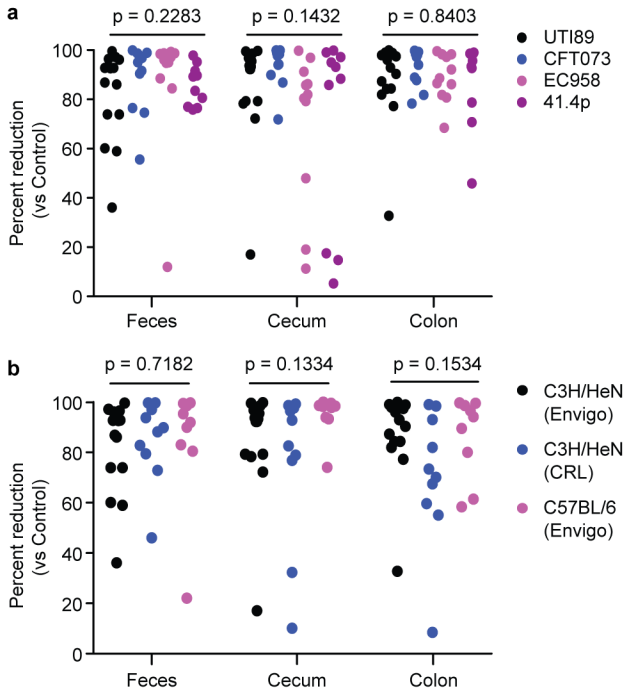

Figure 16. The percent reduction in strains by M4284 treatment is similar in mice colonized with genetically distinct human isolates and in multiple strains of mice colonized by UTI89. (a) The percent reduction in the indicated UPEC strains from M4284-treated versus untreated control C3H/HeN mice from Envigo (based on data presented in Fig. 4c-f). (b) These values were also determined for C3H/HeN mice from Charles Rivers Labs (CRL) and C57BL/6 mice from Envigo (based on data shown in Fig. 4g,h). P values based on Kruskal-Wallis test.

Chapter 4: Conclusions and Future Directions

Significance

The steady increase in the number of clinical infections caused by single and multi-drug resistant bacterial pathogens worldwide highlights the antibiotic crisis we currently face. A recent review on antimicrobial resistance headed by the British government has indicated that unless we intervene now, superbugs could kill more people than cancer by 2050.

One manifestation of this crisis are urinary tract infections (UTI) caused by UPEC. Over a hundred million people are affected by UTIs each year. The global prevalence of UPEC strains resistant to so-called 'last-line antibiotics' like fluoroquinolones and now carbepenems is increasing at an alarming rate and may foreshadow the end of the road for antibiotics in the treatment of some patients with UTIs.

The mechanisms by which UPEC cause acute and recurrent UTIs have been studied extensively; this includes analyses of the roles of chaperone-usher pathway (CUP) pili in colonization of the bladder and kidneys. While UPEC cause infection in the urinary tract, the gut is considered to serve as a primary reservoir from which UPEC strains can emerge to colonize the vagina and peri-urethral area, and subsequently the bladder. However, prior to my thesis work, little was known regarding the mechanism(s) by which UPEC is able to establish itself in the gut.

Ultimately, my research has provided significant advances in our knowledge of UPEC pathogenesis. My work revealed novel *E. coli* virulence factors (type 1 and F17-like pili) that

promote intestinal colonization by UPEC. Identification of a role for F17-like pili in intestinal colonization provides new insights into a previously uncharacterized CUP pilus type. Identification of a role for type 1 pili in intestinal colonization reveals a new, unexpected function for a pilus that is essential for infection in the bladder.

I also present a new antibiotic-sparing approach for precision targeting of UPEC in its intestinal reservoir. If taken to clinical practice, such a treatment would reduce the exposure of the gut bacterial community to antibiotics. Further, administration of high-affinity mannosides offers an opportunity to use these compounds as 'probes' to identify potential interactions between other members of the human gut microbial community and mannose-containing glycans present in the body. Overall, my thesis work provides a powerful example of how anti-microbial measures can selectively deplete a bacterial pathogen, within the context of the complex gut microbial community, during acute infection or from its asymptomatic reservoir.

Future Directions

Where is the UclD ligand-binding site?

Based on the structural homology between UclD and F17G, I identified a putative ligand-binding site on the crystal structure of UclD. Further, due to their location within the putative pocket, I identified six residues that I hypothesize to mediate ligand binding. Moving forward, it will be important to verify this putative binding site. One way to verify that this is the correct site would be a mutagenesis study. By mutating each of the hypothesized 'key' residues and assessing their ability to bind to the upper region of the colonic crypts in mouse sections, I would be able to confirm the location of the binding site. If none of the hypothesized residues result in the loss of crypt binding, then I would turn to *in silico* modeling to predict other regions of the

protein that could contain a ligand-binding site and perform a similar mutagenesis study. Identifying residues that are critical to ligand binding by UclD is necessary for the creation of small-molecule ligand antagonists that could be used to target the function of F17-like pili in the gut.

What is the ligand bound by UclD?

The other essential piece of information required to develop small-molecule ligand antagonists that target UclD is the identity of the ligand bound by the adhesin. No binding of UclD is observed to any ligands present on the Center for Functional Glycomics glycan array nor have we identified a ligand using differential scanning fluorimetry (DSF). However, my work suggests that the ligand bound by UclD is contained within an O-glycan. Excitingly, correspondence with Dr. Richard Cummings, the direction of the Center for Functional Glycomics, has indicated that the center is producing an array containing only structural variations of O-glycans. This 'O-glycan' array will provide a platform tailored toward finding a potential ligand(s) for UclD. In tandem with the "O-glycan" array, I would also perform *in silico* screens to identify ligands that bind virtually within the UclD binding pocket. This type of analysis would allow us to screen a large number of potential ligands, including those contained within O-glycans. Any ligands identified via *in silico* screens or through the 'O-glycan' array would be verified using differential scanning fluorimetry (DSF) and/or Bio-layer Interferometry (BLI).

Does oral mannoside treatment effect the commensal *E. coli* population?

In collaboration with Dr. Jeffrey Gordon and Dr. Andrew Kau, I was able to show that oral mannoside exposure has minimal effects on the overall structure of the mouse fecal microbiota. Interestingly, while most Enterobacteriaceae carry the *fim* operon[1-3], mannoside treatment does not significantly affect the abundance of intestinal Enterobacteriaceae, suggesting that these bacteria may not be expressing type 1 pili during mannoside exposure or that they reside within inaccessible intestinal habitats. However, further examination of the effects of mannoside treatment on gut colonization by different species/strains of Enterobacteriaceae is needed to more fully interpret the significance of these findings.

Because *E. coli* makes up a very small portion of the overall microbiota population, 16S rRNA sequencing is not the most sensitive way to explicitly determine the effect of oral mannoside treatment on this population. A better way to directly assess the effects of oral mannoside treatment on the commensal *E. coli* population would be to examine gnotobiotic mice harboring defined microbiota communities. After inoculating gnotobiotic mice with defined microbiota communities (made up of ~10-15 members that represent bacteria associated with the microbiota of healthy individuals, including different species/strains of Enterobacteriaceae), I could treat the mice with mannosides and then track the colonization levels of the organisms in the defined community, including levels of the type 1 pilus-encoding Enterobacteriaceae. This type of experiment would allow me to directly examine if and/or how mannoside treatment alters the colonization levels of Enterobacteriaceae. Further, performing this experiment in gnotobiotic mice that are also colonized intestinally by UPEC prior to oral mannoside treatment would allow me to determine if mannoside treatment selectively extirpates UPEC while leaving the rest of the microbiota, including the commensal *E. coli* strains, untouched.

One of my hypotheses for why mannoside treatment may not alter type-1 encoding commensal Enterobacteriaceae is that, unlike UPEC strains, these bacteria do not express type 1 pili in the gut. Examining which CUP pilus types are expressed by commensal *E. coli* in naïve mice (that have not been exposed to UPEC or streptomycin, or in mice that have been treated with streptomycin but not inoculated with UPEC) would begin to test the validity of this hypothesis. Performing RT-PCR on RNA extracted from feces, cecal content, or colon content from these mice would be one way to determine which CUP pilus types are being expressed by commensal Enterobacteriaceae. Additionally, I could inoculate gnotobiotic mice with *E. coli* strains that express genetically encoded fluorescent proteins. After treating these mice with a fluorescently conjugated mannoside, I could perform immunohistochemistry on colon sections from these mice. This would allow me to simultaneously investigate the expression of type-1 pili and delineate the localization of *E. coli* in this mouse model.

What are the mannoside structures that work best to target UPEC in the gut?

Not all available mannoside compounds have the same efficacy in the gut. Out of six compounds I tested, two compounds reduced UTI89 titers in the intestines, two had no effect, and two appear to slightly increase UTI89 colonization **(Figure 17)**. Differences in the efficacy of these compounds could be due to a number of variables, including: bioavailability in the gut and/or the ability to withstand cleavage by intestinal enzymes. Testing a panel of structurally distinct mannoside compounds with varied functional groups in our mouse model of UPEC intestinal colonization would provide some insight into which functional groups and core structures are the most effective *in vivo*. Further, analyzing the bioavailability (in the serum, feces, and urine) of compounds that both successfully and unsuccessfully target intestinal UPEC

in mice would provide insight into how changing the chemical structures of the compounds alters the ability of the compound to reach the desired host site.

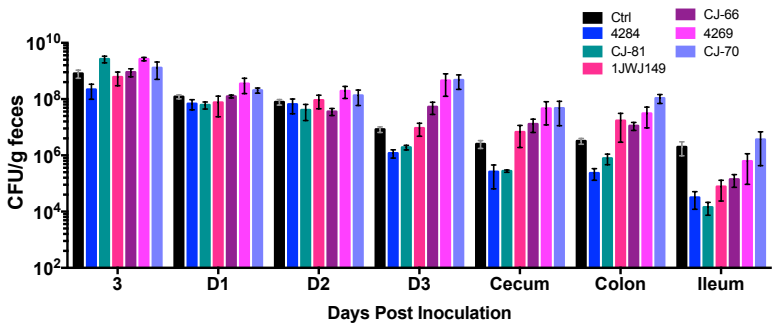

Figure 17. Not all mannoside compounds reduce the intestinal UPEC population. C3H/HeN female mice were pretreated with streptomycin and colonized with UTI89. Starting at 3 days post UTI89 colonization, mice were given three doses of a mannoside compound (100mg/kg) or 10% cyclodextrin (ctrl) (PO). UTI89 levels in the feces and intestinal tissue were assessed 8 hours after the last dose was given.

Does UPEC bind in the colonic crypts *in vivo*?

Using immunofluorescence (IF) studies, our collaborators in Han Remaut's lab found that the purified lectin domains of FimH and UclD bind to distinct areas within mouse colonic crypts. This led us to speculate that *in vivo*, FimH may promote binding to the upper region of the crypts and surface epithelial cuffs while UclD binds a ligand in the lower crypts. However, several limitations of this IF study are: 1) binding was assessed with purified protein, rather than with whole bacteria, and 2) we observed binding to colonic sections that were mounted on microscope slides, rather than *in vivo*.

To address the first point, we chose to examine binding with purified protein, rather than whole bacteria because using bacteria introduces variables that are difficult to control. For example, even when we grow UPEC strains under *in vitro* conditions shown to induce expression of type 1 pili, we still observe expression of other pili (S and P types), by RNA and functional analyses[3,4]. Furthermore, when we genetically engineer the promoter of *fimS* to remain in the Phase ON orientation, thus "locking ON" type 1 pilus expression, there is still some expression of other CUP pilus types[4]. Thus, obtaining a pure population of UPEC expressing exclusively one pilus type is not straightforward and complicated by co-expression of other pilus types. Therefore, we feel that using purified protein is currently the best way to explicitly characterize the role of a specific pilus type in tissue binding.

Addressing the second limitation of our study, colonic sections were used because imaging of bacterial binding *in vivo* is currently limited to techniques like *in vivo* bioluminescence imaging, which provides a general idea of the organ where binding is occurring but cannot provide the cellular detail we gain by imaging tissue sections. However, a major question derived from our findings that purified protein binds within the colonic crypts is: does UPEC bind within the crypts in mice and/or humans or is it an artifact of sectioning tissue?

In order to colonize the colonic epithelium, a bacterium first must overcome the formidable barriers established by the host. The first level of that barrier is the secretion of antimicrobial peptides (AMPs) by colonic enterocytes. AMPs like β-defensins and cathelicidins target a wide range of microbes, including gram positive and negative bacteria, fungi, and viruses, and work to dramatically reduce the number of microbes that can directly interact with the host surface[5]. The second major host barrier is the presence of colonic mucus. The mucus layer is made up of two layers, an outer and inner layer. The outer mucus layer is thicker than the

inner layer (~100 μm in mice) and is commonly colonized by bacteria[6]. The outer layer of mucus is constantly turning over and shedding older mucus into the lumen of the gut, which are then expelled in the feces. The shedding of the outer mucus layer makes it more difficult for bacteria to transit through this layer to colonize the inner layer or epithelium. The inner mucus layer is attached to the colonic epithelium and ranges in thickness from 50 μm in mice to over 100 μm in humans[6]. In the past, it was thought that the inner mucus layer is largely devoid of bacterial colonization. However, recent imaging studies using a fixative that preserves the mucus layer (Carnoy's Fixative) identified bacteria in a "significant fraction" of colonic crypts from healthy mice, indicating that this inner membrane is not sterile[7]. Interestingly, studies profiling crypt-associated bacterial communities using laser microdissection and sequencing found that this habitat is often enriched for Proteobacteria capable of aerobic metabolism, like *E. coli*[8].

However, for UPEC to colonize the crypts they must also be able to access and bind a ligand. Unfortunately, not knowing the ligand for the UclD adhesin limits our ability to determine if a corresponding ligand is present in the lower crypts. Nonetheless, we can explore the presence of a mannose containing ligand in this habitat.

Carcinoembryonic antigen-related cell adhesion molecules (CEACAMs) are a group of immunoglobulin-related glycoproteins that are highly mannosylated. Several CEACAM family members, including CEACAM1, CEACAM6, and CEACAM7, are associated with the normal colorectal mucosa[9]. Excitingly, one of these receptors, CEACAM7, has been shown to localize to the apical surface of highly differentiated epithelial cells in the colorectal mucosa, like those found in the upper crypts and in epithelial surface cuffs[9]. The presence of a highly mannosylated receptor in the same region were we observe FimH binding in our mouse colon sections, suggests that CEACAM7 might act as a ligand for FimH *in vivo*. Another CEACAM that has

been well studied is CEACAM6. While CEACAM6 is expressed at low levels within crypts of healthy individuals, CEACAM6 levels are elevated in the crypts of patients with colorectal cancer[9,10]. One study, using a chronic infection model of CEACAM6 expressing mice, showed that a B2 *E. coli* strain isolated from a patient with colon cancer persists to high levels in the gut, induces colon inflammation, epithelial damages and cell proliferation[11]. This study did not test whether colonization, in these mice, was mediated by type 1 pili, however, my findings suggest that this enhanced intestinal colonization could be mediated by the interaction between type 1 pili and CEACAM6. The ability of FimH to bind to the host intestinal surface *in vivo* is further supported by studies finding that patients with the IBD syndrome Crohn's disease (CD) express abnormally high levels of CEACAM6 on their ileal epithelium[12-15], which is bound by type 1 pili expressing adherent-invasive *E. coli* (AIEC).

Altogether, these data suggest that there is a mannose containing ligand in the upper colonic crypts that could be bound by FimH. However, the thick mucus layer, microbiota, and plethora of AMPs could make accessing the crypts challenging, particularly in a healthy host.

An interesting way to test the ability of FimH or UclD to bind within the crypts in a more physiological setting would be to use intestinal spheroid systems. Spheroids take advantage of proliferative stem/progenitor cells which can be rapidly expanded using conditioned media that contains signaling proteins that promote cellular growth (Wnt3a, R-spondin and Noggin)[16]. Upon differentiation, these cells maintain structural and cellular characteristics of intestinal cells. When grown on a transwell membrane, spheroids form crypts and functional, polarized monolayers covered by a secreted mucus[16]. While spheroids do not completely replicate the intestinal environment (they lack a microbiota and immune system), they would allow us to

determine if the adhesins bind to the same locations in human cells and in the presence of a mucus membrane.

Does the type of intestinal inflammation effect which CUP pili are used for gut colonization?

The majority of characterized CUP adhesins bind glycan moieties; therefore, any changes in the intestinal glycan landscape, including altered expression of glycosylated proteins, could expose ligands for CUP pilus types. Interestingly, previous work has found that the presence of distinct CUP pilus ligands differs between body sites/habitats and, in some cases, is influenced by inflammation. For example, Fml pili promote colonization of the bladder during chronic cystitis, a state of severe, chronic bladder inflammation[17]. The Fml pilus adhesin, FmlH, binds to Gal (β1-3) GalNAc, which is only expressed on the surface of the bladder epithelium during periods of bladder inflammation and remodeling. Accordingly, studies have found that intestinal disorders and dysbioses have divergent effects on the gut environment, altering the composition of the microbiota and stimulating distinct immune responses. Interestingly, the inflammatory state influences the intestinal glycan landscape in the gut of patients with CD. High levels of intestinal inflammation and/or bacterial dysbiosis cause patients with CD to express abnormally high levels of CEACAM6 on their ileal epithelium[12-15]. And as stated before, CEACAM6 is bound by type 1 pili expressing adherent-invasive *E. coli* (AIEC).

To determine how distinct types of intestinal inflammation alter the role of CUP pili in UPEC intestinal colonization, I would examine the ability of individual CUP pilus mutant strains to compete with the isogenic wildtype strain (UTI89) in IL-10 deficient mice, which are prone to spontaneous colitis[18], or in mice treated with dextran sulfate sodium (DSS). DSS is a chemical

inducer of colitis and is an accepted mouse model of IBD[19,20]. DSS, which results in the recruitment of mainly neutrophils to the gut, has a different inflammatory response than streptomycin, which results in recruitment of both neutrophils and inflammatory monocytes[20-23]. Interestingly, I found that treating C3H/HeN mice with DSS, *ad libitum*, greatly enhances UPEC intestinal fitness (**Figure 18**). In DSS treated mice, UTI89 colonization of the gut occurs for a more protracted period of time than is observed in streptomycin treated mice. The distinct impact of these two treatments on the intestinal environment may effect the intestinal glycan landscape in a way that effects which CUP pilus types are used by UPEC to colonize the intestine.

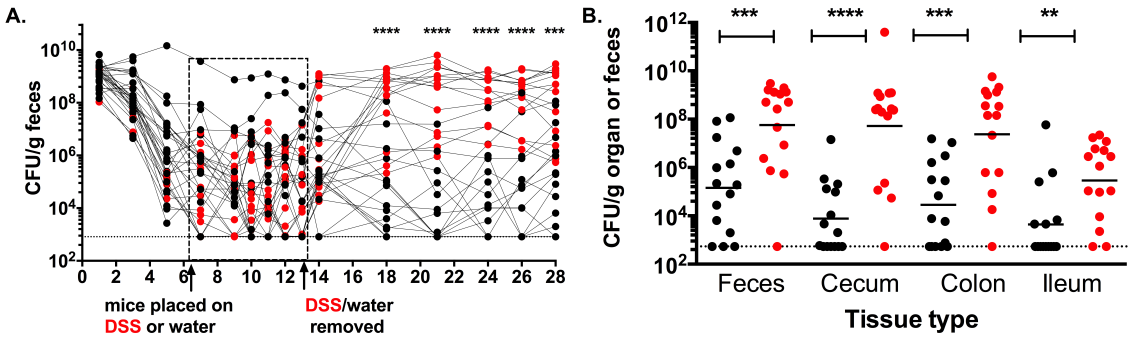

Figure. 18. Stimulating acute colitis in mice increases UTI89 intestinal colonization. Streptomycin treated mice were colonized with UTI89. Starting at 7 days post infection (dpi) mice were provided drinking water supplemented with (red) or without (black) 3% DSS. Longitudinal fecal (A) and tissue (B) (at 28 dpi) show that DSS treatment enhances UPEC intestinal colonization. Mann-Whitney U test, **p<0.01, ***p<0.001, ***p<0.0001.

Which CUP pili promote intestinal colonization by other uropathogens and enteropathogens?

Like UPEC, other uropathogens (such as Proteus, Enterobacter, and Klebsiella species) reside in the gut and are able to cause UTI after being shed in the feces and entering the bladder. However, the bacterial factors that promote intestinal colonization by these uropathogens are understudied. Each of these bacterial species encode a range of CUP pilus types, some of which have been shown to promote UTI[1]. For example, in a mouse model of UTI caused by *Klebsiella pneumoniae*, type 1-mediated binding to mannose is indispensible for invasion into urothelial cells and the formation of IBCs[24]. Yet, a role for CUP pilus types utilizes by these uropathogens in the gut has not been explored. This is an interesting question to pursue since many of these organisms contain CUP pili that are distinct from those carried by UTI89 (for example, Klebsiella species carry type 3 pili, which are absent in UPEC) and thus may uncover roles for other uncharacterized pilus types. Further, identifying bacterial factors, like CUP pilus types, that promote colonization of these non-UPEC uropathogens in the gut is necessary to gain insight into how these organisms cause disease in the host and may provide targets for anti-adhesive drugs.

Following the same experimental plan outlined in Chapter 2, I would identify CUP pilus types that promote intestinal colonization by non-UPEC uropathogens (i.e. creating individual CUP pilus deletion mutants in each background strain and test their ability to compete with an isogenic wildtype strain in the streptomycin mouse model). A benefit of this experimental plan is that it can also be adapted to identify CUP pilus types that promote intestinal colonization by enteropathogens, like AIEC.

Moreover, identification of intestinally expressed CUP pilus types and their corresponding ligands for non-UPEC uropathogens or enteropathogens could allow for the development of ligand antagonists, like mannosides.

An exciting finding would be identifying a role for type 1 pili in intestinal colonization by any of the non-UPEC strains, as this would allow us to test the efficacy of mannosides to target these organisms in the gut.

Perhaps one of the most promising candidates would be Klebsiella species, which carry type 1 pili and, like UPEC, have been shown to use these pili during UTI[24]. If type 1 pili promote Klebsiella intestinal colonization then oral mannoside treatment might be effective at targeting and reducing the Klebsiella population in both the gut and bladder.

Of note, however, sequence variation in the FimH adhesin between UPEC strains and *K. pneumoniae* results in differences in the function of the type 1 pilus in the bladder. In *K. pneumonia,* for example, FimH-dependent biofilm formation is inhibited by heptyl mannose, but not methyl mannose, suggesting that mannose binding to the *K. pneumoniae* FimH may involve contacting residues outside of the mannose binding pocket and thus may be more complex than what occurs in UPEC [24]. Changes in the mannose-FimH interaction in Klebsiella might alter the ability of mannosides to effectively target this organism in the gut. In this case, examining the ability of mannoside to target and reduce type-1 expressing Klebsiella from binding to guinea pig red blood cells *in vitro* (via hemagglutination assays), would be a good start to determine if mannoside could block FimH activity of Klebsiella species.

Another promising candidate might be AIEC, which use type 1 pili and FimH to bind to ligands present in the gut. As discussed earlier, AIEC use type 1 pili to bind to CEACAM6 on the ileal surface during period of intestinal inflammation. To determine if oral mannoside treatment could target and reduce the AIEC population and potentially reduce intestinal inflammation in CD patients, I would intestinally colonize mice (either using my streptomycin model or using IL-10 KO mice) with AIEC and then treat the mice with mannosides. Assessing

the overall number of AIEC present in treated versus control mice would allow me to examine if mannosides target AIEC in the gut.

It would also be interesting to determine if mannoside treatment has any effect on the level or type of intestinal inflammation or the overall structure of the microbiota in mice with IBD-like syndromes (IL-10 deficient mice or DSS treated mice). Microbial dysbiosis is associated with the onset and/or severity of IBD in patients. Therefore, if mannoside treatment is able to reduce the AIEC population in the gut, it might free up niche space or nutrients for competing organisms and thus alter the microbiota structure in a way that could change the inflammatory state. Performing cytokine analyses on serum and fecal, cecal, or colon contents from mice treated with mannosides would provide insight into any effects mannoside treatment might have on the inflammatory state of mouse models of IBD. Further, 16S rRNA profiling of the fecal microbiota of these mice would also allow me to determine how oral mannoside treatment alters the structure of the gut microbiota.

Will oral mannoside treatment work to reduce UPEC in the gut and bladder of humans?

In the end, evaluation of the efficacy and safety of mannosides in the treatment and prevention of UTI in humans will require clinical trials. I envision that such a trial would enroll young females (college age) who have a history of chronic/recurrent UTI (3 or more UTIs a year). Upon experiencing a UTI, these women would be enrolled into the study, an enrollment urine and fecal sample would be collected, and they would receive treatment with an appropriate antibiotic. Following this, half of the women would receive long-term daily treatment with an oral mannoside and half the women would be treated with a placebo control. Longitudinal fecal collection would take place, allowing us to examine the effect of mannoside on the UPEC

population in the gut and on the overall structure of the microbiota over time. Rates of recurrent UTI would also be determined in control vs. mannoside treated individuals.

This study design, which mimics a study that has been done to examine the affects of drinking cranberry juice on UTI frequency[25], would evaluate the efficacy of mannoside treatment on reducing the rate of recurrent UTIs and its effect on the bacteria present in the gut microbiota.

How will UPEC develop resistance to mannosides?

The ability of bacteria to develop and spread resistance to therapeutics and antibiotics is causing a major health care crisis. Creating treatments, like mannosides that can selectively target specific bacteria while leaving the remainder of the microbiota unharmed could help to slow the development and spread of resistance. However, what are the chances that UPEC will develop resistance to mannosides, leaving these compounds ineffective?

Bacteria spread resistance through vertical transmission, where mutations that promote resistance are passed through a population by replication, or through horizontal transmission, where resistance genes can be swapped from one microbe to another. Regardless of how a microbe acquires them, resistance genes can function through a number of distinct mechanisms, including: i) making the cell wall impermeable to the drug, ii) altering the protein bound by the drug, iii) producing an enzyme(s) that cleaves the drug into an inactive form or degrade it, or iv) removing the drug from inside the cell via efflux pumps or transporters[26]. Because mannosides target a virulence factor expressed on the extracellular surface of UPEC, resistance mechanisms that prevent the drug from entering or remaining in the bacterial cell are not of concern. While UPEC might develop or recycle an enzyme to cleave mannosides, this enzyme would need to differentiate mannosides from mannose or risk cleaving the endogenous ligand for the type 1

pilus. Altering the protein bound by the mannosides is also possible, however, there are several reasons why this method of resistance is also not ideal for UPEC.

To develop resistance in this manner, UPEC would need to evolve a FimH protein that is resistant to mannoside binding but retains its ability to bind mannose. However, type 1 pili and the FimH adhesin are highly conserved throughout enterobacteriaceae. In fact, the residues that make up the FimH binding pocket are invariant among all sequenced UPEC strains. Further, unlike antibiotics that kill or stall bacterial growth, mannosides prevent the function of a non-essential colonization factor, creating less selective pressure to develop resistance to the drug.

Despite all this, the development of resistance to mannosides is certainly possible. It may be possible to predict the type of genetic mutations that would provide resistance. Random mutagenesis of the FimH protein followed by screening these mutagenized adhesins for variants that retain D-mannose binding but are resistant to mannoside might provide a resistant variant

What other bacterial genes are important for UPEC intestinal colonization?

I anticipate that bacterial genes other than CUP pili play a role in UPEC intestinal colonization. To determine what other genes are important for gut colonization, I would first want to assess the feasibility of performing a broad unbiased mutagenesis screen of UPEC in the gut. First, I would test for an intestinal bottleneck using an isogenic set of UTI89 derivatives, each carrying a unique genetic barcode tag[27]. A gut colonization bottleneck would preclude my ability to assess the fitness of large collections of different mutants simultaneously in the gut model, and thus make the screening of large random mutant library impractical. If there is no severe gut colonization bottleneck, I would use a transposon mutant library that is already made in UTI89 and screen for mutations that are defective in gut colonization using TnSeq[28].

Impact and Closing Remarks

In this work, I identify novel *E. coli* virulence factors (type 1 and F17-like pili) that promote intestinal colonization. I also present a new antibiotic-sparing approach for precision targeting of UPEC in its intestinal reservoir. If taken to clinical practice, such a treatment would reduce the exposure of the gut bacterial community to antibiotics. Further, administration of high-affinity mannosides offers an opportunity to use these compounds as 'probes' to identify potential interactions between other members of the human gut microbial community and mannose-containing glycans present in this body habitat that affect their fitness.

Identification of the F17-like pilus in intestinal colonization provides new insights into a previously uncharacterized CUP pilus type. This data suggest, unexpectedly, that extra-intestinal pathogenic *E. coli*, like UPEC, acquired an F17-family CUP from intestinal pathogens, and evolved it into a unique virulence factor that promotes the establishment and/or maintenance of an asymptomatic UPEC intestinal reservoir. Identification of genes involved in UPEC colonization of the gut provide new avenues for therapeutic development and may also provide a method to stratify UTI patients for epidemiologic studies of recurrent disease risk as well as for proof of concept clinical studies of the efficacy of CUP-directed treatment regimens: end point markers for such studies could include reduction/elimination of the intestinal reservoir, treatment of acute UTI and reduction in rUTI.

References

1 Wurpel, D. J., Beatson, S. A., Totsika, M., Petty, N. K. & Schembri, M. A. Chaperone-usher fimbriae of Escherichia coli. *PloS One* **8**, e52835, doi:10.1371/journal.pone.0052835 (2013).

2 Jones, C. H. *et al.* FimH adhesin of type 1 pili is assembled into a fibrillar tip structure in the Enterobacteriaceae. *Proc Natl Acad Sci USA* **92**, 2081-2085 (1995).

3 Schreiber, H. L. t. *et al.* Bacterial virulence phenotypes of Escherichia coli and host susceptibility determine risk for urinary tract infections. *Science Translational Med* **9**, doi:10.1126/scitranslmed.aaf1283 (2017).

4 Greene, S. E. *et al.* Pilicide ec240 disrupts virulence circuits in uropathogenic Escherichia coli. *mBio* **5**, e02038, doi:10.1128/mBio.02038-14 (2014).

5 Gallo, R. L. & Hooper, L. V. Epithelial antimicrobial defence of the skin and intestine. *Nature Reviews Immunology* **12**, 503-516, doi:10.1038/nri3228 (2012).

6 Hansson, G. C. Role of mucus layers in gut infection and inflammation. *Current Opinion Microbiol* **15**, 57-62, doi:10.1016/j.mib.2011.11.002 (2012).

7 Swidsinski, A., Loening-Baucke, V., Lochs, H. & Hale, L. P. Spatial organization of bacterial flora in normal and inflamed intestine: a fluorescence in situ hybridization study in mice. *J Gastroenterology : WJG* **11**, 1131-1140 (2005).

8 Pedron, T. *et al.* A crypt-specific core microbiota resides in the mouse colon. *mBio* **3**, doi:10.1128/mBio.00116-12 (2012).

9 Scholzel, S. *et al.* Carcinoembryonic antigen family members CEACAM6 and CEACAM7 are differentially expressed in normal tissues and oppositely deregulated in hyperplastic colorectal polyps and early adenomas. *Am Journal of Pathology* **156**, 595-605, doi:10.1016/S0002-9440(10)64764-5 (2000).

10 Jantscheff, P. *et al.* Expression of CEACAM6 in resectable colorectal cancer: a factor of independent prognostic significance. *J Clinical Oncology* **21**, 3638-3646, doi:10.1200/JCO.2003.55.135 (2003).

11 Raisch, J. *et al.* Colon cancer-associated B2 Escherichia coli colonize gut mucosa and promote cell proliferation. *J Gastroenterology : WJG* **20**, 6560-6572, doi:10.3748/wjg.v20.i21.6560 (2014).

12 Barnich, N. & Darfeuille-Michaud, A. Abnormal CEACAM6 expression in Crohn disease patients favors gut colonization and inflammation by adherent-invasive E. coli. *Virulence* **1**, 281-282, doi:10.4161/viru.1.4.11510 (2010).

13 Dreux, N. *et al.* Point mutations in FimH adhesin of Crohn's disease-associated adherent-invasive Escherichia coli enhance intestinal inflammatory response. *PLoS Pathogens* **9**, e1003141, doi:10.1371/journal.ppat.1003141 (2013).

14 Barnich, N. *et al.* CEACAM6 acts as a receptor for adherent-invasive E. coli, supporting ileal mucosa colonization in Crohn disease. *J Clinical Investigation* **117**, 1566-1574, doi:10.1172/JCI30504 (2007).

15 Carvalho, F. A. *et al.* Crohn's disease adherent-invasive Escherichia coli colonize and induce strong gut inflammation in transgenic mice expressing human CEACAM. *J Experimental Med* **206**, 2179-2189, doi:10.1084/jem.20090741 (2009).

16 VanDussen, K. L. *et al.* Development of an enhanced human gastrointestinal epithelial culture system to facilitate patient-based assays. *Gut* **64**, 911-920, doi:10.1136/gutjnl-2013-306651 (2015).

17 Conover, M. S. *et al.* Inflammation-Induced Adhesin-Receptor Interaction Provides a Fitness Advantage to Uropathogenic E. coli during Chronic Infection. *Cell Host & Microbe* **20**, 482-492, doi:10.1016/j.chom.2016.08.013 (2016).

18 Rennick, D. M. & Fort, M. M. Lessons from genetically engineered animal models. XII. IL-10-deficient (IL-10(-/-) mice and intestinal inflammation. *Am J Physiology.* **278**, G829-833 (2000).

19 Wirtz, S., Neufert, C., Weigmann, B. & Neurath, M. F. Chemically induced mouse models of intestinal inflammation. *Nature Protocols* **2**, 541-546, doi:10.1038/nprot.2007.41 (2007).

20 Rose, W. A., 2nd, Sakamoto, K. & Leifer, C. A. Multifunctional role of dextran sulfate sodium for in vivo modeling of intestinal diseases. *BMC Immunology* **13**, 41, doi:10.1186/1471-2172-13-41 (2012).

21 Ni, J., Chen, S. F. & Hollander, D. Effects of dextran sulphate sodium on intestinal epithelial cells and intestinal lymphocytes. *Gut* **39**, 234-241 (1996).

22 Barthel, M. *et al.* Pretreatment of Mice with Streptomycin Provides a Salmonella enterica Serovar Typhimurium Colitis Model That Allows Analysis of Both Pathogen and Host. *Infection and immunity* **71**, 2839-2858, doi:10.1128/iai.71.5.2839-2858.2003 (2003).

23 Spees, A. M. *et al.* Streptomycin-induced inflammation enhances Escherichia coli gut colonization through nitrate respiration. *mBio* **4**, doi:10.1128/mBio.00430-13 (2013).

24 Rosen, D. A. *et al.* Molecular variations in Klebsiella pneumoniae and Escherichia coli FimH affect function and pathogenesis in the urinary tract. *Infection and Immunity* **76**, 3346-3356, doi:10.1128/IAI.00340-08 (2008).

25 Maki, K. C. *et al.* Consumption of a cranberry juice beverage lowered the number of clinical urinary tract infection episodes in women with a recent history of urinary tract infection. *Am J Clin Nutr* **103**, 1434-1442, doi:10.3945/ajcn.116.130542 (2016).

26 Sommer, G. D. a. M. O. A. How to Fight Back Against Resistance. *American Scientist* **102**, 42-51 (2014).

27 Schwartz, D. J., Chen, S. L., Hultgren, S. J. & Seed, P. C. Population dynamics and niche distribution of uropathogenic Escherichia coli during acute and chronic urinary tract infection. *Infection and Immunity* **79**, 4250-4259, doi:10.1128/IAI.05339-11 (2011).

28 van Opijnen, T., Bodi, K. L. & Camilli, A. Tn-seq: high-throughput parallel sequencing for fitness and genetic interaction studies in microorganisms. *Nature Methods* **6**, 767-772, doi:http://www.nature.com/nmeth/journal/v6/n10/suppinfo/nmeth.1377_S1.html (2009).

Supplementary Tables

Supplementary Table 1: The phylogenetic relationships between F17 homologs as

determined by comparing relatedness of bacterial usher gene sequences.

ENA Sequence ID	Name of Sequence	Percent Identity to UTI89 uclC
ABE10308	Escherichia coli UTI89 putative F17-like fimbrial usher	100
EFJ62248	Escherichia coli MS 200-1 fimbrial usher protein	100
EFU54800	Escherichia coli MS 153-1 fimbrial usher protein	100
EGB83651	Escherichia coli MS 60-1 fimbrial usher protein	100
ESE31717	Escherichia coli A35218R fimbrial usher protein	100
ADN73675	Escherichia coli UM146 putative F17-like fimbrial usher	100
ALD32943	Escherichia coli F17 fimbrial usher	100
EDV68536	Escherichia coli F11 fimbrial usher protein	100
ELC94190	Escherichia coli KTE191 F17-like fimbrial usher	100
ELD03594	Escherichia coli KTE201 F17-like fimbrial usher	100
ELD16276	Escherichia coli KTE206 F17-like fimbrial usher	100
ELE16801	Escherichia coli KTE55 F17-like fimbrial usher	100
ELF44072	Escherichia coli KTE8 F17-like fimbrial usher	100
ELH71006	Escherichia coli KTE215 F17-like fimbrial usher	100
ELI17337	Escherichia coli KTE106 F17-like fimbrial usher	100
ELI42231	Escherichia coli KTE124 F17-like fimbrial usher	100
ELI66860	Escherichia coli KTE131 F17-like fimbrial usher	100
ELI88553	Escherichia coli KTE145 F17-like fimbrial usher	100
EQN12131	Escherichia coli HVH 4 (4-7276109) F17-like fimbrial usher	100
EQO02162	Escherichia coli HVH 28 (4-0907367) F17-like fimbrial usher	100
EQP01733	Escherichia coli HVH 56 (4-2153033) F17-like fimbrial usher	100
EQP59624	Escherichia coli HVH 77 (4-2605759) F17-like fimbrial usher	100
EQQ43504	Escherichia coli HVH 100 (4-2850729) F17-like fimbrial usher	100
EQQ70585	Escherichia coli HVH 111 (4-7039018) F17-like fimbrial usher	100
EQQ80267	Escherichia coli HVH 112 (4-5987253) F17-like fimbrial usher	100
EQS09284	Escherichia coli HVH 143 (4-5674999) F17-like fimbrial usher	100
EQS64201	Escherichia coli HVH 161 (4-3119890) F17-like fimbrial usher	100
EQS94171	Escherichia coli HVH 171 (4-3191958) F17-like fimbrial usher	100
EQV28377	Escherichia coli KOEGE 30 (63a) F17-like fimbrial usher	100
EQV75237	Escherichia coli KOEGE 70 (185a) F17-like fimbrial usher	100
EQX61640	Escherichia coli UMEA 3185-1 F17-like fimbrial usher	100
EQX71663	Escherichia coli UMEA 3193-1 F17-like fimbrial usher	100
EQY26881	Escherichia coli UMEA 3220-1 F17-like fimbrial usher	100
EQY49990	Escherichia coli UMEA 3244-1 F17-like fimbrial usher	100
EQZ33281	Escherichia coli UMEA 3617-1 F17-like fimbrial usher	100
ERA15291	Escherichia coli UMEA 3834-1 F17-like fimbrial usher	100
ERA29104	Escherichia coli UMEA 3955-1 F17-like fimbrial usher	100
ERA85411	Escherichia coli HVH 228 (4-7787030) F17-like fimbrial usher	100
ERB29121	Escherichia coli UMEA 3298-1 F17-like fimbrial usher	100
ESK12150	Escherichia coli UMEA 3290-1 F17-like fimbrial usher	100
ESK22344	Escherichia coli UMEA 3426-1 F17-like fimbrial usher	100
ESK23671	Escherichia coli UMEA 3693-1 F17-like fimbrial usher	100
ETF18627	Escherichia coli HVH 23 (4-6066488) F17-like fimbrial usher	100
EZQ53413	Escherichia coli BIDMC 83 F17-like fimbrial usher	100
KDG55831	Escherichia coli CHS 69 hypothetical protein	100
KDN08559	Escherichia coli Outer membrane usher protein htrE precursor	100
KDO88538	Escherichia coli F17 fimbrial usher	100
KDT41029	Escherichia coli 3-105-05_S4_C2 type VII secretion system (T7SS), usher family protein	100

KDY41355	Escherichia coli 2-427-07_S4_C2 type VII secretion system (T7SS), usher family protein	100
KEJ39633	Escherichia coli 2-460-02_S1_C3 type VII secretion system (T7SS), usher family protein	100
KEO42424	Escherichia coli 2-460-02_S1_C2 type VII secretion system (T7SS), usher family protein	100
KIE65152	Escherichia coli F17 fimbrial usher	100
KLX09881	Escherichia coli F17-like fimbrial usher	100
KLX89280	Escherichia coli F17-like fimbrial usher	100
KLX98072	Escherichia coli F17-like fimbrial usher	100
KLY02293	Escherichia coli F17-like fimbrial usher	100
KNY00060	Escherichia coli F17 fimbrial usher	100
KSX67622	Escherichia coli F17 fimbrial usher	100
KSX77117	Escherichia coli F17 fimbrial usher	100
KSY42022	Escherichia coli F17 fimbrial usher	100
KTK66169	Escherichia coli F17 fimbrial usher	100
KUR86703	Escherichia coli F17 fimbrial usher	100
KUS25287	Escherichia coli F17 fimbrial usher	100
KUS30331	Escherichia coli F17 fimbrial usher	100
KUS39441	Escherichia coli F17 fimbrial usher	100
KUS56802	Escherichia coli F17 fimbrial usher	100
KUS66696	Escherichia coli F17 fimbrial usher	100
KUS97674	Escherichia coli F17 fimbrial usher	100
KUS99347	Escherichia coli F17 fimbrial usher	100
KUV71654	Escherichia coli F17 fimbrial usher	100
KUW51062	Escherichia coli F17 fimbrial usher	100
KUW91068	Escherichia coli F17 fimbrial usher	100
KUW97800	Escherichia coli F17 fimbrial usher	100
KUX04485	Escherichia coli F17 fimbrial usher	100
KUX29835	Escherichia coli F17 fimbrial usher	100
KXL01352	Escherichia coli F17 fimbrial usher	100
KZH53165	Escherichia coli F17 fimbrial usher	100
KZH65083	Escherichia coli F17 fimbrial usher	100
KZJ04397	Escherichia coli F17 fimbrial usher	100
KZP40296	Escherichia coli F17 fimbrial usher	100
AJM76553	Escherichia coli RS218 F17 fimbrial usher	100
KIE78191	Escherichia coli RS218 F17 fimbrial usher	100
ELC78257	Escherichia coli KTE189 F17-like fimbrial usher	100
ELI07650	Escherichia coli KTE104 F17-like fimbrial usher	100
EQW59606	Escherichia coli UMEA 3113-1 F17-like fimbrial usher	100
ERA28987	Escherichia coli UMEA 4075-1 F17-like fimbrial usher	100
EQV60654	Escherichia coli KOEGE 58 (171a) F17-like fimbrial usher	99.9
EOV01926	Escherichia coli KTE195 F17-like fimbrial usher	100
EQP64368	Escherichia coli HVH 78 (4-2735946) F17-like fimbrial usher	100
EQV60901	Escherichia coli KOEGE 58 (171a) F17-like fimbrial usher	99.9
ELL39501	Escherichia coli J96 putative F17-like fimbrial usher	99.7
KLX25294	Escherichia coli F17-like fimbrial usher	99.7
ELD47794	Escherichia coli KTE224 F17-like fimbrial usher	99.7
ELE94443	Escherichia coli KTE87 F17-like fimbrial usher	99.7
ELF33437	Escherichia coli KTE169 F17-like fimbrial usher	99.7
ELF79243	Escherichia coli KTE43 F17-like fimbrial usher	99.7
ELH90555	Escherichia coli KTE218 F17-like fimbrial usher	99.7
ELJ02444	Escherichia coli KTE153 F17-like fimbrial usher	99.7
ELJ33477	Escherichia coli KTE168 F17-like fimbrial usher	99.7
EQN27402	Escherichia coli HVH 7 (4-7315031) F17-like fimbrial usher	99.7
EQN57805	Escherichia coli HVH 20 (4-5865042) F17-like fimbrial usher	99.7
EQO39143	Escherichia coli HVH 38 (4-2774682) F17-like fimbrial usher	99.7
EQO97005	Escherichia coli HVH 55 (4-2646161) F17-like fimbrial usher	99.7

EQP16163	Escherichia coli HVH 61 (4-2736020) F17-like fimbrial usher	99.7
EQP98545	Escherichia coli HVH 89 (4-5885604) F17-like fimbrial usher	99.7
EQU05851	Escherichia coli HVH 197 (4-4466217) F17-like fimbrial usher	99.7
EQU53211	Escherichia coli HVH 207 (4-3113221) F17-like fimbrial usher	99.7
EQV19738	Escherichia coli HVH 225 (4-1273116) F17-like fimbrial usher	99.7
EQW65711	Escherichia coli UMEA 3088-1 F17-like fimbrial usher	99.7
EQX13871	Escherichia coli UMEA 3160-1 F17-like fimbrial usher	99.7
ERA80937	Escherichia coli HVH 160 (4-5695937) F17-like fimbrial usher	99.7
ERF50184	Escherichia coli UMEA 3652-1 F17-like fimbrial usher	99.7
KDY17150	Escherichia coli 2-316-03_S4_C3 type VII secretion system (T7SS), usher family protein	99.7
KIE68021	Escherichia coli F17 fimbrial usher	99.7
KUT57088	Escherichia coli F17 fimbrial usher	99.7
KUX63359	Escherichia coli F17 fimbrial usher	99.7
KZH92368	Escherichia coli F17 fimbrial usher	99.7
KZH92802	Escherichia coli F17 fimbrial usher	99.7
KZJ70388	Escherichia coli F17 fimbrial usher	99.7
KEJ66138	Escherichia coli 3-020-07_S4_C1 type VII secretion system (T7SS), usher family protein	99.7
KSW91158	Escherichia coli F17 fimbrial usher	99.7
KUX58993	Escherichia coli F17 fimbrial usher	99.7
KKA62248	Escherichia coli 9.1649 fimbrial usher protein	99.8
KUS56949	Escherichia coli F17 fimbrial usher	99.8
CAD33726	Escherichia coli putative F17-like fimbrial usher	99.7
ABG71754	Escherichia coli 536 putative F17-like fimbrial usher	99.6
EQW45049	Escherichia coli UMEA 3087-1 F17-like fimbrial usher	99.7
EQW73672	Escherichia coli UMEA 3121-1 F17-like fimbrial usher	99.6
EQW75725	Escherichia coli UMEA 3121-1 F17-like fimbrial usher	99.6
EQY34770	Escherichia coli UMEA 3222-1 F17-like fimbrial usher	99.6
EQY34808	Escherichia coli UMEA 3222-1 F17-like fimbrial usher	99.6
EQT41795	Escherichia coli HVH 185 (4-2876639) F17-like fimbrial usher	99.8
EQT46554	Escherichia coli HVH 185 (4-2876639) F17-like fimbrial usher	99.8
EQU37953	Escherichia coli HVH 204 (4-3112802) F17-like fimbrial usher	99.8
EQW63376	Escherichia coli UMEA 3113-1 F17-like fimbrial usher	99.8
EQU40650	Escherichia coli HVH 204 (4-3112802) F17-like fimbrial usher	99.6
EQQ62500	Escherichia coli HVH 109 (4-6977162) F17-like fimbrial usher	99.6
EQQ82588	Escherichia coli HVH 114 (4-7037740) F17-like fimbrial usher	99.6
EQR09972	Escherichia coli HVH 117 (4-6857191) F17-like fimbrial usher	99.6
EQU89480	Escherichia coli HVH 216 (4-3042952) F17-like fimbrial usher	99.6
EQY63999	Escherichia coli UMEA 3257-1 F17-like fimbrial usher	99.6
KLX39893	Escherichia coli F17-like fimbrial usher	99.6
KLX42170	Escherichia coli F17-like fimbrial usher	99.6
KTK78416	Escherichia fergusonii F17 fimbrial usher	99.6
KUV23781	Escherichia coli F17 fimbrial usher	99.6
KUV45571	Escherichia coli F17 fimbrial usher	99.6
KXL00261	Escherichia coli F17 fimbrial usher	99.6
KZI73335	Escherichia coli F17 fimbrial usher	99.6
EEJ46853	Escherichia coli 83972 fimbrial usher protein	99.7
ESD40481	Escherichia coli 907892 fimbrial usher protein	99.6
EFJ55400	Escherichia coli MS 185-1 fimbrial usher protein	99.6
EFJ93345	Escherichia coli MS 45-1 fimbrial usher protein	99.6
ADN49244	Escherichia coli ABU 83972 putative F17-like fimbrial usher	99.6
ELC24324	Escherichia coli KTE15 F17-like fimbrial usher	99.6
ELC59545	Escherichia coli KTE39 F17-like fimbrial usher	99.6
ELC84925	Escherichia coli KTE188 F17-like fimbrial usher	99.6
ELD42488	Escherichia coli KTE214 F17-like fimbrial usher	99.6
ELD59758	Escherichia coli KTE230 F17-like fimbrial usher	99.6

ELE78785	Escherichia coli KTE86 F17-like fimbrial usher	99.6
ELH41419	Escherichia coli KTE183 F17-like fimbrial usher	99.6
ELJ74739	Escherichia coli KTE88 F17-like fimbrial usher	99.6
ELJ98001	Escherichia coli KTE99 F17-like fimbrial usher	99.6
EOV89522	Escherichia coli KTE89 F17-like fimbrial usher	99.6
EQO41248	Escherichia coli HVH 39 (4-2679949) F17-like fimbrial usher	99.6
EQW11354	Escherichia coli UMEA 3022-1 F17-like fimbrial usher	99.6
EQW13192	Escherichia coli UMEA 3022-1 F17-like fimbrial usher	99.6
EQW51065	Escherichia coli UMEA 3097-1 F17-like fimbrial usher	99.6
EQX17451	Escherichia coli UMEA 3161-1 F17-like fimbrial usher	99.6
EQX36137	Escherichia coli UMEA 3173-1 F17-like fimbrial usher	99.6
EQY06764	Escherichia coli UMEA 3208-1 F17-like fimbrial usher	99.6
EQY24271	Escherichia coli UMEA 3217-1 F17-like fimbrial usher	99.6
EQY50557	Escherichia coli UMEA 3233-1 F17-like fimbrial usher	99.6
EQY95004	Escherichia coli UMEA 3337-1 F17-like fimbrial usher	99.6
EQZ06873	Escherichia coli UMEA 3341-1 F17-like fimbrial usher	99.6
EQZ19130	Escherichia coli UMEA 3490-1 F17-like fimbrial usher	99.6
ERA47360	Escherichia coli UMEA 4076-1 F17-like fimbrial usher	99.6
ERA64849	Escherichia coli HVH 156 (4-3206505) F17-like fimbrial usher	99.6
EQX07927	Escherichia coli UMEA 3159-1 F17-like fimbrial usher	99.6
EQX39702	Escherichia coli UMEA 3175-1 F17-like fimbrial usher	99.6
EQX54816	Escherichia coli UMEA 3178-1 F17-like fimbrial usher	99.6
EQY38465	Escherichia coli UMEA 3221-1 F17-like fimbrial usher	99.6
EQY41172	Escherichia coli UMEA 3230-1 F17-like fimbrial usher	99.6
EQZ85064	Escherichia coli UMEA 3707-1 F17-like fimbrial usher	99.6
EQZ91173	Escherichia coli UMEA 3705-1 F17-like fimbrial usher	99.6
ETF28844	Escherichia coli HVH 83 (4-2051087) F17-like fimbrial usher	99.6
EYB58385	Escherichia coli F17 fimbrial usher	99.6
KEP00361	Escherichia coli F17 fimbrial usher	99.6
KUW14700	Escherichia coli F17 fimbrial usher	99.6
KYS70882	Escherichia coli F17 fimbrial usher	99.6
ELE03318	Escherichia coli KTE53 F17-like fimbrial usher	99.6
ELE37879	Escherichia coli KTE67 F17-like fimbrial usher	99.6
ELH68122	Escherichia coli KTE207 F17-like fimbrial usher	99.6
ELI71746	Escherichia coli KTE133 F17-like fimbrial usher	99.6
EQN00413	Escherichia coli HVH 2 (4-6943160) F17-like fimbrial usher	99.6
EQN45609	Escherichia coli HVH 13 (4-7634056) F17-like fimbrial usher	99.6
EQP06349	Escherichia coli HVH 58 (4-2839709) F17-like fimbrial usher	99.6
EQQ16954	Escherichia coli HVH 92 (4-5930790) F17-like fimbrial usher	99.6
EQQ37550	Escherichia coli HVH 96 (4-5934869) F17-like fimbrial usher	99.6
EQR41036	Escherichia coli HVH 125 (4-2634716) F17-like fimbrial usher	99.6
EQS92042	Escherichia coli HVH 169 (4-1075578) F17-like fimbrial usher	99.6
EQU67332	Escherichia coli HVH 212 (3-9305343) F17-like fimbrial usher	99.6
EQV24276	Escherichia coli HVH 227 (4-2277670) F17-like fimbrial usher	99.6
EQV64639	Escherichia coli KOEGE 56 (169a) F17-like fimbrial usher	99.6
ESP19911	Escherichia coli HVH 86 (4-7026218) F17-like fimbrial usher	99.6
EQR58384	Escherichia coli HVH 132 (4-6876862) F17-like fimbrial usher	99.6
EQS17497	Escherichia coli HVH 144 (4-4451937) F17-like fimbrial usher	99.6
EQU92514	Escherichia coli HVH 218 (4-4500903) F17-like fimbrial usher	99.6
EQV01012	Escherichia coli HVH 220 (4-5876842) F17-like fimbrial usher	99.6
ERA64868	Escherichia coli HVH 157 (4-3406229) F17-like fimbrial usher	99.6
ERA79243	Escherichia coli HVH 159 (4-5818141) F17-like fimbrial usher	99.6
KZI09905	Escherichia coli F17 fimbrial usher	99.6
EQS44918	Escherichia coli HVH 153 (3-9344314) F17-like fimbrial usher	99.6
EQY65807	Escherichia coli UMEA 3264-1 F17-like fimbrial usher	99.6

EQY74298	Escherichia coli UMEA 3268-1 F17-like fimbrial usher	99.6
EQZ69900	Escherichia coli UMEA 3687-1 F17-like fimbrial usher	99.6
EQZ74168	Escherichia coli UMEA 3694-1 F17-like fimbrial usher	99.6
ERA06117	Escherichia coli UMEA 3821-1 F17-like fimbrial usher	99.6
ERA44053	Escherichia coli UMEA 4207-1 F17-like fimbrial usher	99.6
ESJ99313	Escherichia coli HVH 98 (4-5799287) F17-like fimbrial usher	99.6
ESK27829	Escherichia coli UMEA 3342-1 F17-like fimbrial usher	99.6
EYB60166	Escherichia coli F17 fimbrial usher	99.6
KEP02518	Escherichia coli F17 fimbrial usher	99.6
KHO56518	Escherichia coli F17 fimbrial usher	99.6
KUS42725	Escherichia coli F17 fimbrial usher	99.6
EQP44047	Escherichia coli HVH 74 (4-1034782) F17-like fimbrial usher	99.6
EQT05774	Escherichia coli HVH 172 (4-3248542) F17-like fimbrial usher	99.6
EQV53030	Escherichia coli KOEGE 43 (105a) F17-like fimbrial usher	99.6
EQV55245	Escherichia coli KOEGE 44 (106a) F17-like fimbrial usher	99.6
EQV65664	Escherichia coli KOEGE 61 (174a) F17-like fimbrial usher	99.6
EQW35180	Escherichia coli UMEA 3053-1 F17-like fimbrial usher	99.6
EQR30454	Escherichia coli HVH 121 (4-6877826) F17-like fimbrial usher	99.6
OAC27962	Escherichia coli F17-like fimbrial usher	99.6
ELJ78821	Escherichia coli KTE94 F17-like fimbrial usher	97.9
EOX21851	Escherichia coli KTE185 F17-like fimbrial usher	97.9
ELH20199	Escherichia coli KTE194 F17-like fimbrial usher	79.9
ELI19171	Escherichia coli KTE113 F17-like fimbrial usher	79.9
EQV28775	Escherichia coli KOEGE 30 (63a) F17-like fimbrial usher	79.9
EQW14192	Escherichia coli UMEA 3014-1 F17-like fimbrial usher	79.9
EQX15781	Escherichia coli UMEA 3160-1 F17-like fimbrial usher	79.9
EQX72890	Escherichia coli UMEA 3193-1 F17-like fimbrial usher	79.9
ERA29942	Escherichia coli UMEA 4075-1 F17-like fimbrial usher	79.9
KXL21895	Escherichia coli F17 fimbrial usher	79.9
KUW45549	Escherichia coli F17 fimbrial usher	79.9
AGS60699	Proteus mirabilis BB2000 fimbrial usher protein	79.4
AND13784	Proteus mirabilis F17 fimbrial usher	79.5
EKB01574	Proteus mirabilis WGLW6 hypothetical protein	79.5
KSA05685	Proteus mirabilis F17 fimbrial usher	79.5
KGA58547	Proteus vulgaris hypothetical protein	79.3
CAR41290	Proteus mirabilis fimbrial usher protein	79.2
KGQ15598	Proteus mirabilis F17 fimbrial usher	79.2
KGA89929	Proteus mirabilis hypothetical protein	79.2
KGZ05032	Proteus mirabilis F17 fimbrial usher	79.2
KGZ39655	Proteus mirabilis F17 fimbrial usher	79.1
KSW14302	Proteus mirabilis F17 fimbrial usher	79.1
KSW23593	Proteus mirabilis F17 fimbrial usher	79.1
EEI46422	Proteus mirabilis ATCC 29906 fimbrial usher protein	79.1
KGY29288	Proteus mirabilis F17 fimbrial usher	79.1
KGY42554	Proteus mirabilis F17 fimbrial usher	79.1
KGY46341	Proteus mirabilis F17 fimbrial usher	79.1
KXB98825	Proteus mirabilis fimbrial usher protein	79
KKC58837	Proteus mirabilis F17 fimbrial usher	79.1
ETE47402	Salmonella enterica subsp fimbrial usher protein	58.1
KUR52793	Salmonella enterica subsp.F17 fimbrial usher	58.1
CAX67955	Salmonella enterica putative fimbrial biogenesis usher protein	59.1
EHY70493	Salmonella enterica subsp. fimbrial usher protein	59
ENZ87754	Salmonella enterica subsp.Outer membrane usher protein htrE precursor	59
ESE91231	Salmonella enterica subsp. fimbrial usher protein	60.6
ANA20601	Salmonella enterica subsp. diarizonae F17 fimbrial usher	59.2

ANA24823	Salmonella enterica subsp. diarizonae F17 fimbrial usher	59.2
ANA29166	Salmonella enterica subsp. diarizonae F17 fimbrial usher	59.2
ESJ19560	Salmonella enterica subsp fimbrial usher protein	59.3
ESE86375	Salmonella enterica subsp. fimbrial usher protein	59.5
ACT33470	Escherichia coli Vir68 F17 fimbrial usher protein	58.9
EGI36603	Escherichia coli TA271 outer membrane usher protein HifC	58.9
KHG75394	Escherichia coli F17 fimbrial usher	58.9
KHI16177	Escherichia coli F17 fimbrial usher	58.9
KHI55142	Escherichia coli F17 fimbrial usher	58.9
KXQ50743	Escherichia coli F17 fimbrial usher	58.9
KIG88168	Escherichia coli F17 fimbrial usher	58.8
EID64834	Escherichia coli W26 outer membrane usher protein HifC	58.9
KLG28392	Escherichia coli F17 fimbrial usher	58.9
KIG29732	Escherichia coli F17 fimbrial usher	58.9
KHI29822	Escherichia coli F17 fimbrial usher	58.9
AAA92620	Escherichia coli transmembrane protein	59.6
ERA04437	Escherichia coli UMEA 3805-1 F17-like fimbrial usher	59.6
EQO74630	Escherichia coli HVH 46 (4-2758776) F17-like fimbrial usher	59.6
EQS48079	Escherichia coli HVH 153 (3-9344314) F17-like fimbrial usher	59.6
KIO84626	Escherichia coli 97.0264 fimbrial usher protein	59.6
KXL74806	Escherichia coli F17 fimbrial usher	59.6
KXL87851	Escherichia coli F17 fimbrial usher	59.6
KXM02269	Escherichia coli F17 fimbrial usher	59.6
KXM18522	Escherichia coli F17 fimbrial usher	59.6
KXM45748	Escherichia coli F17 fimbrial usher	59.6
KXN29657	Escherichia coli F17 fimbrial usher	59.6
KXN32898	Escherichia coli F17 fimbrial usher	59.6
OAC11594	Escherichia coli fimbrial transmembrane protein F17a-C	59.6
OAC27624	Escherichia coli fimbrial transmembrane protein F17a-C	59.7
KQJ38281	Escherichia coli F17 fimbrial usher	58.8
EKI47004	Escherichia coli N1 transmembrane protein	58.9
KHJ08306	Escherichia coli F17 fimbrial usher	59.1
EGX03870	Escherichia coli STEC MHI813 outer membrane usher protein hifC	59.6
EOU64766	Escherichia coli KTE19 F17-like fimbrial usher	59.7
KHI17420	Escherichia coli F17 fimbrial usher	59
KIG71063	Escherichia coli F17 fimbrial usher	59
KHG81555	Escherichia coli F17 fimbrial usher	59.8
KHH99754	Escherichia coli F17 fimbrial usher	59.8
KIG38390	Escherichia coli F17 fimbrial usher	59.8
KHG83618	Escherichia coli F17 fimbrial usher	59.7
ACT33558	Escherichia coli Vir68 hypothetical protein	42
EYZ95685	Escherichia coli O119:H4 str. 03-3458 deoxyribonuclease HsdR	42
EGI36568	Escherichia coli TA271 putative fimbrial usher protein	42
EKH08978	Escherichia coli FRIK920 putative outer membrane usher protein	43.6
EKH17933	Escherichia coli PA34 putative outer membrane usher protein	43.6
EKH20639	Escherichia coli FDA506 putative outer membrane usher protein	43.6
EKH25450	Escherichia coli FDA507 putative outer membrane usher protein	43.6
EKH32471	Escherichia coli FDA504 putative outer membrane usher protein	43.6
EKH39969	Escherichia coli FRIK1999 putative outer membrane usher protein	43.6
EKH49904	Escherichia coli NE1487 putative outer membrane usher protein	43.6
EKH59659	Escherichia coli FRIK2001 putative outer membrane usher protein	43.6
EKH67664	Escherichia coli PA4 putative outer membrane usher protein	43.6
EKH77367	Escherichia coli PA23 putative outer membrane usher protein	43.6
EKH77904	Escherichia coli PA49 putative outer membrane usher protein	43.6
EKH83279	Escherichia coli PA45 putative outer membrane usher protein	43.6

EKH92578	Escherichia coli TT12B putative outer membrane usher protein	43.6
EKH96483	Escherichia coli MA6 putative outer membrane usher protein	43.6
EKI11323	Escherichia coli CB7326 putative outer membrane usher protein	43.6
EKI69610	Escherichia coli EC1736 putative outer membrane usher protein	43.6
EKJ30920	Escherichia coli EC1868 putative outer membrane usher protein	43.6
EKJ31064	Escherichia coli EC1866 putative outer membrane usher protein	43.6
EKJ45004	Escherichia coli EC1869 putative outer membrane usher protein	43.6
EKJ47884	Escherichia coli NE098 putative outer membrane usher protein	43.6
EKJ49469	Escherichia coli EC1870 putative outer membrane usher protein	43.6
EKJ63277	Escherichia coli FRIK523 putative outer membrane usher protein	43.6
EKJ65985	Escherichia coli 0.1304 putative outer membrane usher protein	43.6
EKK33136	Escherichia coli 5.2239 type VII secretion system (T7SS), usher family protein	43.6
EKK33786	Escherichia coli 6.0172 putative outer membrane usher protein	43.6
EKK58486	Escherichia coli 8.0586 type VII secretion system (T7SS), usher family protein	43.6
EKK78428	Escherichia coli 8.0416 putative outer membrane usher protein	43.6
EKK89063	Escherichia coli 10.0821 type VII secretion system (T7SS), usher family protein	43.6
EKV83394	Escherichia coli 89.0511 type VII secretion system (T7SS), usher family protein	43.6
EKV99677	Escherichia coli 90.2281 type VII secretion system (T7SS), usher family protein	43.6
EKW00030	Escherichia coli 90.0039 type VII secretion system (T7SS), usher family protein	43.6
EKW00417	Escherichia coli 90.0091 type VII secretion system (T7SS), usher family protein	43.6
EKW16280	Escherichia coli 93.0056 type VII secretion system (T7SS), usher family protein	43.6
EKW16942	Escherichia coli 93.0055 type VII secretion system (T7SS), usher family protein	43.6
EKW17713	Escherichia coli 94.0618 type VII secretion system (T7SS), usher family protein	43.6
EKW33758	Escherichia coli 95.0183 type VII secretion system (T7SS), usher family protein	43.6
EKW48481	Escherichia coli 96.0428 type VII secretion system (T7SS), usher family protein	43.6
EKW54352	Escherichia coli 96.0939 type VII secretion system (T7SS), usher family protein	43.6
EKW66086	Escherichia coli 96.0932 type VII secretion system (T7SS), usher family protein	43.6
EKW81431	Escherichia coli 97.1742 type VII secretion system (T7SS), usher family protein	43.6
EKW85444	Escherichia coli 97.0007 type VII secretion system (T7SS), usher family protein	43.6
EKW93747	Escherichia coli 99.0713 type VII secretion system (T7SS), usher family protein	43.6
EKW95043	Escherichia coli 99.0672 type VII secretion system (T7SS), usher family protein	43.6
EKY42416	Escherichia coli 96.0109 type VII secretion system (T7SS), usher family protein	43.6
ELV20957	Escherichia coli 99.0814 type VII secretion system (T7SS), usher family protein	43.6
ELV28748	Escherichia coli 99.0815 type VII secretion system (T7SS), usher family protein	43.6
ELV56195	Escherichia coli 99.1753 type VII secretion system (T7SS), usher family protein	43.6
ELV72838	Escherichia coli ATCC 700728 type VII secretion system (T7SS), usher family protein	43.6
ELV73067	Escherichia coli PA11 type VII secretion system (T7SS), usher family protein	43.6
ELV79731	Escherichia coli 99.1805 type VII secretion system (T7SS), usher family protein	43.6
ELV87097	Escherichia coli PA13 type VII secretion system (T7SS), usher family protein	43.6
ELV94460	Escherichia coli PA2 type VII secretion system (T7SS), usher family protein	43.6
ELW08784	Escherichia coli PA8 type VII secretion system (T7SS), usher family protein	43.6
ELW19147	Escherichia coli 7.1982 type VII secretion system (T7SS), usher family protein	43.6
ELW21161	Escherichia coli 99.1781 type VII secretion system (T7SS), usher family protein	43.6
ELW24342	Escherichia coli 99.1762 type VII secretion system (T7SS), usher family protein	43.6
ELW37584	Escherichia coli 3.4880 type VII secretion system (T7SS), usher family protein	43.6
ELW42989	Escherichia coli 95.0083 type VII secretion system (T7SS), usher family protein	43.6
ELW44766	Escherichia coli 99.0670 type VII secretion system (T7SS), usher family protein	43.6
ERB76857	Escherichia coli B107 type VII secretion system (T7SS), usher family protein	43.6
ERB87400	Escherichia coli B26-1 type VII secretion system (T7SS), usher family protein	43.6
ERB97963	Escherichia coli B26-2 type VII secretion system (T7SS), usher family protein	43.6
ERC04184	Escherichia coli B28-2 type VII secretion system (T7SS), usher family protein	43.6
ERC05409	Escherichia coli B28-1 type VII secretion system (T7SS), usher family protein	43.6
ERC12039	Escherichia coli B29-1 type VII secretion system (T7SS), usher family protein	43.6
ERC21172	Escherichia coli B29-2 type VII secretion system (T7SS), usher family protein	43.6
ERC23962	Escherichia coli B36-1 type VII secretion system (T7SS), usher family protein	43.6

ERC27098	Escherichia coli B36-2 type VII secretion system (T7SS), usher family protein	43.6
ERC35253	Escherichia coli B7-1 type VII secretion system (T7SS), usher family protein	43.6
ERC44510	Escherichia coli B7-2 type VII secretion system (T7SS), usher family protein	43.6
ERC44972	Escherichia coli B93 type VII secretion system (T7SS), usher family protein	43.6
ERC50784	Escherichia coli B94 type VII secretion system (T7SS), usher family protein	43.6
ERC69414	Escherichia coli type VII secretion system (T7SS), usher family protein	43.6
ERC84429	Escherichia coli T234_00 type VII secretion system (T7SS), usher family protein	43.6
ERC89721	Escherichia coli 14A type VII secretion system (T7SS), usher family protein	43.6
ERD03249	Escherichia coli B104 type VII secretion system (T7SS), usher family protein	43.6
ERD03476	Escherichia coli B103 type VII secretion system (T7SS), usher family protein	43.6
ERD04377	Escherichia coli 2886-75 type VII secretion system (T7SS), usher family protein	43.6
ERD18377	Escherichia coli B105 type VII secretion system (T7SS), usher family protein	43.6
ERD19275	Escherichia coli B106 type VII secretion system (T7SS), usher family protein	43.6
ERD20316	Escherichia coli B108 type VII secretion system (T7SS), usher family protein	43.6
ERD33082	Escherichia coli B109 type VII secretion system (T7SS), usher family protein	43.6
ERD34566	Escherichia coli B112 type VII secretion system (T7SS), usher family protein	43.6
ERD41195	Escherichia coli B113 type VII secretion system (T7SS), usher family protein	43.6
ERD50200	Escherichia coli B114 type VII secretion system (T7SS), usher family protein	43.6
ERD51964	Escherichia coli B15 type VII secretion system (T7SS), usher family protein	43.6
ERD53995	Escherichia coli B17 type VII secretion system (T7SS), usher family protein	43.6
ERD66870	Escherichia coli B40-2 type VII secretion system (T7SS), usher family protein	43.6
ERD67707	Escherichia coli B49-2 type VII secretion system (T7SS), usher family protein	43.6
ERD68267	Escherichia coli B40-1 type VII secretion system (T7SS), usher family protein	43.6
ERD80446	Escherichia coli B5-2 type VII secretion system (T7SS), usher family protein	43.6
ERD83897	Escherichia coli B83 type VII secretion system (T7SS), usher family protein	43.6
ERD87954	Escherichia coli B84 type VII secretion system (T7SS), usher family protein	43.6
ERD94118	Escherichia coli B85 type VII secretion system (T7SS), usher family protein	43.6
ERE09951	Escherichia coli type VII secretion system (T7SS), usher family protein	43.6
ERE24559	Escherichia coli T1282_01 type VII secretion system (T7SS), usher family protein	43.6
ERE35233	Escherichia coli B90 type VII secretion system (T7SS), usher family protein	43.6
ETJ78460	Escherichia coli ATCC BAA-2192 fimbrial protein	43.6
EYV59047	Escherichia coli O157:H7 str. 2009EL2109 fimbrial protein	43.6
EYV68242	Escherichia coli O157:H7 str. 2009EL1705 fimbrial protein	43.6
EYV81494	Escherichia coli O157:H7 str. K5806 fimbrial protein	43.6
EYV86677	Escherichia coli O157:H7 str. F7350 fimbrial protein	43.6
EYW03298	Escherichia coli O157:H7 str. 2011EL-2312 fimbrial protein	43.6
EYW21095	Escherichia coli O157:H7 str. 2011EL-2114 fimbrial protein	43.6
EYW38000	Escherichia coli O157:H7 str. 2011EL-2113 fimbrial protein	43.6
EYW38081	Escherichia coli O157:H7 str. 2011EL-2112 fimbrial protein	43.6
EYW42507	Escherichia coli O157:H7 str. 2011EL-2111 fimbrial protein	43.6
EYW47992	Escherichia coli O157:H7 str. 2011EL-2108 fimbrial protein	43.6
EYW50954	Escherichia coli O157:H7 str. 2011EL-2109 fimbrial protein	43.6
EYW52560	Escherichia coli O157:H7 str. 2011EL-2107 fimbrial protein	43.6
EYW58006	Escherichia coli O157:H7 str. 2011EL-2106 fimbrial protein	43.6
EYW66459	Escherichia coli O157:H7 str. 2011EL-2105 fimbrial protein	43.6
EYW69628	Escherichia coli O157:H7 str. 2011EL-2104 fimbrial protein	43.6
EYW78793	Escherichia coli O157:H7 str. 2011EL-2103 fimbrial protein	43.6
EYW79101	Escherichia coli O157:H7 str. 2011EL-2101 fimbrial protein	43.6
EYW87064	Escherichia coli O157:H7 str. 2011EL-2099 fimbrial protein	43.6
EYW92680	Escherichia coli O157:H7 str. 08-4169 fimbrial protein	43.6
EYX08878	Escherichia coli O157:H7 str. 08-3037 fimbrial protein	43.6
EYX09370	Escherichia coli O157:H7 str. 08-3527 fimbrial protein	43.6
EYX22958	Escherichia coli O157:H7 str. 2011EL-2097 fimbrial protein	43.6
EYX27122	Escherichia coli O157:H7 str. 2011EL-2098 fimbrial protein	43.6
EYX31783	Escherichia coli O157:H7 str. 2011EL-2096 fimbrial protein	43.6

EYX41317	Escherichia coli O157:H7 str. 2011EL-2093 fimbrial protein	43.6
EYX42359	Escherichia coli O157:H7 str. 2011EL-2094 fimbrial protein	43.6
EYX49506	Escherichia coli O157:H7 str. 2011EL-2091 fimbrial protein	43.6
EYX49623	Escherichia coli O157:H7 str. 2011EL-2092 fimbrial protein	43.6
EYX53190	Escherichia coli O157:H7 str. 2011EL-2090 fimbrial protein	43.6
EYZ27349	Escherichia coli O157:H7 str. 07-3091 fimbrial protein	43.6
EYZ39043	Escherichia coli O157:H7 str. 06-4039 fimbrial protein	43.6
EYZ50667	Escherichia coli O157:H7 str. 06-3745 fimbrial protein	43.6
EYZ53932	Escherichia coli O55:H7 str. 06-3555 fimbrial protein	43.6
EZA86831	Escherichia coli O157:H7 str. F6142 fimbrial protein	43.6
EZA96722	Escherichia coli O157:H7 str. F6750 fimbrial protein	43.6
EZB05142	Escherichia coli O157:H7 str. F6749 fimbrial protein	43.6
EZB09946	Escherichia coli O157:H7 str. F6751 fimbrial protein	43.6
EZB13848	Escherichia coli O157:H7 str. F7377 fimbrial protein	43.6
EZB34113	Escherichia coli O157:H7 str. H2495 fimbrial protein	43.6
EZB34923	Escherichia coli O157:H7 str. G5303 fimbrial protein	43.6
EZB41263	Escherichia coli O157:H7 str. K1420 fimbrial protein	43.6
EZB51029	Escherichia coli O157:H7 str. K1793 fimbrial protein	43.6
EZB57624	Escherichia coli O157:H7 str. K1792 fimbrial protein	43.6
EZB68752	Escherichia coli O157:H7 str. K1795 fimbrial protein	43.6
EZB70893	Escherichia coli O157:H7 str. K1796 fimbrial protein	43.6
EZB76896	Escherichia coli O157:H7 str. K1845 fimbrial protein	43.6
EZB84586	Escherichia coli O157:H7 str. K1927 fimbrial protein	43.6
EZB85896	Escherichia coli O157:H7 str. K2188 fimbrial protein	43.6
EZB86437	Escherichia coli O157:H7 str. K1921 fimbrial protein	43.6
EZB93552	Escherichia coli O157:H7 str. K2192 fimbrial protein	43.6
EZB97777	Escherichia coli O157:H7 str. K2324 fimbrial protein	43.6
EZC02291	Escherichia coli O157:H7 str. K2191 fimbrial protein	43.6
EZC11600	Escherichia coli O157:H7 str. K2581 fimbrial protein	43.6
EZC16351	Escherichia coli O157:H7 str. K2622 fimbrial protein	43.6
EZC20510	Escherichia coli O157:H7 str. K2845 fimbrial protein	43.6
EZC23600	Escherichia coli O157:H7 str. K2854 fimbrial protein	43.6
EZC33166	Escherichia coli O157:H7 str. K4396 fimbrial protein	43.6
EZC64017	Escherichia coli O157:H7 str. K5453 fimbrial protein	43.6
EZC65918	Escherichia coli O157:H7 str. K5448 fimbrial protein	43.6
EZC69249	Escherichia coli O157:H7 str. K5449 fimbrial protein	43.6
EZC78925	Escherichia coli O157:H7 str. K5460 fimbrial protein	43.6
EZC79564	Escherichia coli O157:H7 str. K5602 fimbrial protein	43.6
EZC86329	Escherichia coli O157:H7 str. K5467 fimbrial protein	43.6
EZC93672	Escherichia coli O157:H7 str. K5607 fimbrial protein	43.6
EZC99468	Escherichia coli O157:H7 str. K5609 fimbrial protein	43.6
EZD03089	Escherichia coli O157:H7 str. K5852 fimbrial protein	43.6
EZD13398	Escherichia coli O157:H7 str. K6590 fimbrial protein	43.6
EZD75223	Escherichia coli O157:H7 str. K7140 fimbrial protein	43.6
EZD89123	Escherichia coli O157:NM str. 08-4540 fimbrial protein	43.6
EZE56112	Escherichia coli O157:H7 str. 2009C-4258 fimbrial protein	43.6
EZE82006	Escherichia coli O157:H7 str. 2009EL1449 fimbrial protein	43.6
EZF03468	Escherichia coli O157:H7 str. 2011EL-2313 fimbrial protein	43.6
EZQ44480	Escherichia coli O157: str. 2010EL-2045 fimbrial protein	43.6
EZQ53020	Escherichia coli O157: str. 2010EL-2044 fimbrial protein	43.6
KIY27912	Escherichia coli fimbrial protein	43.6
KIZ10804	Escherichia coli fimbrial protein	43.6
KKF84503	Escherichia coli O157:H7 fimbrial protein	43.6
KKK27660	Escherichia coli fimbrial protein	43.6
KKY48541	Escherichia coli O157:H7 fimbrial protein	43.6

KOZ06857	Escherichia coli fimbrial protein	43.6
KOZ10810	Escherichia coli fimbrial protein	43.6
KOZ16101	Escherichia coli fimbrial protein	43.6
KOZ29806	Escherichia coli fimbrial protein	43.6
KOZ48678	Escherichia coli fimbrial protein	43.6
KOZ53952	Escherichia coli fimbrial protein	43.6
KOZ57012	Escherichia coli fimbrial protein	43.6
KOZ72847	Escherichia coli fimbrial protein	43.6
KOZ97762	Escherichia coli fimbrial protein	43.6
KPH29271	Escherichia coli fimbrial protein	43.6
KPH37240	Escherichia coli fimbrial protein	43.6
KPH42145	Escherichia coli fimbrial protein	43.6
KPP14588	Escherichia coli fimbrial protein	43.6
KPP19808	Escherichia coli fimbrial protein	43.6
KPP35187	Escherichia coli fimbrial protein	43.6
KPP45378	Escherichia coli fimbrial protein	43.6
KPP48065	Escherichia coli fimbrial protein	43.6
KPP51659	Escherichia coli fimbrial protein	43.6
KRQ15005	Escherichia coli O157:H7 fimbrial protein	43.6
KYT92957	Escherichia coli fimbrial protein	43.6
ADD55863	Escherichia coli O55:H7 str. CB9615 Putative outer membrane usher protein	43.6
AEZ39843	Escherichia coli O55:H7 str. RM12579 outer membrane usher protein	43.6
AFJ28284	Escherichia coli Xuzhou21 putative outer membrane usher protein	43.6
AIG67653	Escherichia coli O157:H7 str. EDL933 outer membrane fimbrial usher protein	43.6
ALH91049	Escherichia coli O157:H7 fimbrial protein	43.6
AMW50839	Escherichia coli fimbrial protein	43.6
ANE66650	Escherichia coli fimbrial protein	43.6
ANG67852	Escherichia coli O157:H7 fimbrial protein	43.6
ANG73402	Escherichia coli O157:H7 fimbrial protein	43.6
ANG79029	Escherichia coli O157:H7 fimbrial protein	43.6
ANW39262	Escherichia coli O157:H7 fimbrial protein	43.6
AOD12137	Escherichia coli fimbrial protein	43.6
BAB34701	Escherichia coli O157:H7 str. Sakai putative outer membrane usher protein	43.6
EDU87258	Escherichia coli O157:H7 str. EC4501 fimbrial usher protein	43.6
EDU89867	Escherichia coli O157:H7 str. EC869 fimbrial usher protein	43.6
EDU96778	Escherichia coli O157:H7 str. EC508 fimbrial usher protein	43.6
EEC27388	Escherichia coli O157:H7 str. TW14588 fimbrial usher protein	43.6
EFW67105	Escherichia coli O157:H7 str. EC1212 putative outer membrane usher protein	43.6
EFX21873	Escherichia coli O55:H7 str. 3256-97 putative outer membrane usher protein	43.6
EGD62345	Escherichia coli O157:H7 str. 1125 putative outer membrane usher protein	43.6
EGD69322	Escherichia coli O157:H7 str. 1044 putative outer membrane usher protein	43.6
EHU62991	Escherichia coli DEC3A fimbrial Usher family protein	43.6
EHU75376	Escherichia coli DEC3C fimbrial Usher family protein	43.6
EHU80135	Escherichia coli DEC3D fimbrial Usher family protein	43.6
EHU81960	Escherichia coli DEC3E fimbrial Usher family protein	43.6
EHU95993	Escherichia coli DEC4A fimbrial Usher family protein	43.6
EHV00739	Escherichia coli DEC4B fimbrial Usher family protein	43.6
EHV11958	Escherichia coli DEC4C fimbrial Usher family protein	43.6
EHV12403	Escherichia coli DEC4D fimbrial Usher family protein	43.6
EHV27572	Escherichia coli DEC4F fimbrial Usher family protein	43.6
EHV28099	Escherichia coli DEC5A fimbrial Usher family protein	43.6
EHV34607	Escherichia coli DEC5B fimbrial Usher family protein	43.6
EHV41319	Escherichia coli DEC5C fimbrial Usher family protein	43.6
EIN27548	Escherichia coli FRIK1996 putative outer membrane usher protein	43.6
EIN28653	Escherichia coli FDA517 putative outer membrane usher protein	43.6

EIN44971	Escherichia coli 93-001 putative outer membrane usher protein	43.6
EIN47324	Escherichia coli FRIK1985 putative outer membrane usher protein	43.6
EIN80149	Escherichia coli PA10 putative outer membrane usher protein	43.6
EIN81204	Escherichia coli PA15 putative outer membrane usher protein	43.6
EIN91451	Escherichia coli PA22 putative outer membrane usher protein	43.6
EIO20073	Escherichia coli PA31 putative outer membrane usher protein	43.6
EIO20293	Escherichia coli PA32 putative outer membrane usher protein	43.6
EIO22332	Escherichia coli PA33 putative outer membrane usher protein	43.6
EIO30655	Escherichia coli PA40 putative outer membrane usher protein	43.6
EIO43631	Escherichia coli PA42 putative outer membrane usher protein	43.6
EIO44995	Escherichia coli PA39 putative outer membrane usher protein	43.6
EIO61076	Escherichia coli TW10246 putative outer membrane usher protein	43.6
EIO67789	Escherichia coli TW11039 putative outer membrane usher protein	43.6
EIO71388	Escherichia coli TW07945 putative outer membrane usher protein	43.6
EIO84707	Escherichia coli TW10119 putative outer membrane usher protein	43.6
EIO85331	Escherichia coli TW09098 putative outer membrane usher protein	43.6
EIP16971	Escherichia coli TW14301 putative outer membrane usher protein	43.6
EIP18683	Escherichia coli O157:H7 str. TW14313 putative outer membrane usher protein	43.6
EIP19202	Escherichia coli EC4421 putative outer membrane usher protein	43.6
EIP30962	Escherichia coli EC4422 putative outer membrane usher protein	43.6
EIP49382	Escherichia coli EC4436 putative outer membrane usher protein	43.6
EIP61961	Escherichia coli EC1738 putative outer membrane usher protein	43.6
EIP64455	Escherichia coli EC4437 putative outer membrane usher protein	43.6
EIP69570	Escherichia coli EC1734 putative outer membrane usher protein	43.6
EIP81532	Escherichia coli EC1863 putative outer membrane usher protein	43.6
EKK33536	Escherichia coli 3.4870 type VII secretion system (T7SS), usher family protein	43.6
OAN04922	Escherichia coli O157:H7 fimbrial protein	43.6
AAG55651	Escherichia coli O157:H7 str. EDL933 putative usher protein	43.6
CTR59674	Escherichia coli usher protein	43.6
CTS24352	Escherichia coli usher protein	43.6
CTV79962	Escherichia coli usher protein	43.6
CUA30582	Escherichia coli usher protein	43.6
EFX27205	Escherichia coli O55:H7 str. USDA 5905 putative outer membrane usher protein	43.6
EKH97331	Escherichia coli 5905 putative outer membrane usher protein	43.6
EFX31563	Escherichia coli O157:H7 str. LSU-61 putative outer membrane usher protein	43.6
EKW70091	Escherichia coli 96.0107 type VII secretion system (T7SS), usher family protein	43.6
ERC71947	Escherichia coli Bd5610_99 type VII secretion system (T7SS), usher family protein	43.5
ERC88804	Escherichia coli T924_01 type VII secretion system (T7SS), usher family protein	43.6
KOZ32122	Escherichia coli fimbrial protein	43.6
EZB38362	Escherichia coli O157:H7 str. H2498 fimbrial protein	43.5
KOZ19538	Escherichia coli fimbrial protein	43.6
KPO75320	Escherichia coli fimbrial protein	43.5
KPP21245	Escherichia coli fimbrial protein	43.5
EFX12225	Escherichia coli O157:H- str. 493-89 putative outer membrane usher protein	43.5
EFX17137	Escherichia coli O157:H- str. H 2687 putative outer membrane usher protein	43.5
EHU93417	Escherichia coli DEC3F fimbrial Usher family protein	43.5
EIO52001	Escherichia coli TW06591 putative outer membrane usher protein	43.5
EKI14407	Escherichia coli 5412 putative outer membrane usher protein	43.5
KJJ47841	Escherichia coli fimbrial protein	43.5
KOZ57645	Escherichia coli fimbrial protein	43.5
KOZ67216	Escherichia coli fimbrial protein	43.5
KOZ82091	Escherichia coli fimbrial protein	43.5
KOZ82732	Escherichia coli fimbrial protein	43.5
KOZ92844	Escherichia coli fimbrial protein	43.5
EFX07263	Escherichia coli O157:H7 str. G5101 putative outer membrane usher protein	43.7

EKI14888	Escherichia coli EC96038 putative outer membrane usher protein	43.7
EKK75680	Escherichia coli 10.0869 type VII secretion system (T7SS), usher family protein	43.7
ELW04498	Escherichia coli PA48 type VII secretion system (T7SS), usher family protein	43.7
EYY42224	Escherichia coli O157:H7 str. 2010C-4979C1 fimbrial protein	43.7
EHU64177	Escherichia coli DEC3B fimbrial Usher family protein	43.6
EHV42696	Escherichia coli DEC5D fimbrial Usher family protein	43.6
EIN28899	Escherichia coli FDA505 putative outer membrane usher protein	43.6
EIN47052	Escherichia coli FRIK1990 putative outer membrane usher protein	43.6
EIN64062	Escherichia coli PA5 putative outer membrane usher protein	43.6
EIN64660	Escherichia coli PA9 putative outer membrane usher protein	43.6
EIN81979	Escherichia coli PA14 putative outer membrane usher protein	43.6
EIO05906	Escherichia coli PA28 putative outer membrane usher protein	43.6
EIO42576	Escherichia coli PA41 putative outer membrane usher protein	43.6
EIP02169	Escherichia coli TW09195 putative outer membrane usher protein	43.6
EKH46243	Escherichia coli FRIK1997 putative outer membrane usher protein	43.6
EKI52599	Escherichia coli PA38 putative outer membrane usher protein	43.6
EKI72347	Escherichia coli EC1737 putative outer membrane usher protein	43.6
EKJ16694	Escherichia coli EC1864 putative outer membrane usher protein	43.6
EKK61703	Escherichia coli 8.2524 type VII secretion system (T7SS), usher family protein	43.6
EKV82226	Escherichia coli 88.1042 type VII secretion system (T7SS), usher family protein	43.6
EKV83788	Escherichia coli 88.1467 type VII secretion system (T7SS), usher family protein	43.6
EKW33566	Escherichia coli 95.0943 type VII secretion system (T7SS), usher family protein	43.6
EKW52543	Escherichia coli 96.0427 type VII secretion system (T7SS), usher family protein	43.6
EKW66188	Escherichia coli 97.0003 type VII secretion system (T7SS), usher family protein	43.6
EKY43968	Escherichia coli 97.0010 type VII secretion system (T7SS), usher family protein	43.6
ELV42265	Escherichia coli 99.0816 type VII secretion system (T7SS), usher family protein	43.6
ELV59010	Escherichia coli 99.1775 type VII secretion system (T7SS), usher family protein	43.6
ELV60235	Escherichia coli 99.1793 type VII secretion system (T7SS), usher family protein	43.6
ERB87602	Escherichia coli B102 type VII secretion system (T7SS), usher family protein	43.6
ERD95759	Escherichia coli B86 type VII secretion system (T7SS), usher family protein	43.6
ERE34518	Escherichia coli B89 type VII secretion system (T7SS), usher family protein	43.6
ERE38404	Escherichia coli Tx1686 type VII secretion system (T7SS), usher family protein	43.6
ERE19084	Escherichia coli 09BKT024447 type VII secretion system (T7SS), usher family protein	43.6
EKI58398	Escherichia coli EC1735 putative outer membrane usher protein	43.6
EKH58316	Escherichia coli NE037 putative outer membrane usher protein	43.8
EHV49910	Escherichia coli DEC5E fimbrial Usher family protein	41.9
CTT89937	Escherichia coli usher protein	43.6
EFF07341	Escherichia coli B185 outer membrane usher protein	43.6
KOA35398	Escherichia coli fimbrial protein	43.6
EGX10205	Escherichia coli STEC_MHI813 fimbrial Usher family protein	43.5
KJW46289	Escherichia coli fimbrial protein	43.5
ELG90062	Escherichia coli KTE146 hypothetical protein	43.4
ANO88318	Escherichia coli fimbrial protein	43.3
EHN88119	Escherichia coli TA124 hypothetical protein	43.4
CDP68350	Escherichia coli D6-113.11 Putative outer membrane usher protein	43.7
CDU35541	Escherichia coli D6-113.11 Putative outer membrane usher protein	43.7
KHI45262	Escherichia coli fimbrial protein	43.8
KUS76798	Escherichia coli fimbrial protein	43.8
ELC99050	Escherichia coli KTE193 hypothetical protein	43.6
ELI31921	Escherichia coli KTE112 hypothetical protein	43.6
EQZ68447	Escherichia coli UMEA 3671-1 hypothetical protein	43.7
EQW90693	Escherichia coli UMEA 3124-1 hypothetical protein	43.9
EGI22399	Escherichia coli M718 putative fimbrial usher protein	43.5
KNZ99685	Escherichia coli fimbrial protein	43.5
ESA67030	Escherichia coli 113290 fimbrial usher protein	43.7

KFD74598	Escherichia coli fimbrial protein	43.7
ESM39020	Escherichia coli BWH 32 hypothetical protein	43.6
KYT01105	Escherichia coli fimbrial protein	43.8
KYU52385	Escherichia coli fimbrial protein	43.8
EHN96543	Escherichia coli E101 hypothetical protein	43.8
EQZ93543	Escherichia coli UMEA 3718-1 hypothetical protein	43.7

Supplementary Table 2: The carriage of F17-like pili in rUTI UPEC strains.

Strain	Pathotype	Clade	BioProject	F17-like Carriage	Sample Time Point**
536	UPEC	B2	PRJNA16235	Yes	
11128	EHEC	B1	PRJDA32513		
11368	EHEC	B1	PRJDA32509		
12009	EHEC	B1	PRJDA32511		
55989	EAEC	B1	PRJNA33413		
2009EL-2050	EHEC	B1	PRJNA81097		
2009EL-2071	EHEC	B1	PRJNA81099		
2011C-3493	EHEC	B1	PRJNA81095		
ABU 83972	ABU	B2	PRJNA38725	Yes	
APEC O1	APEC	B2	PRJNA16718		
APEC O78	APEC	B1	PRJNA184588		
ATCC 8739	Commensal	A	PRJNA18083		
BL21(DE3)	Lab Strain	A	PRJNA20713		
BW2952	Lab Strain	A	PRJNA33775		
CB9615	EPEC	E	PRJNA42729		
CE10	NMEC	F	PRJNA63597		
CFT073	UPEC	B2	PRJNA313		
clone D i14	UPEC	B2	PRJNA52023		
clone D i2	UPEC	B2	PRJNA52021		
DH1	Lab Strain	A	PRJDA52077		
DH10B	Lab Strain	A	PRJNA20079		
E2348/69	EPEC	B2	PRJEA32571		
E24377A	ETEC	B1	PRJNA13960		
EC4115	EHEC	E	PRJNA27739		
ED1a	Commensal	B2	PRJNA33409		
EDL933	EHEC	E	PRJNA259		
H10407	ETEC	A	PRJEA42749		
HS	Commensal	A	PRJNA13959		
IAI39	UPEC	F	PRJNA33411		
IHE3034	NMEC	B2	PRJNA43693		
K12 MG1655	Commensal	A	PRJNA40075		
LF82	AIEC	B2	PRJNA33825		
NRG 857C	AIEC	B2	PRJNA41221		
REL606	Lab Strain	A	PRJNA18281		
RM12579	EPEC	E	PRJNA68245		
S88	Commensal	B2	PRJNA33375		
SE11	Commensal	B1	PRJNA18057		
SE15	Commensal	B2	PRJDA19053		
SMS-3-5	Environmental	F	PRJNA19469		
TW14359	EHEC	E	PRJNA30045		

UM146	AIEC	B2	PRJNA50883	Yes	
UMNK88	ETEC	A	PRJNA42137		
UTI89	UPEC	B2	PRJNA16259	Yes	
W	Lab Strain	B1	PRJNA48011		
W3110	Lab Strain	A	PRJNA16351		
Xuzhou21	EHEC	E	PRJNA45823		
2.1a*	UPEC	A	PRJNA269984		Enrollment UTI
2.2r*	UPEC	D	PRJNA269984		Different-strain rUTI
5.1a*	UPEC	B1	PRJNA269984		Enrollment UTI
5.2p*	UPEC	B2	PRJNA269984	Yes	Prior to Recurrence
5.3r*	UPEC	B2	PRJNA269984	Yes	Different-strain rUTI
9.1a*	UPEC	D	PRJNA269984		Enrollment UTI
9.2p*	UPEC	B1	PRJNA269984		Prior to Recurrence
9.3r*	UPEC	B1	PRJNA269984		Different-strain rUTI
11.1a*	UPEC	A	PRJNA269984		Enrollment UTI
11.2p*	UPEC	A	PRJNA269984		Prior to Recurrence
11.3r*	UPEC	A	PRJNA269984		Same-strain rUTI
12.1a*	UPEC	B2	PRJNA269984	Yes	Enrollment UTI
12.2p*	UPEC	B2	PRJNA269984	Yes	Prior to Recurrence
12.3r*	UPEC	B2	PRJNA269984	Yes	Same-strain rUTI
12.4r*	UPEC	B2	PRJNA269984	Yes	Same-strain rUTI
17.1a*	UPEC	B2	PRJNA269984	Yes	Enrollment UTI
17.2p*	UPEC	B2	PRJNA269984	Yes	Prior to Recurrence
17.3r*	UPEC	B2	PRJNA269984	Yes	Same-strain rUTI
20.1a*	UPEC	B2	PRJNA269984	Yes	Enrollment UTI
20.2r*	UPEC	B2	PRJNA269984	Yes	Same-strain rUTI
20.3r*	UPEC	B2	PRJNA269984	Yes	Same-strain rUTI
21.1a*	UPEC	B2	PRJNA269984	Yes	Enrollment UTI
21.2p*	UPEC	B2	PRJNA269984	Yes	Prior to Recurrence
21.3r*	UPEC	B2	PRJNA269984	Yes	Same-strain rUTI
26.1a*	UPEC	B2	PRJNA269984	Yes	Enrollment UTI
26.2p*	UPEC	B2	PRJNA269984	Yes	Prior to Recurrence
26.3r*	UPEC	B2	PRJNA269984	Yes	Same-strain rUTI
31.1a*	UPEC	B1	PRJNA269984		Enrollment UTI
31.2p*	UPEC	B1	PRJNA269984		Prior to Recurrence
31.3r*	UPEC	B2	PRJNA269984		Different-strain rUTI
34.1a*	UPEC	B2	PRJNA269984	Yes	Enrollment UTI
34.2r*	UPEC	B2	PRJNA269984	Yes	Same-strain rUTI
35.1a*	UPEC	B2	PRJNA269984	Yes	Enrollment UTI
35.2p*	UPEC	B2	PRJNA269984	Yes	Prior to Recurrence

35.3r*	UPEC	B2	PRJNA269984	Yes	Same-strain rUTI
41.1a*	UPEC	B2	PRJNA269984	Yes	Enrollment UTI
41.2p*	UPEC	B2	PRJNA269984	Yes	Prior to Recurrence
41.3r*	UPEC	B2	PRJNA269984	Yes	Same-strain rUTI
41.4p*	UPEC	B1	PRJNA269984		Prior to Recurrence
41.5r*	UPEC	B1	PRJNA269984		Different-strain rUTI
56.1a*	UPEC	B1	PRJNA269984		Enrollment UTI
56.2r*	UPEC	B2	PRJNA269984	Yes	Different-strain rUTI
56.3r*	UPEC	B2	PRJNA269984	Yes	Same-strain rUTI

* Collected during a previous longitudinal study on recurrent UTI (ref. 18)
** Sample time point as defined in [REF]

Supplementary Table 3: UclD X-ray collection and refinement statistics

	$_{HR}$UclD^{LD} (5NWP)	UclD^{LD} (5VQ5)
Data collection		
Space group	$P2_1$	$P2_12_12_1$
Cell dimensions		
a, *b*, *c* (Å)	31.0, 91.9, 64.9	39.0, 58.6, 175.1
α, β, γ (°)	90.0, 96.5, 90.0	90.0, 90.0, 90.0
Resolution (Å) [a]	91.87 – 1.05 (1.11-1.05)	55.60-1.6 (1.66-1.60)
R_{merge} [a]	0.079 (0.336)	0.05 (0.43)
$I/\sigma(I)$ [a]	11.9 (2.1)	17.68 (1.43)
$CC_{1/2}$ [a]	99.6 (86.0)	0.998 (0.659)
Completeness (%)[a]	88.6 (43.8)	99.97 (99.98)
Redundancy [a]	5.0 (2.0)	2.0 (2.0)
Refinement		
Resolution (Å)	91.87 - 1.05	55.60 - 1.60
No. reflections	144393	108142
R_{work} / R_{free}	0.118 / 0.143	0.172 / 0.218
No. atoms	6890	3289
Protein	6223	2804
Iodide	/	6
Sulphate	1	/
Water	662	479
B factors		
Protein	10.7	22.4
Iodide	/	62.6

Sulphate	11.0	/
Water	23.9	36.2
R.m.s. deviations		
Bond lengths (Å)	0.028	0.002
Bond angles (°)	2.281	0.58

Number of crystals for each structure should be noted in footnote.

[a] Values in parentheses are for highest-resolution shell.